

NATIONAL BUREAU OF STANDARDS REPORT

10 481

INTERIM REPORT ON THE THERMODYNAMICS OF CHEMICAL SPECIES IMPORTANT IN AEROSPACE TECHNOLOGY

(The previous reports in this series have the NBS Report Nos. 6297, 6484, 6645, 6928, 7093, 7192, 7437, 7587, 7796, 8033, 8186, 8504, 8628, 8919, 9028, 9389, 9500, 9601, 9803, 9905, 10004, 10074, and 10326.)



U.S. DEPARTMENT OF COMMERCE
NATIONAL BUREAU OF STANDARDS

U. S. Air Force, Office of Scientific Research
Agreement No. AFOSR-ISSA-70-0002, Project No. 9750-01.
INTERIM REPORT ON THE THERMODYNAMICS OF CHEMICAL SPECIES IMPORTANT
IN AEROSPACE TECHNOLOGY

1 July 1971

Approved for Public Release; Distribution Unlimited

Qualified requestors may obtain additional copies from the Defense Documentation Center; all others should apply to the Clearinghouse for Federal Scientific and Technical Information.

NATIONAL BUREAU OF STANDARDS REPORT

NBS PROJECT

2320423
3160401
3160404
3160405
3160426

1 July 1971

NBS REPORT

10 481

INTERIM REPORT ON THE THERMODYNAMICS OF CHEMICAL SPECIES IMPORTANT IN AEROSPACE TECHNOLOGY

(The previous reports in this series have the NBS Report Nos. 6297, 6484, 6645, 6928, 7093, 7192, 7437, 7587, 7796, 8033, 8186, 8504, 8628, 8919, 9028, 9389, 9500, 9601, 9803, 9905, 10004, 10074, and 10326.)

Reference: U. S. Air Force, Office of Scientific Research, Agreement No. AFOSR-ISSA-70-0002, Project No. 9750-01.

IMPORTANT NOTICE

NATIONAL BUREAU OF STANDARDS
for use within the Government.
and review. For this reason, the
whole or in part, is not authorized
Bureau of Standards, Washington, D.C.
the Report has been specifically

Approved for public release by the
Director of the National Institute of
Standards and Technology (NIST)
on October 9, 2015.

These accounting documents intended
to be subjected to additional evaluation
and listing of this Report, either in
the Office of the Director, National
Institute of Standards and Technology,
by the Government agency for which
copies for its own use.



U.S. DEPARTMENT OF COMMERCE
NATIONAL BUREAU OF STANDARDS

U. S. Air Force, Office of Scientific Research
Agreement No. AFOSR-ISSA-70-0002, Project No. 9750-01.
INTERIM REPORT ON THE THERMODYNAMICS OF CHEMICAL SPECIES IMPORTANT
IN AEROSPACE TECHNOLOGY
1 July 1971
Approved for Public Release; Distribution Unlimited

CONDITIONS OF REPRODUCTION

Reproduction, translation, publication, use and disposal in whole or in part by or for the United States Government is permitted.

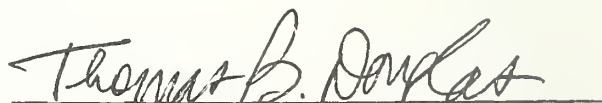
FOREWORD

Structure, propulsion, and guidance of new or improved weapons delivery systems are dependent in crucial areas of design on the availability of accurate thermodynamic data. Data on high-temperature materials, new rocket propellant ingredients, and combustion products (including exhaust ions) are, in many cases, lacking or unreliable. This broad integrated research program at the National Bureau of Standards supplies new or more reliable thermodynamic properties essential in several major phases of current propulsion development and application. Measured are compounds of those several chemical elements important in efficient propulsion fuels; those substances most affecting ion concentrations in such advanced propulsion concepts as ion propulsion; and the transition and other refractory metals (and their pertinent compounds) which may be suitable as construction materials for rocket motors, rocket nozzles, and nose cones that will be durable under extreme conditions of high temperature and corrosive environment. The properties determined extend in temperature up to 6000 degrees Kelvin. The principal research activities are experimental, and involve developing new measurement techniques and apparatus, as well as measuring heats of reaction, of fusion, and of vaporization; specific heats; equilibria involving gases; several thermophysical properties in fast processes at very high temperatures; spectra of the infrared, matrix-isolation, microwave, and electronic types; and mass spectra. Some of these techniques, by relating thermodynamic properties to molecular or crystal structures, make it possible to tabulate reliably these properties over far wider ranges of temperature and pressure than those actually employed in the basic investigations.

ABSTRACT

The NBS program is presently devoted to reliable measurements of the thermodynamic and other thermophysical properties of refractory metals and their Aerospace-important compounds. This report presents in detail recent results and critical analyses of several experimental investigations completed or in progress, literature surveys, and new measurement-method developments. All experimental values obtained are compared thoroughly with the previously published results. The subjects may be enumerated under three broad categories. (1) Properties of metals -- Using a subsecond pulse-heating technique, the heat capacity, electrical resistivity, and hemispherical total and normal spectral emittances were measured for tungsten (2000-3600 K) and niobium (1500 - 2700 K), with estimated inaccuracies of 2%-3% (heat capacity), 0.5%-1% (electrical resistivity), and 3% (the emittances). Using a similar fast technique, preliminary work gave for tungsten a melting point of 3692 K (IPTS-1968), with an estimated uncertainty of 15 K. The enthalpy of molybdenum, measured by drop-type calorimetry 1170-2100 K, agrees closely for drawn-annealed and zone-refined samples, with an estimated uncertainty generally within 1% for the derived heat capacity. The measured emissivities of tungsten, molybdenum, tantalum,

and niobium were found to be higher than those predicted by a classical theoretical relation to electrical resistivity (at 2000 K by amounts ranging from 10% for Nb to over 50% for W, but by progressively less at higher temperatures). (2) Properties of compounds -- MoF₅ was prepared, with a cryoscopically indicated purity of 99.85 mol %. After developing a technique for preventing its decomposition, preliminary values for its vapor pressure and heat of vaporization have been obtained by the transpiration method. To measure its heat of formation by oxidation to MoF₆, the heat of solution of MoF₆ was undertaken, and preliminary results indicate that the published₆ value is far in error (besides disagreeing by 14 kcal/mole from the published fluorine-combustion value). Using double-boiler Knudsen cells to suppress the polymer bands, the infrared spectrum of NbF₅ (matrix-isolated and some gas-phase) was observed, and was interpreted₅ to yield the six infrared-active fundamental frequencies of the monomer molecule, assuming it to have C_{4v} symmetry. The known composition and thermal properties, as well as sample-characterization techniques, of the systems Mo-C, Ta-C, and Nb-B are reviewed, and criteria for samples suitable for accurate drop calorimetry are discussed as background to measurements in progress. (3) New measurement techniques -- A high-speed (millisecond) method of measuring the thermal expansion of electrical conductors at high temperatures was developed, and tests on platinum (300-700 K) show agreement with steady-state data well within the estimated 5% uncertainty of the new method. Refinements being considered are enumerated. A rotating attenuator for the generation of subsecond-duration sawtooth-shape radiance pulses is described; the observed radiance variation scatters by the order of 0.5% from the calculated values. Various optical methods (primarily photoelectric and photographic) for measuring transient high temperatures with millisecond- and microsecond-order time resolution are critically reviewed. The advantages and limitations of the various methods are discussed, and estimates of the uncertainties given. Applications to solids above 1500 K are emphasized, such as in measuring their various thermophysical properties and in determining surface temperatures and temperature gradients in ram-jet combustion and ablating materials. Short-time (millisecond) fluctuations of the temperature of a graphite arc were measured (at about 3800 K), and were found to be 3 to 4 K, being comparable to those reported over a period of seconds using a slower pyrometer.


Thomas B. Douglas



Charles W. Beckett

TABLE OF CONTENTS

	<u>Page</u>
Foreword	i
Abstract	i
Chap. 1. <u>HIGH-SPEED (SUBSECOND) MEASUREMENT OF HEAT CAPACITY, ELECTRICAL RESISTIVITY, AND THERMAL RADIATION PROPERTIES OF TUNGSTEN IN THE RANGE 2000 TO 3600 K</u> (by A. Cezairliyan and J. L. McClure)	1
Abstract	1
1. Introduction	2
2. Measurements	2
Fig. 1. Photomicrographs of the tungsten specimen	4
Table 1. Impurities in tungsten specimen.	6
3. Experimental Results	7
3.1 Heat Capacity	7
Table 2. Heat capacity, electrical resistivity, hemispherical total and normal spectral emittances of tungsten.	8
3.2 Electrical Resistivity.	9
3.3 Hemispherical Total Emittance	9
3.4 Normal Spectral Emittance	9
4. Estimate of Errors	10
5. Discussion	10
Table 3. Tungsten heat capacity difference (previous literature values minus present-work values) in percent	12
Fig. 2. Heat capacity of tungsten reported in the literature	13
Table 4. Tungsten electrical resistivity difference (previous literature values minus present-work) in percent	14
Fig. 3. Electrical resistivity of tungsten reported in the literature.	15
Fig. 4. Hemispherical total emittance of tungsten reported in the literature	16
Fig. 5. Normal spectral emittance of tungsten at $\lambda = 650$ nm reported in the literature.	17
Table 5. Electrical resistivity of tungsten at 293 K.	18
Table 6. Excess heat capacity Δc in equation (5) and estimated vacancy contribution to heat capacity of tungsten.	20

TABLE OF CONTENTS (Continued)

	<u>Page</u>
Fig. 6. Heat capacity of tungsten according to equation (6)	22
6. References	23
Chap. 2. <u>PRELIMINARY RESULTS ON THE MEASUREMENT OF MELTING POINT OF TUNGSTEN BY A PULSE HEATING METHOD</u> (by Ared Cezairliyan)	26
Abstract	26
1. Introduction	26
2. Results	27
3. Discussion	28
Table 1. Melting point of tungsten reported in the literature	29
4. References	31
Chap. 3. <u>HIGH-SPEED (SUBSECOND) MEASUREMENT OF HEAT CAPACITY, ELECTRICAL RESISTIVITY, AND THERMAL RADIATION PROPERTIES OF NIOBIUM IN THE RANGE 1500 TO 2700 K</u> (by Ared Cezairliyan)	33
Abstract	33
1. Introduction	34
2. Measurements	34
Fig. 1. Photomicrographs of the niobium specimen.	36
3. Experimental Results	37
Table 1. Impurities in niobium specimen.	38
Table 2. Heat capacity, electrical resis- tivity, hemispherical total emit- tance and normal spectral emittance of niobium.	39
3.1 Heat Capacity	40
3.2 Electrical Resistivity.	40
3.3 Hemispherical Total Emittance	41
3.4 Normal Spectral Emittance	41
4. Estimate of Errors	42
5. Discussion	42
Table 3. Niobium heat capacity difference (previous literature minus present- work values) in percent	44
Fig. 2. Heat capacity of niobium reported in the literature	45
Table 4. Niobium electrical resistivity dif- ference (previous literature minus present-work values) in percent	46

TABLE OF CONTENTS (Continued)

	<u>Page</u>
Fig. 3. Electrical resistivity of niobium reported in the literature	47
Fig. 4. Hemispherical total emittance of niobium reported in the literature.	48
Fig. 5. Normal spectral emittance of niobium at $\lambda = 650$ nm reported in the literature	49
Acknowledgement	51
Fig. 6. Heat capacity of niobium according to equation (6)	52
6. References.	53
Chap. 4. <u>DEPARTURE OF EMITTANCE-RESISTIVITY RELATION FROM THEORETICAL PREDICTIONS FOR REFRACTORY METALS AT HIGH TEMPERATURES</u> (by Ared Cezairliyan).	55
Fig. 1. Variation of the ratio of measured emittance to computed emittance as a function of temperature for niobium, molybdenum, tantalum, and tungsten	57
References.	58
Chap. 5. <u>THE RELATIVE ENTHALPY AND HEAT CAPACITY OF MOLYBDENUM METAL FROM 1170 TO 2100 K</u> (by Shigeru Ishihara and Thomas B. Douglas).	59
Abstract.	59
I. Introduction.	59
II. Samples	60
Qualitative Spectrochemical Analyses	60
Spark-Source Mass Spectrometry	61
Electronic Characterization.	61
Sample Annealing Prior to Enthalpy Measurements.	61
Table 1A. Qualitative spectrochemical analyses of the molybdenum samples, in weight %	62
Table 1B. Mass-spectrometric analyses of a representative specimen of Samples A and B.	63
III. Calorimetric Apparatus and Method	64
IV. Enthalpy Data and Empirical Equations for Relative Enthalpy and Heat Capacity of Molybdenum.	66
Table 2. Individual enthalpy measurements on molybdenum.	68
Table 3A. Heat capacity and enthalpy of molybdenum (in joules)	70

TABLE OF CONTENTS (Continued)

	<u>Page</u>
Table 3B. Heat capacity and enthalpy of molybdenum (in calories)	71
Table 3C. Corrections for molybdenum to convert to IPTS-48 and IPTS-68 scales	72
V. Comparison with Previous Investigators and Compilers	73
VI. Discussion of Errors	73
Table 4. Outline of reported measurements of the enthalpy or heat capacity of molybdenum metal above 1000 K.	74
Fig. 1. Comparison of molybdenum $H_T - H_{298.15}$ values of various investigators	75
Fig. 2. Comparison of molybdenum heat-capacity values of various investigators	76
Table 5. Percentage deviation of the values of enthalpy and heat capacity of molybdenum adopted by various compilers from those of the present work (Eq 1)	77
(1) Effects of Sample Impurities	78
(2) Effects of Temperature Errors	79
VII. Acknowledgements	80
VIII. References	81
 Chap. 6. <u>THE HEAT OF FORMATION OF $\text{MoF}_6(\ell)$ BY SOLUTION CALORIMETRY; ANALYSIS OF PRELIMINARY EXPERIMENTS</u> (by R. L. Nuttall, K. L. Churney, and M. V. Kilday)	84
Introduction	84
Reaction Scheme of Solution Experiments	86
Experimental Procedure	89
Analysis of Results	90
(A) Heat of Solution of $\text{NaF}(c)$	90
(B) Heat of Solution of $\text{MoO}_3(c)$	90
(C) Heat of Solution of $\text{MoF}_6(\ell)$	92
References	95
 Chap. 7. <u>PROVISIONAL RESULTS ON THE PREPARATION, MELTING, AND VAPORIZATION OF MoF_5</u> (by Ralph F. Krause, Jr.)	97
Abstract	97
Literature Survey	97
Table 1. Chemical analyses of some molybdenum fluorides	98
Table 2. Estimate of the change in enthalpy of Eqs 1 and 2, using the data of Cady and Hargreaves	100

TABLE OF CONTENTS (Continued)

	<u>Page</u>
Preparation.	101
Melting and Purity	103
Table 3. Observed melting data on samples of MoF ₅ and MoF ₆	104
Vaporization by Entrainment.	105
Table 4. Preliminary results of vaporizing a sample of MoF ₅ by entrainment.	106
References	108
 Chap. 8. <u>THE INFRARED SPECTRUM OF MATRIX ISOLATED NbF₅</u> (by Nicolo Acquista and Stanley Abramowitz)	110
Abstract	110
Introduction	111
Experimental	112
Experimental Results	113
Fig. 1. The gas phase infrared spectrum of NbF ₅	114
Fig. 2. The infrared spectrum of matrix iso- lated NbF ₅	115
Fig. 3. Infrared spectra of matrix isolated NbF ₅	116
Conclusion	117
Table I. Observed bands and vibrational assign- ment for NbF ₅	118
References	119
 Chap. 9. <u>SURVEY OF THE SYSTEMS Mo-C, Ta-C AND Nb-B WITH EMPHASIS ON COMPOUNDS SUITABLE FOR ENTHALPY MEASUREMENT BY DROP CALORIMETRY, INCLUDING A LITERATURE SURVEY OF ENTHALPY AND HEAT CAPACITY DATA ON SELECTED COMPOUNDS FROM THESE SYSTEMS</u> (by David A. Ditmars)	120
I. Introduction	120
II. Stable Phases Suitable for Calorimetric Measure- ment	120
A. Phase Diagrams -- General Features.	120
Fig. 1. Phase diagram of the system Mo-C (ref. [1]).	121
Fig. 2. Phase diagram of the system Ta-C (ref. [1])	122
Fig. 3. Phase diagram of the system Nb-B (ref. [1])	123

TABLE OF CONTENTS (Continued)

	<u>Page</u>
B. Methods of Synthesis and Sample Characterization	125
1. Synthesis	125
2. Sample Characterization	126
III. Literature	126
A. General References	126
Table 1. Reported investigations of enthalpy and heat capacity of solid Mo_2C , TaC , Ta_2C , NbB , and NbB_2	127
References	128
Chap. 10. <u>A HIGH-SPEED METHOD OF MEASURING THERMAL EXPANSION OF ELECTRICAL CONDUCTORS</u> (by Ared Cezairliyan)	130
Fig. 1. Optics of the high-speed thermal expansion measurement system	131
References	134
Chap. 11. <u>ROTATING OPTICAL ATTENUATOR FOR THE GENERATION OF SUB-SECOND DURATION SAWTOOTH SHAPE RADIANCE PULSES</u> (by Ared Cezairliyan)	135
Abstract	135
1. Introduction	136
2. Method and Apparatus	136
Fig. 1. Functional diagram of the optical system for the generation of sub-second duration sawtooth shape radiance pulses	137
Fig. 2. The attenuator disk and the diaphragm opening	139
3. Results	141
Fig. 3. Oscilloscope trace photographs of linear and quadratic pulses	142
Table 1. Summary of experimental parameters and results	143
4. Conclusion	144
5. References	145
Chap. 12. <u>OPTICAL METHODS OF MEASURING TRANSIENT HIGH TEMPERATURES</u> (by Ared Cezairliyan)	146
Abstract	146

Chapter 1

HIGH-SPEED (SUBSECOND) MEASUREMENT OF HEAT CAPACITY, ELECTRICAL RESISTIVITY, AND THERMAL RADIATION PROPERTIES OF TUNGSTEN IN THE RANGE 2000 TO 3600 K

A. Cezairliyan and J. L. McClure
National Bureau of Standards
Washington, D.C. 20234

Abstract

Measurements of heat capacity, electrical resistivity, hemispherical total and normal spectral emittances of tungsten above 2000 K by a pulse heating technique are described. Duration of an individual experiment, in which the specimen is heated from room temperature to near its melting point is less than one second. Temperature measurements are made with a photoelectric pyrometer. Experimental quantities are recorded with a digital data acquisition system, which has a full-scale signal resolution of one part in 8000. Time resolution of the entire system is 0.4 ms. Results on the above properties of tungsten in the range 2000 to 3600 K are reported and are compared with those in the literature. Estimated inaccuracy of measured properties in the above temperature range is: 2 to 3 percent for heat capacity, 1 percent for electrical resistivity, 3 percent for hemispherical total and normal spectral emittances.

1. Introduction

Tungsten has the highest melting point (above 3600 K) of any known metal. Because of the difficulties involved in performing accurate experiments by conventional techniques at temperatures above approximately 2500 K, a high-speed method was developed to measure heat capacity, electrical resistivity, hemispherical total emittance and normal spectral emittance of electrical conductors. In this paper, application of this technique to measurements on tungsten in the temperature range 2000 to 3600 K is described.

The method is based on rapid resistive self-heating of the specimen from room temperature to near its melting point. During the short experiment, which lasts less than one second, current flowing through the specimen, potential across the specimen and specimen temperature are measured. Temperature measurements are made with a high-speed photoelectric pyrometer [1]. Recordings of experimental quantities are made with a digital data acquisition system, which has a time resolution of 0.4 ms, and a full-scale signal resolution of one part in 8000. Details regarding the construction and operation of the measurement system, and other pertinent information, such as formulation of relations for properties etc., are given in earlier publications [2,3] in connection with measurements on molybdenum and tantalum.

2. Measurements

The measurements were made in the temperature interval 1900 to 3600 K. To optimize the operation of the pyrometer, this temperature interval was divided into four ranges: low, 1900 to 2200 K; medium, 2150 to 2500 K; high, 2450 to 2900 K; and very high, 2850 to 3600 K.

Two experiments were conducted in each range; and three additional experiments were conducted in each of the first three ranges in which the surface radiance of the specimen was measured. Before the start of the experiments, the specimen was annealed by subjecting it to approximately 30 heating pulses (up to 3200 K).

The duration of the current pulses in the experiments ranged from 410 to 630 ms depending on the desired final temperature. The average heating rate of the specimen was: 7100 K s^{-1} at 2000 K, 5600 K s^{-1} at 3000 K, and 3700 K s^{-1} at 3600 K. At these temperatures, radiative heat losses from the specimen amounted to approximately 3, 12, and 27 per cent of the input power, respectively. All of the experiments were conducted with the specimen in a vacuum environment of approximately 10^{-4} torr.

The data on voltage, current, and temperature were used to obtain third degree polynomial functions for each quantity in terms of time, which then provided the input information for the determination of properties.

The pyrometer was calibrated before and after the entire set of experiments against a tungsten-filament standard lamp, which in turn was calibrated against the NBS temperature standard. The digital recording system, including the differential amplifiers, was also calibrated before and after the entire set of experiments. The details of the calibration procedures are given in an earlier publication [2].



0.1 mm

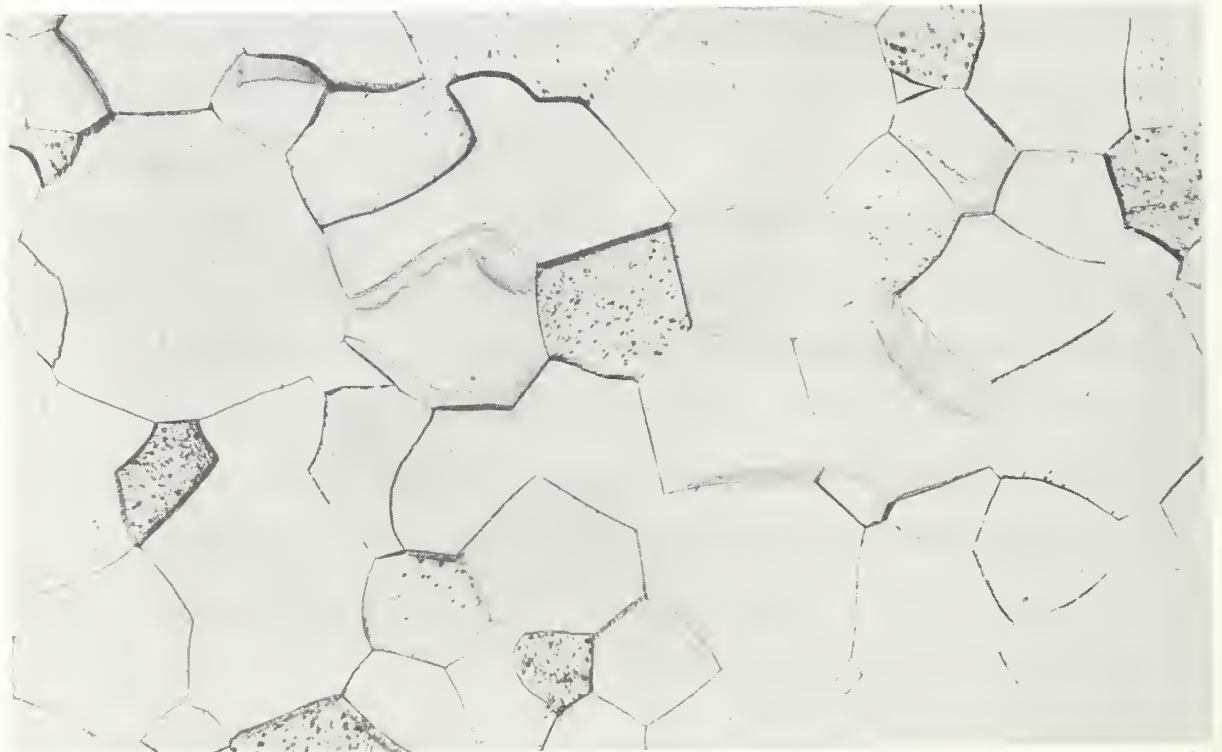


FIGURE 1. Photomicrographs of the tungsten specimen before (upper photograph) and after (lower photograph) the entire set of experiments.

The specimen was a tube fabricated from a tungsten rod by removing the center portion by an electro-erosion technique. The outer surface of the specimen was polished to reduce heat loss due to thermal radiation. The nominal dimensions of the specimen were: length, 4 in. (101 mm); outside diameter, 0.25 in. (6.3 mm); and wall thickness, 0.02 in. (0.5 mm).

Specimen characterization was made by the following methods: photomicrography, spectrochemical analysis, and residual resistivity ratio. Photomicrographs of the specimen (figure 1) indicate that considerable grain growth took place as the result of pulse heating to high temperatures. A list of the nature and composition of impurities in the specimen, at the end of the entire set of experiments as determined by spectrochemical analysis¹, is given in table 1. The residual resistivity ratio of the specimen (ratio of electrical resistivity at 273 K to that at 4 K), measured before the experiments, was 41.

The "effective" mass of the specimen was calculated from the total mass by the ratio of the geometric surface area between voltage probes to total surface area. Length measurements at room temperature were made with a micrometer microscope. The cross-sectional area of the specimen was calculated from the mass, density, and geometry. Density of the tungsten specimen was measured at 293 K to be $19.23 \times 10^3 \text{ kg m}^{-3}$. This compares favorably with a previously cited value of $19.3 \times 10^3 \text{ kg m}^{-3}$ [4].

¹Spectrochemical analysis of the tungsten specimen was made by the Lamp Metals and Components Department of the General Electric Company.

TABLE 1

Impurities in Tungsten Specimen

Impurity	Composition, ppm (by weight)
Al	5
B	<2
Ca	15
Cr	5
Co	<2
Cu	10
Fe	60
Mg	<2
Mn	<2
Mo	310
Nb	<20
Ni	<2
Pb	<2
Si	5
Sn	<2
Sr	<2
Th	<250
Ti	10
Zr	30

450 < Total < 740

3. Experimental Results

This section presents the results on the thermophysical properties determined from the measured quantities. All values are based on the 1968 International Practical Temperature Scale [5]. In all computations, the geometrical quantities are based on their room temperature (298 K) dimensions. The experimental results are represented by polynomial functions in temperature which were obtained by least squares approximation of the individual points. The final values on properties at 100 degree temperature intervals computed using the functions are presented in table 2.

3. 1. Heat Capacity

Heat capacity was computed from data taken during the heating period. A correction for power loss due to thermal radiation was made using the results on hemispherical total emittance. The function for heat capacity (standard deviation = 0.7 percent) that is valid in the temperature range 2000 to 3600 K is:

$$c_p = -25.71 + 6.331 \times 10^{-2} T - 2.459 \times 10^{-5} T^2 + 3.638 \times 10^{-9} T^3 \quad (1)$$

where T is in K and c_p in $J \text{ mol}^{-1} \text{ K}^{-1}$. In the computations of the heat capacity, the atomic weight of tungsten was taken as 183.85.

To determine the effect of thermal cycling on heat capacity the results of four additional experiments covering the range 2000 to 3300 K were compared with those reported above. The average difference between the two sets of results was less than 0.1 percent which is smaller than the measurement resolution. This indicates that the measurements were not sensitive to thermal cycling.

TABLE 2

Heat capacity, electrical resistivity, hemispherical total and normal spectral emittances of tungsten.

Temp. K	c_p J mol ⁻¹ K ⁻¹	ρ^a 10 ⁻⁸ Ω m	ϵ^a	$\epsilon_{N,\lambda}$
2000	31.65	56.22	0.318 ^b	0.379
2100	32.49	59.74	.321 ^b	.379
2200	33.29	63.25	.324 ^b	.379
2300	34.08	66.77	.326	.379
2400	34.89	70.28	.329	.379
2500	35.72	73.80	.332	.379
2600	36.61	77.31	.335	.379
2700	37.57	80.83	.338	.379
2800	38.63	84.34	.340	.379
2900	39.81	87.86	.343	.379
3000	41.14	91.37	.346	.379
3100	42.62	94.89	.349	
3200	44.29	98.40	.351	
3300	46.17	101.92	.354	
3400	48.27	105.43	.357	
3500	50.63	108.95		
3600	53.25	112.46		

^aBased on ambient temperature (298 K) dimensions.

^bExtrapolated from higher temperature results.

3. 2. Electrical Resistivity

The electrical resistivity of tungsten was determined from the same experiments that were used to calculate the heat capacity. The function for electrical resistivity (standard deviation = 0.4 percent) that is valid in the temperature range 2000 to 3600 K is:

$$\rho = -14.08 + 3.515 \times 10^{-2} T \quad (2)$$

where T is in K and ρ in $10^{-8} \Omega\text{m}$. The results of thermal cycling indicates an average difference of less than 0.5 percent in electrical resistivity.

3.3. Hemispherical Total Emittance

Hemispherical total emittance was computed using data taken during both heating and initial free cooling periods in the experiments. The function for hemispherical total emittance (standard deviation = 1 percent) that is valid in the temperature range 2300 to 3400 K is:

$$\epsilon = 0.2627 + 2.770 \times 10^{-5} T \quad (3)$$

where T is in K.

3.4. Normal Spectral Emittance

Normal spectral emittance was computed using data from three sets of two experiments, one in which the pyrometer was aimed at the surface of the specimen, and another in which it was aimed at the blackbody hole in the specimen. The target on the surface was a narrow flat ground along the specimen. The measurements were made at the effective wavelength of the pyrometer interference filter (650 nm; bandwidth 10 nm). The function for normal spectral emittance (standard deviation = 0.2 percent) that is valid in the temperature range 2000 to

3000 K is:

$$\epsilon_{n,\lambda} = 0.3804 - 5.060 \times 10^{-7} T \quad (4)$$

where T is in K.

4. Estimate of Errors

Estimates of errors in measured and computed quantities lead to the following estimates of errors in the properties over the temperature range 2000 to 3600 K.

Heat capacity: 2 percent at 2000 K, 3 percent at 3600 K.

Electrical resistivity: 1 percent

Hemispherical total emittance: 3 percent

Normal spectral emittance: 3 percent

Details regarding the estimates of errors and their combination in high-speed experiments using the present measurement system are given in a previous publication [2]. Specific items in the error analysis were recomputed whenever the present conditions differed from those in the earlier publication.

5. Discussion

The heat capacity and electrical resistivity results of this work are compared graphically with those in the literature in figures 2 and 3, respectively. Numerical comparisons are given in tables 3 and 4. It may be seen that present results agree favorably with most others at 2000 K. Considerable disagreement in heat capacity exists above 2500 K. This may be expected, since above this temperature ^{accuracy} of heat capacity measured by conventional methods decreases rapidly.

Estimates of errors in papers cited lead to an estimate of inaccuracies in previously reported heat capacity and electrical resistivity of approximately 5 to 15 and 1 to 5 percent, respectively, in the temperature range considered. Measurements of the electrical resistivity of tungsten corresponding to 293 K, as well as values reported in the literature, are given in table 5.

The results for hemispherical total and normal spectral emittances of this work and those in the literature are presented in figures 4 and 5, respectively. Because of the strong dependence of emittance on surface conditions, considerable deviations exist in the results of various investigators.

Heat capacity results at high temperatures are considerably higher than the Dulong and Petit value of $3R$. Some of this departure is due to $c_p - c_v$ and the electronic terms. However, they do not account for the entire departure. Heat capacity above the Debye temperature may be expressed by

$$c_p = A - \frac{B}{T^2} + CT + \Delta c \quad (5)$$

where the constant term is $3R$ ($24.943 \text{ J mol}^{-1} \text{ K}^{-1}$), the term in T^{-2} is the first term in the expansion of the Debye function, the term in T represents $c_p - c_v$ and electronic contributions, and the quantity Δc represents excess in measured heat capacity at high temperatures, which is not accounted for by the first three terms. The coefficients $B(7.72 \times 10^4)$ and $C(2.33 \times 10^{-3})$ were obtained from data on heat capacity at room and moderate temperatures (at 298.15 and 1000 K) given by Hultgren et al. [6].

TABLE 3

Tungsten heat capacity difference (previous literature values
minus present work values) in percent

Investigator	Ref.	Year	Method	Temperature, K										
				2000	2200	2400	2600	2800	3000	3200	3400	3600		
Worthing	10	1918	pulse	+1.6	+0.3	-0.7								
Jaeger and Rosenbohm	11	1930	drop	-3.2 ^a										
Hoch and Johnston	12	1961	drop	-4.7	-7.3	-9.7	-12	-15						
Kirillin et al.	13	1963	drop	+1.6	-0.4	-2.1	-4.0	-6.7	-9.7					
Kraftmakher and Strelkov	14	1963	modul.	-1.4	-2.4	-3.6	-4.0	-3.2	-0.8	+3.4	+9.5	+17		
Lowenthal	15	1963	modul.	-1.5	-2.3	-2.4								
Hein and Flagella	16	1968	drop	- .03	-0.7	-0.6	-0.2	-0.1	-0.7	-2.4				
Leibowitz et al.	17	1968	drop					-1.8	-4.1	-7.5	-12	-17		
West and Ishihara	18		drop	+1.0	+0.4	+0.8	+1.9							

^a Extrapolated from 1873 K

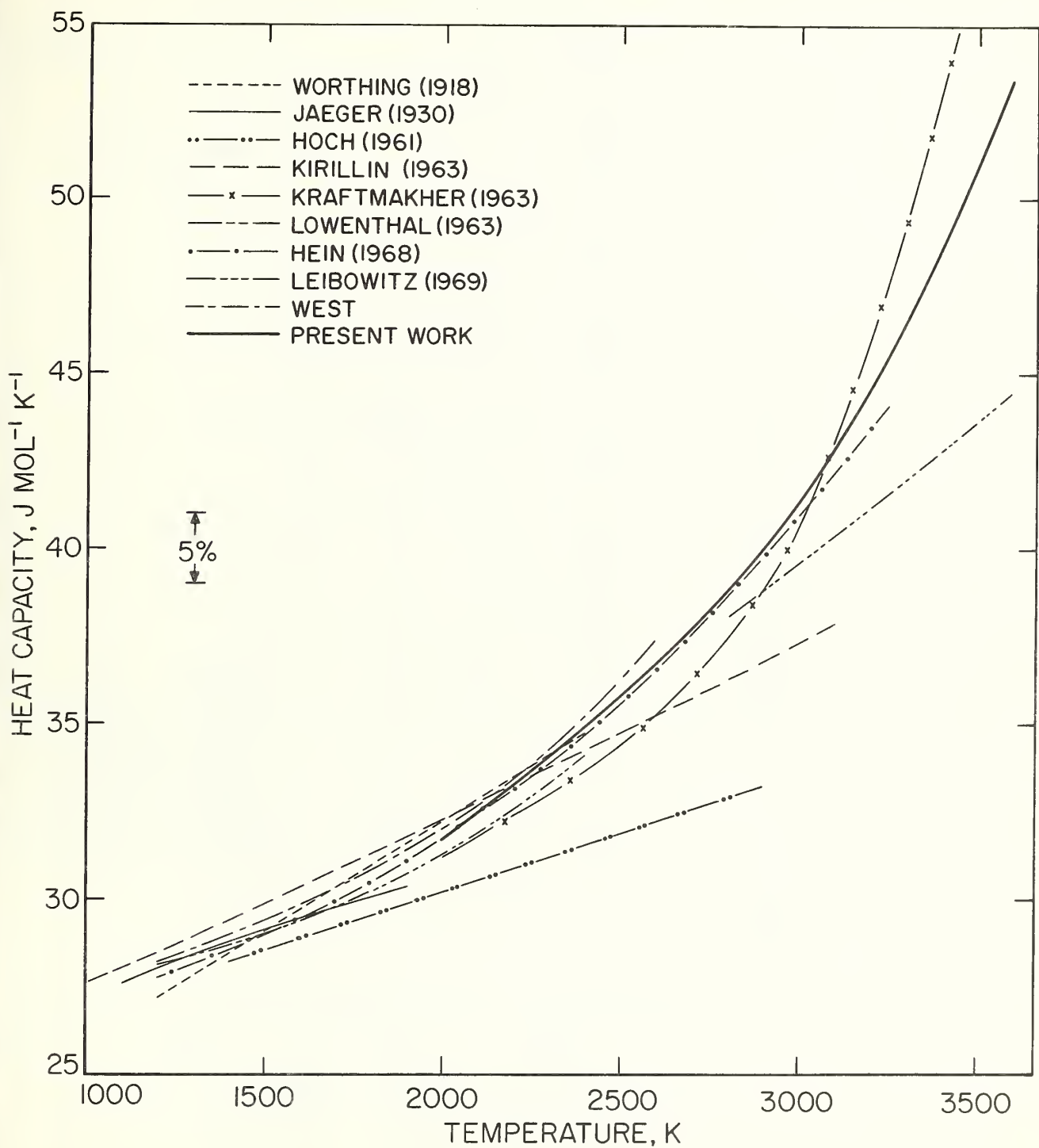


FIGURE 2. Heat capacity of tungsten reported in the literature.

TABLE 4

Tungsten electrical resistivity difference (previous literature values minus present work) in percent

Investigator	Ref.	Year	Temperature, K									
			2000	2200	2400	2600	2800	3000	3200	3400	3600	
Forsythe and Worthing	19	1925	+5.1	+4.7	+4.6	+4.8	+4.9	+5.2	+5.5	+5.9		
Jones	20	1926	+0.8	+0.2	+0.1	+0.1	+0.4	+0.7	+1.2	+1.7	+2.2	
Forsythe and Watson	32	1934	-0.9	-1.3	-1.5	-1.4	-1.3	-1.1				
Osborn	21	1941	-0.4	-0.6								
Platunov and Fedorov	22	1964	+1.1	+1.2	+1.9	+2.2	+2.4	+2.5	+2.5			
Neimark and Voronin	23	1967	+1.2	+0.7	+0.5							

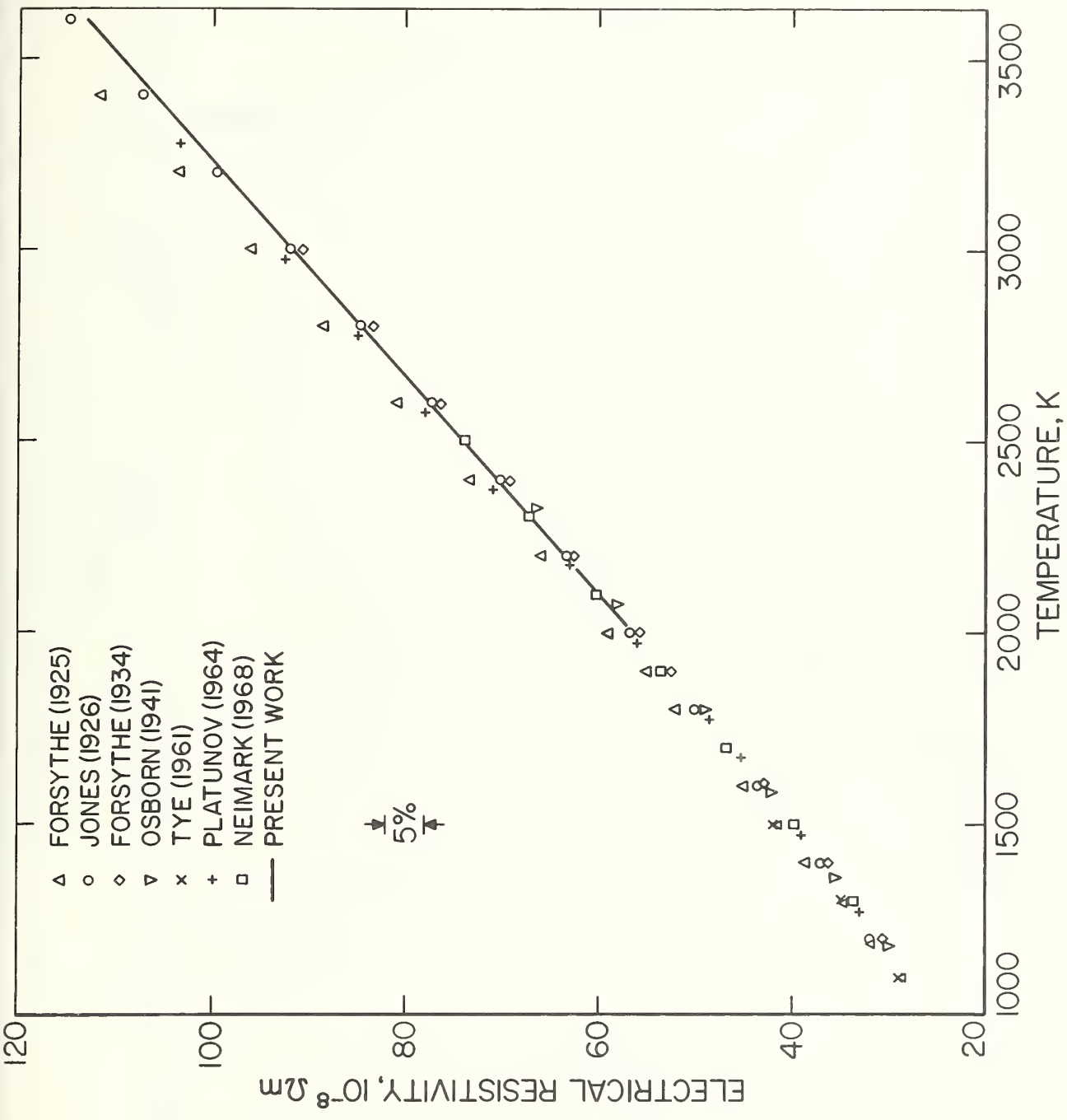


FIGURE 3. Electrical resistivity of tungsten reported in the literature.

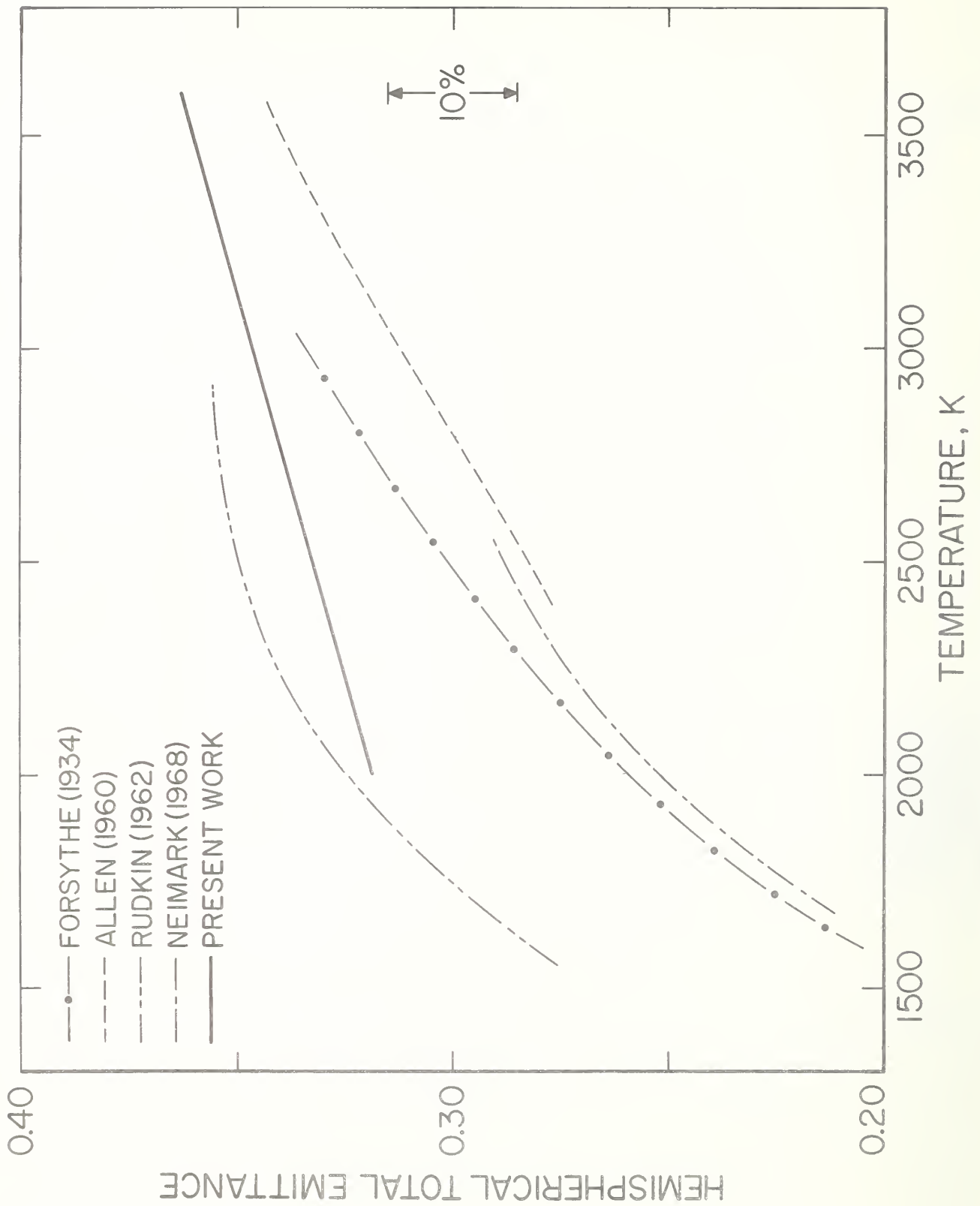


FIGURE 4. Hemispherical total emittance of tungsten reported in the literature.

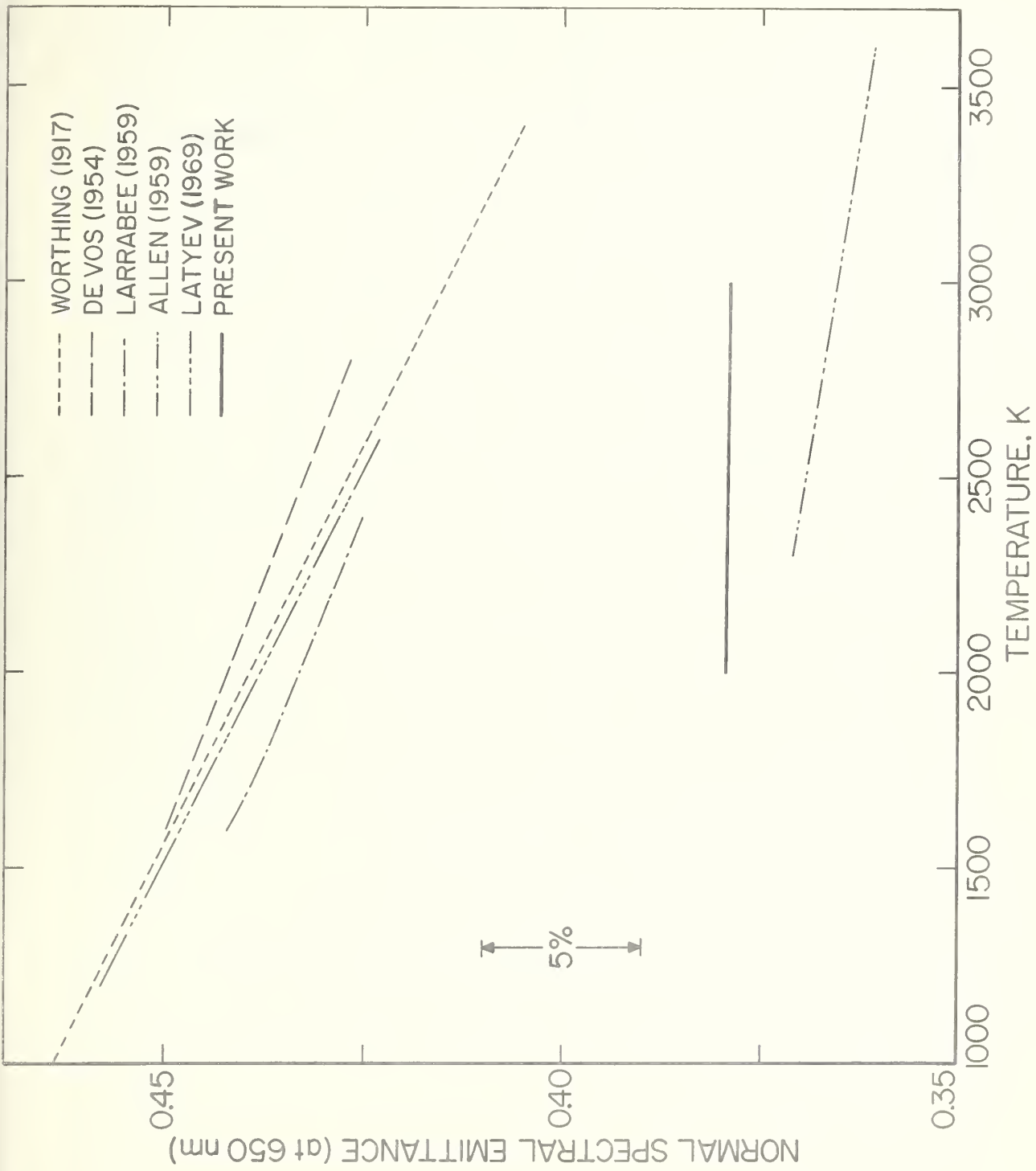


FIGURE 5. Normal spectral emittance of tungsten at $\lambda = 650$ nm reported in the literature.

TABLE 5

Electrical Resistivity of Tungsten at 293 K.

Investigator	Ref.	Year	Resistivity $10^{-8} \Omega\text{m}$
Forsythe and Worthing	19	1925	5.46
Jones	20	1926	5.49
Forsythe and Watson	32	1934	5.50
White and Woods	31	1959	5.29 ^a
Tye	24	1961	5.45
Present Work			5.45

^aideal resistivity.

Using eq (5) and the heat capacity results of this work, the quantity Δc was computed for temperatures above 2000 K. The results are tabulated in table 6. The estimated uncertainty in the computed Δc may be as high as $1 \text{ J mol}^{-1} \text{ K}^{-1}$. This was obtained from the combined uncertainties in the coefficients in eq (5) and the measured heat capacities.

Although the mechanisms of vacancy generation become important at high temperatures, it was not possible to attribute the high values entirely to vacancies. To demonstrate this, a crude estimate of the contribution of vacancies to heat capacity was made using the method described in a previous publication [2]. The reported values for vacancy formation energy of tungsten are 3.3 eV [7] and 3.6 eV [8]. Results of quenching experiments on various refractory elements [7,9] have indicated that vacancy concentrations are probably in the range 0.01 to 0.1 percent at their melting points. Estimates corresponding to a vacancy concentration of 0.1 percent at the melting point and a vacancy formation energy of 3.3 eV are given in table 6. The results indicate that vacancy contribution is small, less than $0.8 \text{ J mol}^{-1} \text{ K}^{-1}$ (upper limit) at 3600 K, and does not account for high heat capacity values.

If the entire difference between measured and computed [using eq (5)] heat capacities is attributed to vacancies, a value of 1.3 eV for energy and 12 percent for concentration at the melting point are obtained. Both of these values seem to be unrealistic for tungsten.

TABLE 6

Excess heat capacity Δc in equation (5) and estimated vacancy contribution to heat capacity of tungsten.

T K	Δc J mol ⁻¹ K ⁻¹	c_{vac} J mol ⁻¹ K ⁻¹
2000	2.07	0.0005
2200	3.24	0.002
2400	4.37	0.009
2600	5.62	0.03
2800	7.18	0.06
3000	9.21	0.14
3200	11.90	0.26
3400	15.41	0.47
3600	19.93	0.79

To give a simple expression for the heat capacity of tungsten over a wide temperature range, an empirical term in T^4 for the quantity Δc in eq (5) was substituted. The coefficient of this term was obtained from the results of the present work in conjunction with the values given by Hultgren et al. [6] at temperatures below 1000 K. Then, eq (5) for the range 300 to 3600 K becomes

$$c_p = 24.943 - \frac{7.72 \times 10^4}{T^2} + 2.33 \times 10^{-3} T + 1.18 \times 10^{-13} T^4 \quad (6)$$

where T is in K and c_p in $J \text{ mol}^{-1} \text{ K}^{-1}$. Average deviation of the individual points from the function over the temperature range considered is 0.2 percent. Equation (6) is presented graphically in figure 6.

The experimental results reported in this paper have further substantiated the feasibility of accurate simultaneous measurement of selected properties above 2000 K by a millisecond ^{resolution} pulse method. The technique is particularly attractive at high temperatures where conventional methods fail to give accurate results.

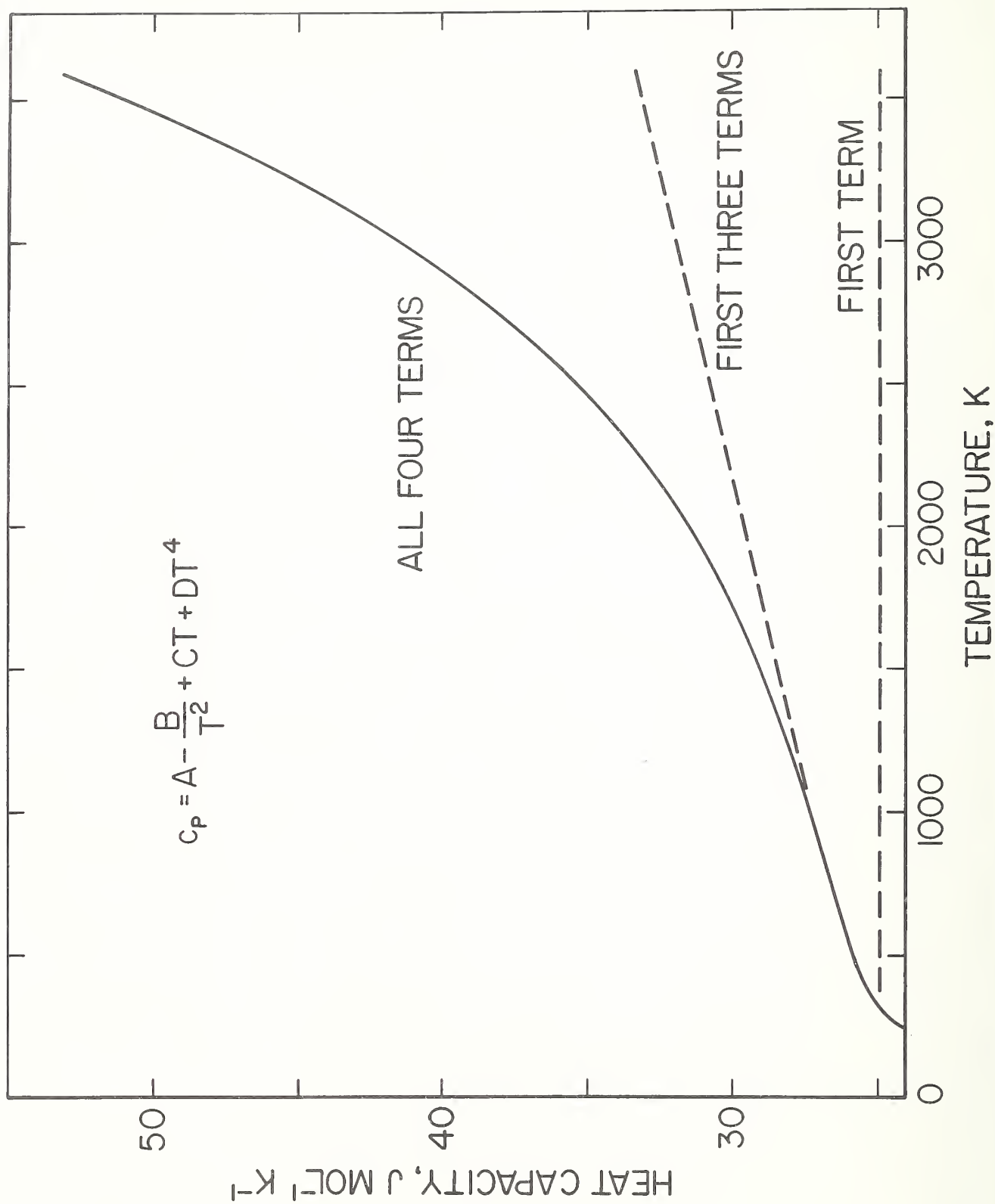


FIGURE 6. Heat capacity of tungsten according to equation (6).

6. References

- [1] Foley, G. M., High-speed optical pyrometer, Rev. Sci. Instr. 41, 827 (1970).
- [2] Cezairliyan, A., M. S. Morse, H. A. Berman, and C. W. Beckett, High-speed (subsecond) measurement of heat capacity, electrical resistivity, and thermal radiation properties of molybdenum in the range 1900 to 2800 K, J. Res. Nat. Bur. Stand. (U.S.) 74A (Phys. and Chem.), 65 (1970).
- [3] Cezairliyan, A., J. L. McClure, and C. W. Beckett, High-speed (subsecond) measurement of heat capacity, electrical resistivity, and thermal radiation properties of tantalum in the range 1900 to 3200 K, J. Res. Nat. Bur. Stand. (U.S.), to be published.
- [4] Tietz, T. E. and J. W. Wilson, Behavior and properties of refractory metals, Stanford University Press, California (1965), p. 28.
- [5] International Practical Temperature Scale of 1968, Metrologia 5, 35 (1969).
- [6] Hultgren, R., R. L. Orr, P. D. Anderson, and K. K. Kelly, Selected Values of Thermodynamic Properties of Metals and Alloys, John Wiley, New York (1963).
- [7] Schultz, H., "Quenching of vacancies in tungsten," in Lattice Defects in Quenched Metals, R. M. J. Cotterill, M. Doyama, J. J. Jackson and M. Meshi, eds., Academic Press, New York (1965), p. 761.
- [8] Gripshover, R. J., M. Khoshnevisan, J. S. Zetts, and J. Bass, A study of vacancies in tungsten wires quenched in superfluid helium, Phil. Mag. 22, 757 (1970).
- [9] Meakin, J. D., A. Lawley, and R. C. Koo, "Vacancy loops in quenched molybdenum," in Lattice Defects in Quenched Metals, R. M. J. Cotterill, M. Doyama, J. J. Jackson, and M. Meshi, eds., Academic Press, New York (1965), p. 767.
- [10] Worthing, A. G., Atomic heats of tungsten and of carbon at incandescent temperatures, Phys. Rev. 12, 199 (1918).
- [11] Jaeger, F. M. and E. Rosenbohm, Exact measurement of specific heat of solid substances at high temperatures, III: Pd and W, Proc. K. Ak. V. Wetensch. 33, 457 (1930).

- [12] Hoch, M. and H. L. Johnston, A high-temperature drop calorimeter, the heat capacities of tantalum and tungsten between 1000 and 3000 K, J. Chem. Phys. 65, 855 (1961).
- [13] Kirillin, V. A., A. E. Sheindlin, V. Ya. Chekhovskoi, and V. A. Petrov, Thermodynamic properties of tungsten, Russ. J. Phys. Chem. 37, 1212 (1963).
- [14] Kraftmakher, Ya. A. and P. G. Strelkov, Energy of formation of and concentration of vacancies in tungsten, Solid State Physics(USSR) 4, 1662 (1963).
- [15] Lowenthal, G. C., The specific heat of metals between 1200 K and 2400 K, Australian J. Phys. 16, 47 (1963).
- [16] Hein, R. A. and P. N. Flagella, Enthalpy measurements of UO_2 and tungsten to 3260 K, General Electric Report GEMP-578, 1968.
- [17] Leibowitz, L., M. G. Chasanov and L. W. Mishler, The enthalpy of solid tungsten from 2800 K to its melting point, Trans. Met. Soc. AIME 245, 981 (1969).
- [18] West, E. D. and S. Ishihara, Enthalpy of tungsten, Private communication.
- [19] Forsythe, W. E. and A. G. Worthing, The properties of tungsten and the characteristics of tungsten lamps, Astrophys. J. 61, 146 (1925).
- [20] Jones, H. A., A temperature scale for tungsten, Phys. Rev. 28, 202 (1926).
- [21] Osborn, R. H., Thermal conductivities of tungsten and molybdenum at incandescent temperatures, J. Opt. Soc. Am. 31, 428 (1941).
- [22] Platunov, E. S. and V. B. Fedorov, Use of photographic pyrometry in thermal studies, High Temp. 2, 568 (1964).
- [23] Neimark, B. E. and L. K. Voronin, Thermal conductivity, specific electrical resistivity, and total emissivity of refractory metals at high temperatures, High Temperature 6, 999 (1968).
- [24] Tye, R. P., Preliminary measurements on the thermal and electrical conductivities of molybdenum, niobium, tantalum, and tungsten, J. Less-Common Metals 3, 13 (1961).
- [25] Allen, R. D., L. F. Glasier, and P. L. Jordan, Spectral emissivity, total emissivity, and thermal conductivity of molybdenum, tantalum, and tungsten above 2300 K, J. Appl. Phys. 31, 1382 (1960).

- [26] Rudkin, R. L., W. J. Parker, and R. J. Jenkins, "Measurement of the thermal properties of metals at elevated temperatures," in Temperature Its Measurement and Control in Science and Industry, C. M. Herzfeld, ed., Vol. III, part 2, p. 523, Reinhold, New York, (1962).
- [27] Worthing, A. G., The true temperature scale of tungsten and its emissive power at incandescant temperatures, Phys. Rev. 10, 377 (1917).
- [28] DeVos, J. C., A new determination of the emissivity of tungsten ribbon, Physica 20, 690 (1954).
- [29] Larrabee, R. D., Spectral emissivity of tungsten, J. Opt. Soc. Am. 49, 619 (1959).
- [30] Latyev, L. N., V. Ya. Chekhovskoi, and E. N. Shestakov, Experimental determination of emissive power of tungsten in the visible region of the spectrum in the temperature range 1200 to 2600 K, High Temperature 7, 610 (1969).
- [31] White, G. K. and S. B. Woods, Electrical and thermal resistivity of the transition elements at low temperatures, Phil. Trans. Royal Soc. (London) 251, 273 (1959).
- [32] Forsythe, W. E. and E. M. Watson, Resistance and radiation of tungsten as a function of temperature, J. Opt. Soc. Am. 24, 114 (1934).

Chapter 2

PRELIMINARY RESULTS ON THE MEASUREMENT OF MELTING POINT OF TUNGSTEN BY A PULSE HEATING METHOD

Ared Cezairliyan
National Bureau of Standards
Washington, D. C. 20234

Abstract

A subsecond duration pulse heating method is used to measure the melting point of tungsten. Preliminary work yields a value of 3692 K, with an estimated inaccuracy of 15 K.

1. Introduction

Serious difficulties are encountered in the measurement of melting point of substances at temperatures above 2500 K by conventional methods. Most of the problems inherent in these methods are eliminated by using high-speed measurement techniques. Application of a high-speed (pulse heating) technique to the accurate measurement of the melting point of molybdenum is described in the literature [1].

In the present study, the same pulse heating technique is used for the measurement of the melting point of tungsten. The specimen, which is in tubular form, was heated in vacuum from room temperature to its melting point in 0.7 s by a single heavy-current pulse. During

the pulse period, specimen temperature was measured with a high-speed photoelectric pyrometer [2], which permits 1200 temperature evaluations per second. The pyrometer's target was a small hole fabricated in the wall at the middle of the specimen to approximate blackbody conditions. The recordings of temperature were made with a high-speed digital data acquisition system [3], which is capable of recording data with a full-scale signal resolution of approximately one part in 8000 and a time resolution of 0.4 ms. Details regarding the construction and operational characteristics of the entire measurement system are given elsewhere [3, 4].

2. Results

The tungsten specimen was a tube of the following nominal dimensions: length, 4 in. (102 mm); outside diameter, 0.25 in. (6.3 mm); thickness, 0.02 in. (0.5 mm). The outer surface of the specimen was polished to reduce heat loss due to thermal radiation. The specimen was 99.9⁺ percent pure. Spectrochemical analysis indicated the presence of the following impurities in ppm by weight: Mo, 310; Th, <250; Fe, 60; Zr, 30; Ca and Nb, <20 each; Cu and Ti, 10 each; Al, Cr and Si, 5 each; B, Co, Mg, Mn, Ni, Pb, Sn, Sr, <2 each. All measurements reported in this paper, unless stated otherwise, are based on the International Practical Temperature Scale of 1968 (ITS-1968) [5].

Specimen temperature near and during the initial melting period was measured. The plateau in temperature indicates the region of solid and liquid equilibria. By averaging temperature points on the plateau, a value of 3692 K was obtained for the melting point of tungsten with a standard deviation (individual point) of 1.3 K.

Sources and estimates of errors in experiments similar to the one conducted in this study are given in detail in other publications [1, 3]. Estimated inaccuracy in the melting point is 15 K.

3. Discussion

As may be seen in Table 1, considerable differences exist in the tungsten melting points reported in the literature. In order to have a common ground for comparisons, all reported values were converted to IPTS-1968. It is interesting to note that, in general, the reported values increase chronologically. The measurements were performed either before 1930 or after 1960. The melting points reported prior to 1915, as was summarized by Langmuir [6], were lower than that of Langmuir by as much as 50 to 500 K. Experimental difficulties, including pyrometry problems, encountered in high temperature quasi steady-state measurements might have been responsible for the large discrepancies. Another source of the discrepancies could have been the differences in the purity of the various tungsten specimens.

Probably, the most reliable measurement performed on the melting point of tungsten before 1930 was that of Worthing [8] which is 22 K below the present value; however, this difference is within the combined uncertainties of the two results. The average value of the melting points reported by three investigators [11, 15, 16] since 1960 is 3693 K; average and maximum differences from this value being 7 K and 10 K, respectively. The melting point obtained in this study is 1 K lower than the above average.

TABLE 1

Melting Point of Tungsten Reported in the Literature

Investigator	Ref.	Year	T _{Au} (K)	c ₂ (cm K)	Melting Point, K	
					as reported	on IPTS-1968
Langmuir	6	1915	1335	1.439	3540 ± 30	3559
Luckey	7	1917			3623	
Worthing	8	1917	1336	1.435	3675 ± 15	3670
Henning and Heuse	14	1923	1336	1.430	3643	3616
Pirani	9	1923	1336	1.430	3660 ± 60	3633
Forsythe and Worthing	10	1925	1336	1.433	3655	3641
Zalabak	15	1961	1336.15	1.438	3680	3687
Allen	11	1962	1336.15	1.438	3682 ± 20	3689
Rudy and Harmon	16	1966	1336.15	1.438	3696	3703
IPTS-1968*	5	1968	1337.58	1.4388	3660	3660
Present Work			1337.58	1.4388	3692 ± 15	3692

* Recommended as secondary reference point on IPTS-1968.

The presence of impurities in a specimen alters (in general, reduces) the melting point of the element. Based on the Raoult-Van't Hoff equation, the melting point depression for the tungsten specimen (with total amount of impurities less than 0.1 percent) is estimated to be less than 3 K. Also, under the present operating conditions, it is very unlikely that the effect of superheating, if present at all, is more than a fraction of a degree.

4. References

- [1] Cezairliyan, A., M. S. Morse, and C. W. Beckett. Measurement of melting point and electrical resistivity (above 2840 K) of molybdenum by a pulse heating method. *Rev. Int. Hautes Temper. et Refract.* 7, 382 (1970).
- [2] Foley, G. M. High-speed optical pyrometer. *Rev. Sci. Instr.* 41, 827 (1970).
- [3] Cezairliyan, A., M. S. Morse, H. A. Berman, and C. W. Beckett. High-speed (subsecond) measurement of heat capacity, electrical resistivity, and thermal radiation properties of molybdenum in the range 1900 to 2800 K. *J. Res. Nat. Bur. Stand. (U.S.)* 74A (Phys. and Chem.), 65 (1970).
- [4] Cezairliyan, A. Design and operational characteristics of a high-speed (millisecond) system for the measurement of thermophysical properties at high temperatures. *J. Res. Nat. Bur. Stand. (U.S.)* 75C (Eng. and Instr.), 7 (1971).
- [5] International Practical Temperature Scale of 1968. *Metrologia* 5, 35 (1969).
- [6] Langmuir, I. The melting point of tungsten. *Phys. Rev.* 6, 138 (1915).
- [7] Luckey, G. P. The tungsten arc under pressure. *Phys. Rev.* 9, 129 (1917).
- [8] Worthing, A. G. The true temperature scale of tungsten and its emissive powers at incandescent temperatures. *Phys. Rev.* 10, 377 (1917).

- [9] Pirani, M. and H. Alterthum. A method of measuring the melting points of metals having high melting points. *Zeitschrift Electrochemie* 29, 5 (1923).
- [10] Forsythe, W. E. and A. G. Worthing. The properties of tungsten and the characteristics of tungsten lamps. *Astrophys. J.* 61, 146 (1925).
- [11] Allen, R. D. Techniques for melting point determination on an electrically heated refractory metal. *Nature* 193, 769 (1962).
- [12] Jones, H. A. A temperature scale for tungsten. *Phys. Rev.* 28, 202 (1926).
- [13] Ubbelohde, A. R. *Melting and crystal structure* (Clarendon Press, Oxford, 1965).
- [14] Henning, F. and W. Heuse. Melting points of platinum and tungsten. *Zeit. Physik* 16, 63 (1923).
- [15] Zalabak, C. R. NASA Tech. Note, TND-761, 1961.
- [16] Rudy, E. and D. P. Harmon. AFML-TR-65-2, Part I, Vol. VI, Air Force Materials Laboratory Research and Technology Division, Dayton, Ohio, (1966).

Chapter 3

HIGH-SPEED (SUBSECOND) MEASUREMENT OF HEAT CAPACITY, ELECTRICAL RESISTIVITY, AND THERMAL RADIATION PROPERTIES OF NIOBIUM IN THE RANGE 1500 TO 2700 K

Ared Cezairliyan
National Bureau of Standards
Washington, D. C. 20234

Measurements of heat capacity, electrical resistivity, hemispherical total emittance, and normal spectra emittance of niobium in the temperature range 1500 to 2700 K by a subsecond duration pulse heating technique are described. Results on the above properties are reported and are compared with those in the literature. A sharp increase in heat capacity above 2000 K was observed. Electrical resistivity showed a negative departure from linearity in the curve of electrical resistivity against temperature. Estimated inaccuracy of measured properties is: 2 percent for heat capacity, 0.5 percent for electrical resistivity, and 3 percent for hemispherical total and normal spectral emittances.

1. Introduction

Because of the difficulties involved in performing accurate experiments at high temperatures by conventional techniques, a high-speed method was developed to measure heat capacity, electrical resistivity, hemispherical total emittance, and normal spectral emittance of electrical conductors. In this paper, application of this technique to measurements on niobium in the temperature range 1500 to 2700 K is described.

The method is based on rapid resistive self-heating of the specimen from room temperature to near its melting point. During the short experiment, which lasts less than one second, current flowing through the specimen, potential across the specimen and specimen temperature are measured. The experimental quantities are recorded with a digital recording system, which has a time resolution of 0.4 ms, and a full-scale signal resolution of one part in 8000. Details regarding the construction and operation of the measurement system, the methods of measuring experimental quantities, and other pertinent information, such as formulation of relations for properties, etc. are given in earlier publications [1, 2]¹.

2. Measurements

Measurements were made on two specimens designated as niobium-1 and niobium-2. Each specimen was a tube of the following nominal dimensions; length, 4 in. (101 mm); outside diameter, 0.25 in. (6.3 mm); and wall thickness, 0.02 in. (0.5 mm), ^{A hole} fabricated in the wall at the middle of the specimen approximated blackbody conditions for the high-speed photoelectric pyrometer [3].

¹Figures in brackets indicate the literature references at the end of this paper.

The measurements were made in the temperature interval 1500 to 2700 K. To optimize the operation of the pyrometer, this temperature interval was divided into six ranges: I, 1500 to 1650 K; II, 1600 to 1800 K; III, 1750 to 1950 K; IV, 1900 to 2200 K; V, 2100 to 2550 K; VI, 2400 to 2700 K.

In each of the first five temperature ranges, two experiments were conducted on niobium-1 and one on niobium-2; in the last range, one experiment was conducted on each specimen. A total of three additional experiments in the ranges II, III, and IV were performed on niobium-1 in which the surface radiance of the specimen was measured.

Before the start of the experiments, each specimen was annealed by subjecting it to 30 heating pulses (up to 2400 K). All the experiments were conducted with the specimens in a vacuum environment of approximately 10^{-4} torr.

To optimize the operation of the measurement system, heating rate of the specimens was varied depending on the desired temperature range by adjusting the value of the resistance in series with the specimen. Duration of the current pulses in the experiments ranged from 390 to 450 ms; and the average heating rate of the specimens was approximately 5200 K s^{-1} . Radiative heat losses from the specimens amounted to approximately 1 percent at 1500 K, 3 percent at 2000 K, and 10 percent at 2700 K of the input power.

Characterization of one of the specimens (niobium-1) was made by the following methods: photomicrography, spectrochemical analysis, and residual resistivity ratio. Photomicrographs of the specimen, shown in

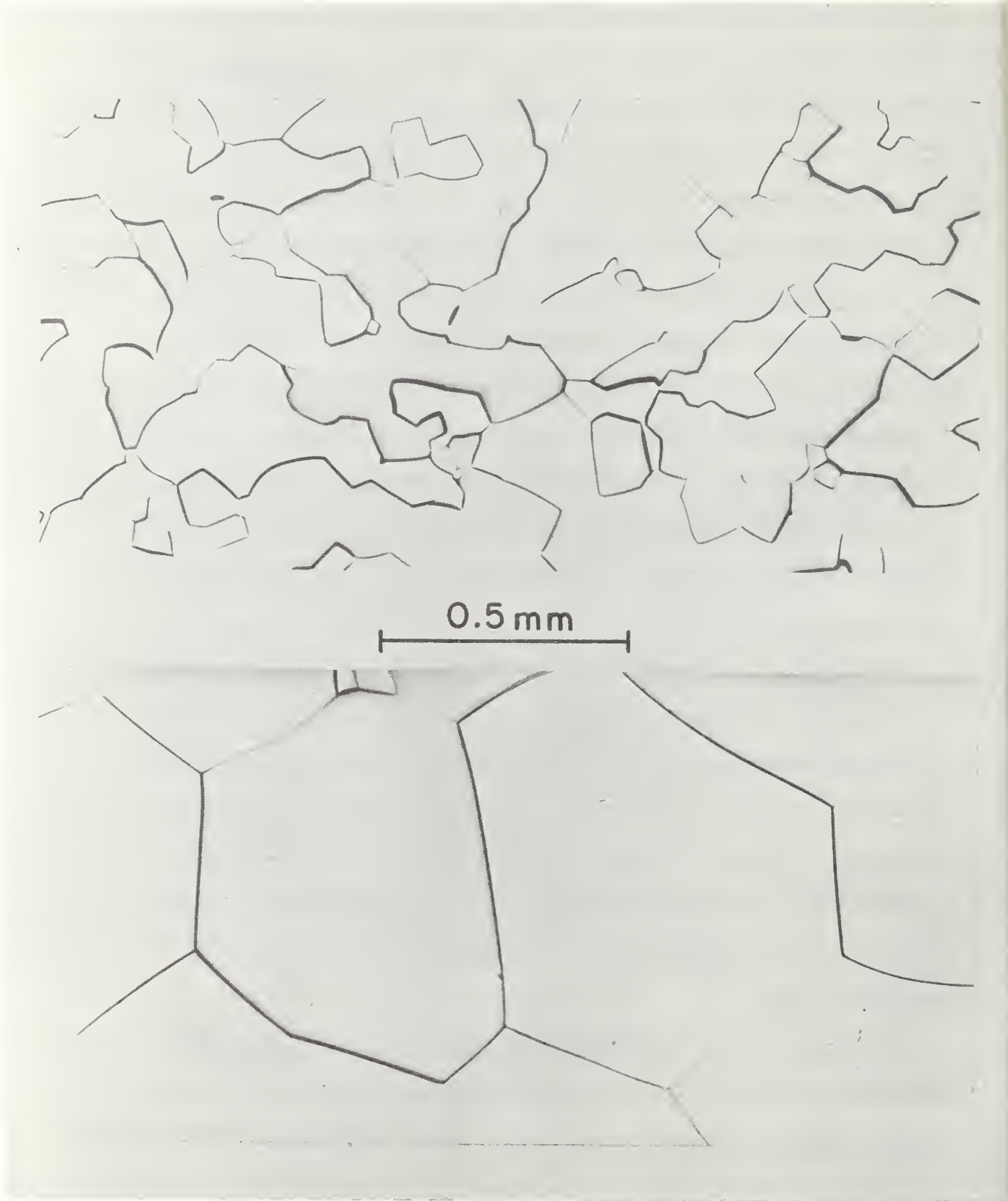


FIGURE 1. Photomicrographs of the niobium specimen before (upper photograph) and after (lower photograph) the entire set of experiments.

figure 1, indicate that considerable grain growth took place as the result of pulse heating to high temperatures. A list of the nature and composition of impurities in the specimen, at the end of the entire set of experiments as determined by spectrochemical analysis, is given in table 1. The residual resistivity ratio (ratio of electrical resistivity at 273 K to the residual resistivity) of the specimen, measured before the experiments, was 11.

The data on voltage, current, and temperature were used to obtain third degree polynomial functions for each quantity in terms of time, which then provided the input information for the determination of properties.

3. Experimental Results

This section presents the thermophysical properties determined from the measured quantities. All values are based on the 1968 International Practical Temperature Scale [4]. In all computations, the geometrical quantities are based on their room temperature (298 K) dimensions. The experimental results are represented by polynomial functions in temperature obtained by least squares approximation of the individual points. The final values on properties at 100 degree temperature intervals computed using the functions are presented in table 2.

TABLE 1

Impurities in Niobium Specimen

Impurity	Amount ppm	Impurity	Amount ppm
Al	5	Mo	5
As	<5	Ni	<1
B	<1	Pb	<1
Bi	<5	Sb	<10
Ca	<1	Si	<5
Cd	<5	Sn	3
Co	<1	Ta	450
Cr	<1	Te	<5
Cu	<1	Ti	<1
Fe	<3	V	<1
Hf	<50	W	<100
Mg	<1	Zn	<10
Mn	<1	Zr	<5

470 < Total < 680

TABLE 2

Heat capacity, electrical resistivity, hemispherical total emittance and normal spectral emittance of niobium

Temp. K	c_p J mol ⁻¹ K ⁻¹	ρ^a 10 ⁻⁸ Ω m	ϵ^a	$\epsilon_{N,\lambda}$
1500	29.48	57.58		
1600	30.11	60.41		
1700	30.73	63.20	0.217	0.353
1800	31.35	65.96	0.230	0.352
1900	32.02	68.68	0.242	0.352
2000	32.75	71.37	0.254	0.351
2100	33.57	74.02	0.264	0.351
2200	34.53	76.63	0.274	0.351
2300	35.64	79.20	0.282	0.350
2400	36.94	81.74	0.290	
2500	38.46	84.25	0.297	
2600	40.23	86.71	0.303	
2700	42.28	89.14		

^aBased on ambient temperature (298 K) dimensions.

3.1. Heat Capacity

Heat capacity was computed from data taken during the heating period. A correction for power loss due to thermal radiation was made using the results on hemispherical total emittance. The standard deviation of the individual data points from a third degree polynomial function in the range 1500 to 2700 K for each specimen is 0.7 percent for niobium-1 and 0.9 percent for niobium-2. The average absolute difference between the results on two specimens is 0.7 percent. The function for heat capacity (standard deviation = 0.8 percent) that represents the combined results of the two specimens in the temperature interval 1500 to 2700 K is:

$$c_p = -3.395 + 4.855 \times 10^{-2} T - 2.531 \times 10^{-5} T^2 + 5.035 \times 10^{-9} T^3 \quad (1)$$

where T is in K and c_p is in $J \text{ mol}^{-1} \text{ K}^{-1}$. In the computations of heat capacity, the atomic weight of niobium was taken as 92.91.

3.2 Electrical Resistivity

The electrical resistivity of niobium was determined from the same experiments that were used to calculate heat capacity. The standard deviation of the individual data points from a second degree polynomial function in the range 1500 to 2700 K for each specimen is 0.2 percent for both niobium-1 and niobium-2. The average absolute difference between the results on two specimens is 0.5 percent. The function for electrical resistivity (standard deviation = 0.3 percent) that represents the combined results of the two specimens in the temperature interval 1500 to 2700 K is:

$$\rho = 10.74 + 3.396 \times 10^{-2} T - 1.823 \times 10^{-6} T^2 \quad (2)$$

where T is in K, and ρ is in $10^{-8} \Omega\text{m}$. In the computations of the specimen's

cross-sectional area, which is needed for the computations of electrical resistivity, the density of niobium was taken as $8.57 \times 10^3 \text{ kg m}^{-3}$ [5]. The measurements, before pulse experiments, of the electrical resistivity of the two niobium specimens at 293 K with a Kelvin bridge were in agreement within 0.1 percent. Electrical resistivity of niobium at 293 K obtained by averaging the results of the two specimens is $15.9 \times 10^{-8} \Omega\text{m}$.

3.3 Hemispherical Total Emittance

Hemispherical total emittance was computed for niobium-1 using data taken during both heating and initial free cooling periods. The function for hemispherical total emittance (standard deviation = 0.4 percent) that represents the results in the temperature range 1700 to 2650 K is:

$$\epsilon = -0.144 + 2.88 \times 10^{-4} T - 4.46 \times 10^{-8} T^2 \quad (3)$$

where T is in K.

3.4. Normal Spectral Emittance

Normal spectral emittance was computed for niobium-1 using data from three sets of two experiments, one in which the pyrometer was aimed at the surface of the specimen, and another in which it was aimed at the blackbody hole in the specimen. The measurements were made at the effective wavelength of the pyrometer interference filter (650 nm; bandwidth 10 nm). The function for normal spectral emittance (standard deviation = 0.6 percent) that represents the results in the temperature range 1700 to 2300 K is:

$$\epsilon_{N,\lambda} = 0.361 - 4.77 \times 10^{-6} T \quad (4)$$

where T is in K.

4. Estimate of Errors

Estimates of errors in measured and computed quantities lead to the following estimates of errors in the properties over the temperature range 1500 to 2700 K: heat capacity, 2 percent; electrical resistivity, 0.5 percent; hemispherical total emittance, 3 percent; normal spectral emittance, 3 percent. Details regarding the estimates of errors and their combination in high-speed experiments using the present measurement system are given in a previous publication [2]. Specific items in the error analysis were recomputed whenever the present conditions differed from those in the earlier publication.

In all the earlier experiments with the present high-speed system, the lowest temperature at which measurements were made was 1900 K. In the present work, the measurements were extended down to 1500 K without creating any significant uncertainties in temperature measurements. The imprecision¹ of temperature measurements was 0.7 K at 1500 K, and 0.5 K at 1900 K. The imprecision of voltage and current measurements was less than 0.02 and 0.03 percent, respectively, over the entire temperature range.

5. Discussion

The heat capacity and electrical resistivity results of this work are compared graphically with those in the literature in figures 2 and 3, respectively. Numerical comparisons are given in tables 3 and 4. Heat capacity results of this work are, in general, lower than those of most other investigators, with the exception of Kraftmacher [8].

¹Imprecision refers to the standard deviation of an individual point as computed from the difference between measured value and that from the smooth function obtained by the least squares method.

Electrical resistivity results are in good agreement with those of others. Estimates of errors in papers cited lead to an estimate of inaccuracies in previously reported heat capacity and electrical resistivity of approximately 5 to 10 and 1 to 3 percent, respectively.

The present result of the electrical resistivity of niobium corresponding to 293 K is $15.9 \times 10^{-8} \Omega\text{m}$; those reported in the recent literature range from $14.6 \times 10^{-8} \Omega\text{m}$ [13] to $16.9 \times 10^{-8} \Omega\text{m}$ [12].

The results for hemispherical total emittance and normal spectral emittance of this work and those in the literature are presented in figures 4 and 5, respectively. Deviations in the results of various investigators may largely be attributed to the differences in specimen surface conditions.

Similar to the earlier results on molybdenum [2], tantalum [21], and tungsten[22] obtained with the present measurement system, heat capacity of niobium at high temperatures is considerably higher than the Dulong and Petit value of $3R$. Some of this departure is due to $c_p - c_v$ and the electronic terms. However, they do not account for the entire difference. Heat capacity above the Debye temperature may be expressed by

$$c_p = A - \frac{B}{T^2} + CT + \Delta c \quad (5)$$

where the constant term is $3R$ ($24.943 \text{ J mol}^{-1} \text{ K}^{-1}$), the term in T^{-2} is the first term in the expansion of the Debye function, the term in T represents $c_p - c_v$ and electronic contributions, and the quantity Δc

TABLE 3
 Niobium heat capacity difference (previous literature minus present
 work values) in percent

Investigator	Ref.	Year	Method	Temperature, K							
				1500	1700	1900	2100	2300	2500	2700	
Jaeger and Veenstra	6	1934	drop	+2.4	+1.8	+1.3					
Lowenthal	7	1963	modul.	+4.8	+4.1	+3.6	+2.6	+0.7			
Kraftmakher	8	1963	modul.	-3.6	-3.4	-3.1	-2.9	-3.2	-4.0	-5.5	
Conway and Hein	9	1965	drop	-2.6	+2.6	+7.2	+10.6	+12.0	+11.0		
Kirillin et al.	10	1965	drop	+5.2	+5.1	+6.3	+8.2	+10.4	+12.3	+13.6	

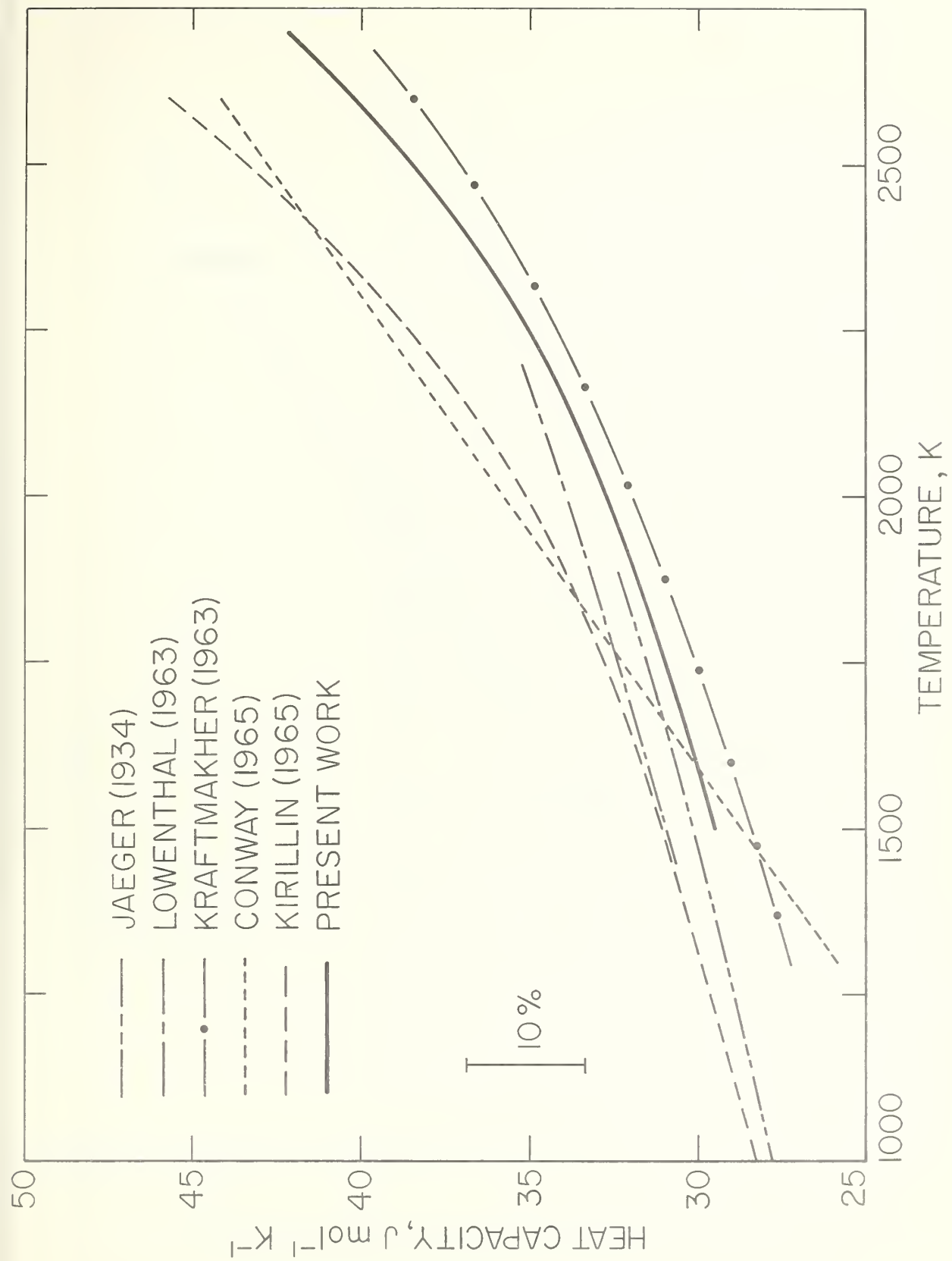


FIGURE 2. Heat capacity of niobium reported in the literature.

TABLE 4

Niobium electrical resistivity difference (previous literature minus present work values) in percent

Investigator	Ref.	Year	Temperature, K					
			1500	1700	1900	2100	2300	2500
Reimann	11	1936			-2.7	-2.8	-2.9	
Tye	12	1961	+3.6	+3.9				
Gebhardt et al.	13	1966	-0.6	-0.6	-0.5	-0.1	+0.4	+1.0
Neimark and Voronin	14	1968	+1.0	+1.4	+1.6	+1.7	+1.6	

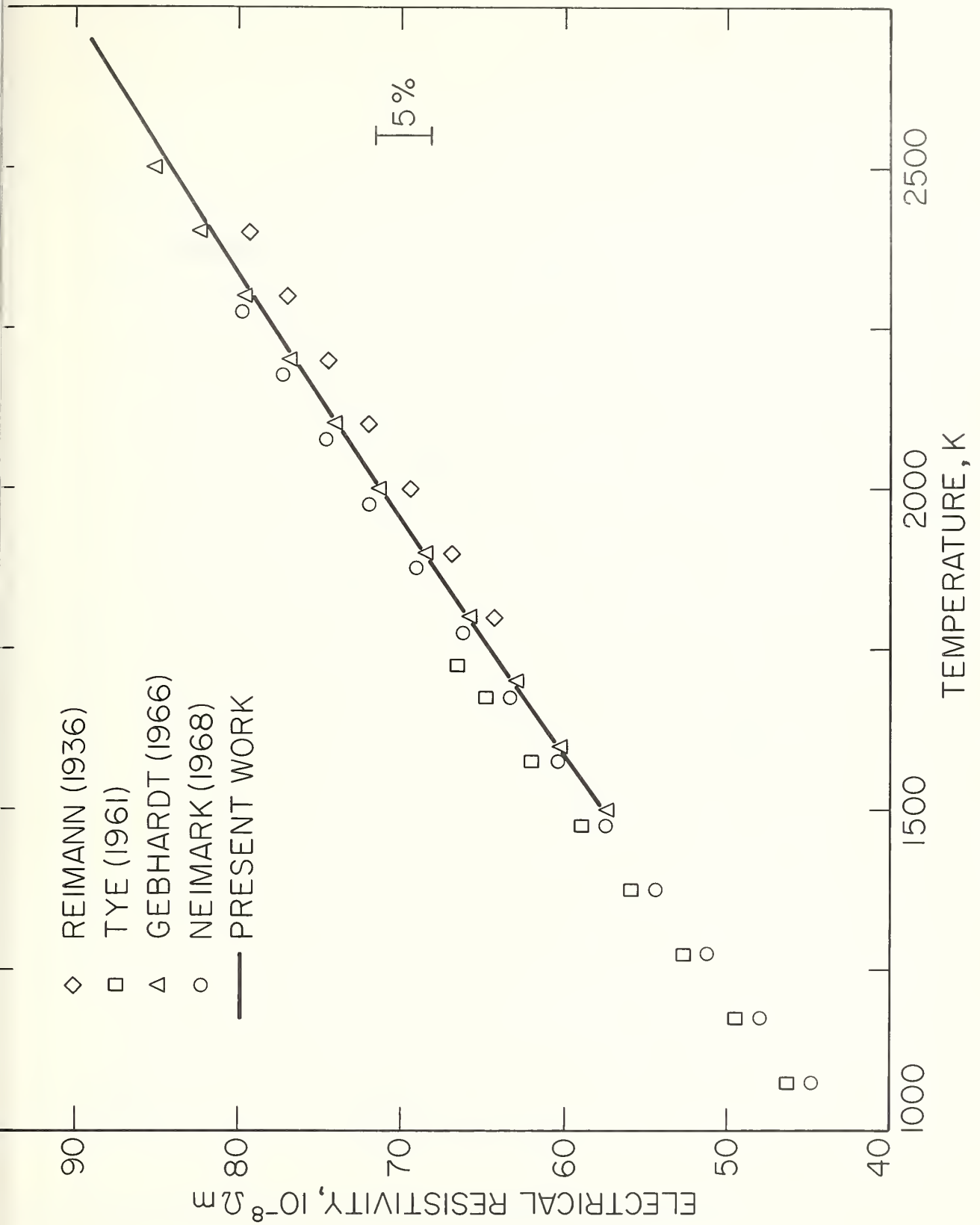


FIGURE 3. Electrical resistivity of niobium reported in the literature.

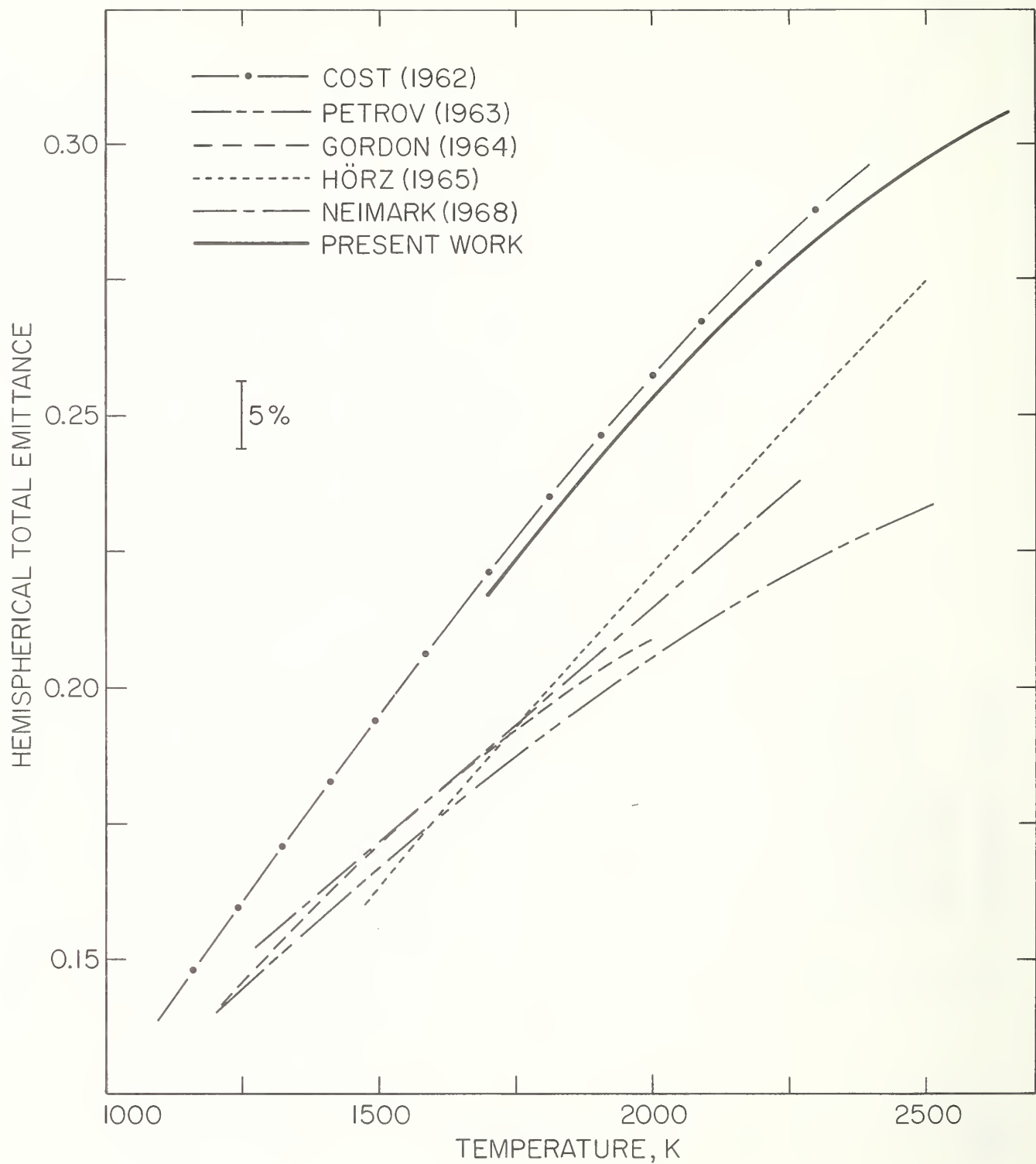


FIGURE 4. Hemispherical total emittance of niobium reported in the literature.

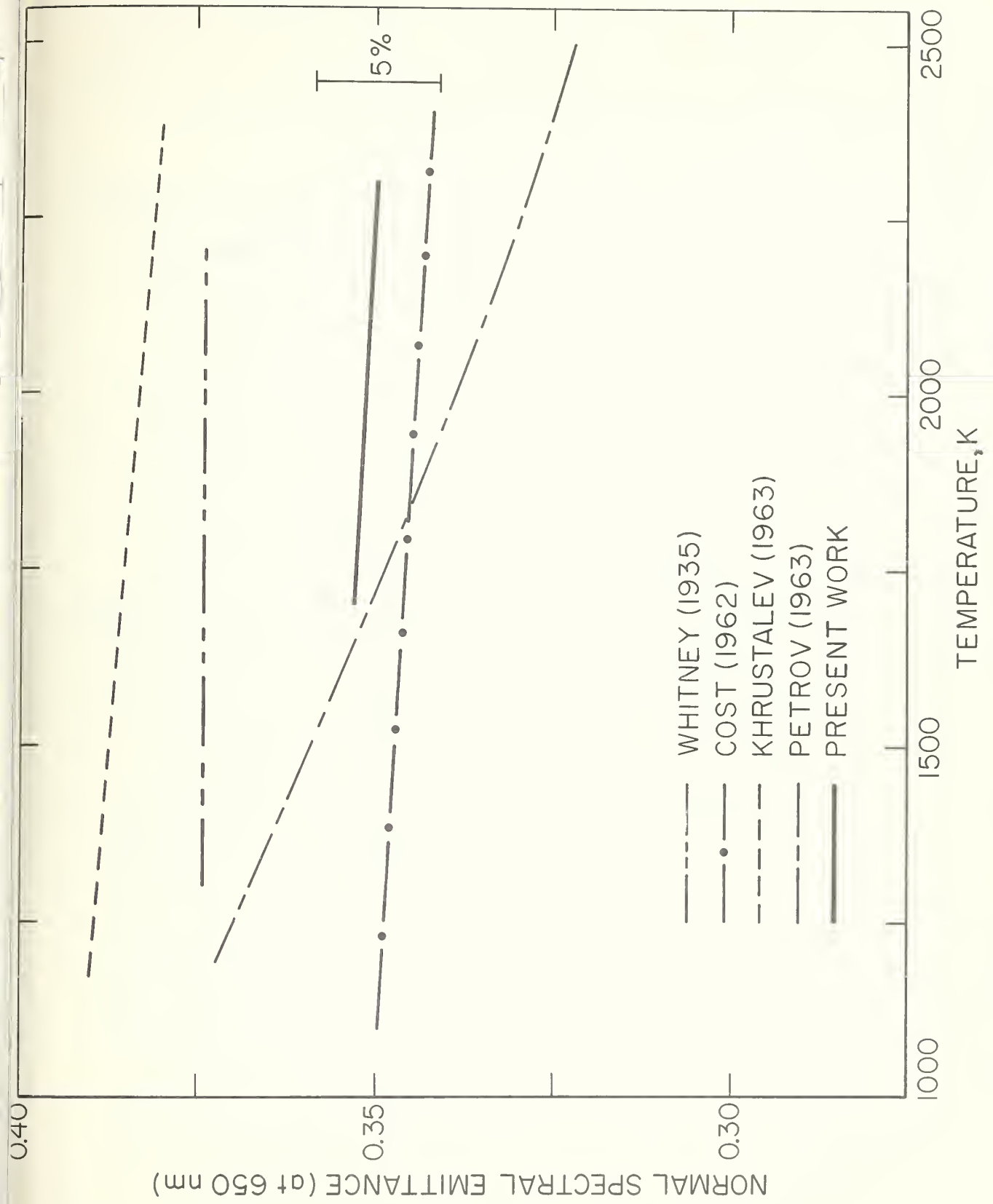


FIGURE 5. Normal spectral emittance of niobium at $\lambda = 650$ nm reported in the literature.

represents excess in measured heat capacity at high temperatures, which is not accounted/for by the first three terms. The coefficients $B(9.6 \times 10^4)$ and $C(2.9 \times 10^{-3})$ were obtained from data on heat capacity at 200 K and 1000 K given by Hultgren et al. [23].

Using eq (5) and the heat capacity results of this work, the quantity Δc was computed for temperatures above 1500 K. The results for Δc in $\text{J mol}^{-1} \text{K}^{-1}$ are: 0.2 at 1500 K, 2.0 at 2000 K, 6.3 at 2500 K, and 9.5 at 2700 K.

Although the mechanisms of vacancy generation become important at high temperatures, it was not possible to attribute the high heat capacity values entirely to vacancies. To demonstrate this, a crude estimate of the contribution of vacancies to heat capacity was made using the method described in a previous publication [2]. The results indicate that vacancy contribution would be small, less than $0.05 \text{ J mol}^{-1} \text{K}^{-1}$ at 2000 K and $0.5 \text{ J mol}^{-1} \text{K}^{-1}$ at 2700 K, and would not account for the high heat capacity values. If the entire difference between measured and computed [using the first three terms in eq (5)] heat capacities is attributed to vacancies, values of 1.3 eV for vacancy formation energy and 3.5 percent for vacancy concentration at the melting point are obtained. Both of these values seem to be unrealistic for niobium.

To give a simple expression for the heat capacity of niobium over a wide temperature range, an empirical term for the quantity Δc in eq (5) was substituted. Trials indicated that a term in T^5 describes the experimental results better than a term in T^4 . The coefficient of this term was obtained from the results of the present work in conjunction with the

values given by Hultgren et al. [23] at temperatures below 1000 K. Then, eq (5) for the range 300 to 2700 K becomes

$$c_p = 24.943 - \frac{9.6 \times 10^4}{T^2} + 2.9 \times 10^{-3} T + 6.4 \times 10^{-17} T^5 \quad (6)$$

where T is in K and c_p is in $\text{J mol}^{-1} \text{K}^{-1}$. Average absolute deviation of the individual points from the function over the temperature range considered is 0.4 percent. Equation (6) is presented graphically in figure 6.

Earlier work on tantalum [21], which also belongs to Group V, indicated that the quantity Δc in eq (5) is best represented by a term in T^5 . However, the results on molybdenum [2] and tungsten [22], which belong to Group VI, indicated that the same quantity is best described by a term in T^4 . The significance of this is not apparent at this time.

Electrical resistivity of niobium, in the range of present measurements, showed a negative departure from linearity in the curve of electrical resistivity against temperature. A similar trend was also observed for tantalum [21].

Acknowledgement

The author expresses his gratitude to Dr. C. W. Beckett for his continued interest and encouragement of research in high-speed methods of measuring thermophysical properties. The contributions of Mr. M. S. Morse in connection with electronic instrumentation are also greatly appreciated.

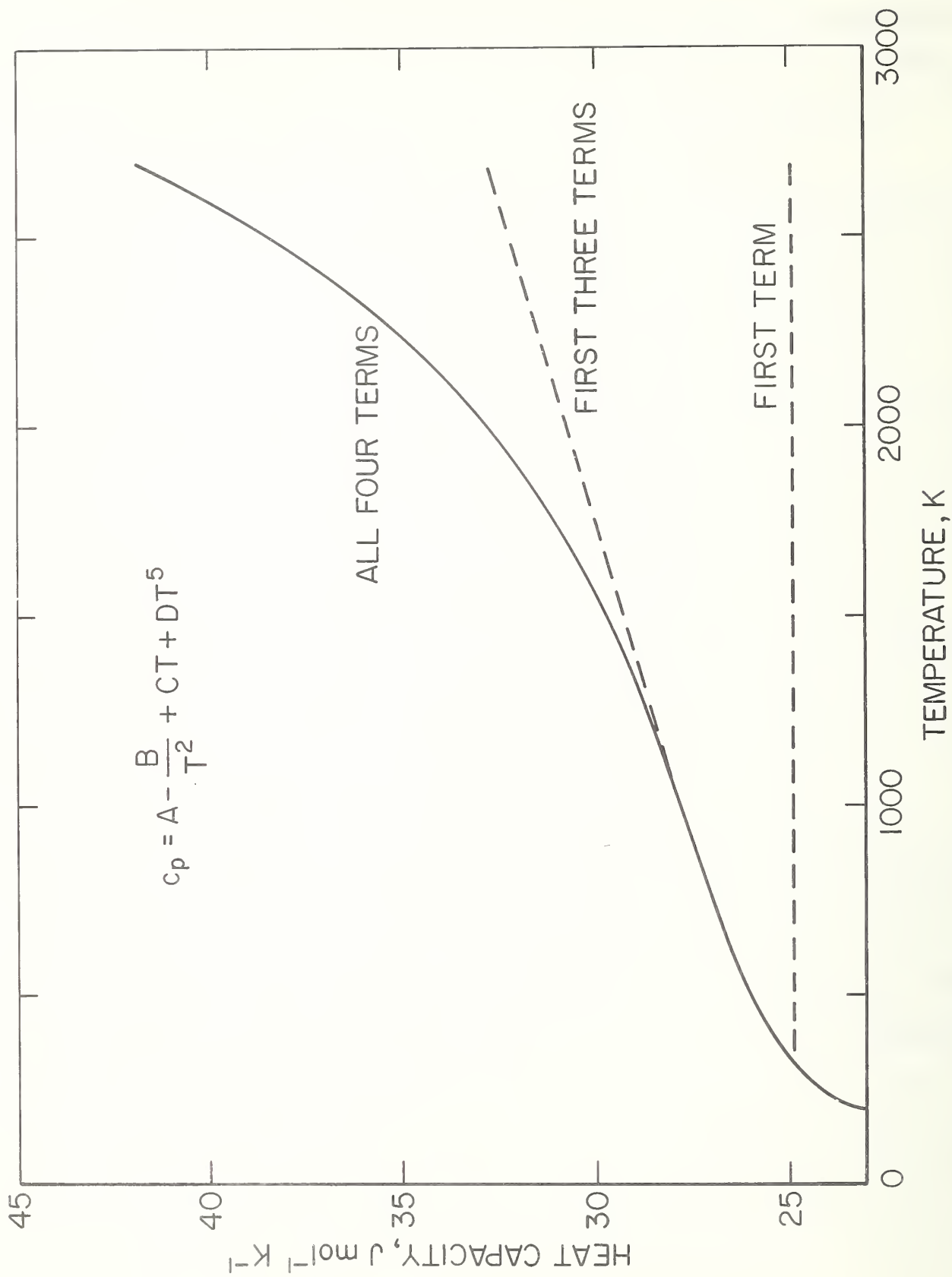


FIGURE 6. Heat capacity of niobium according to equation (6).

6. References

- [1] Cezairliyan, A. Design and operational characteristics of a high-speed (millisecond) system for the measurement of thermophysical properties at high temperatures. J. Res. Nat. Bur. Stand. (U.S.) 75C (Eng. and Instr), 7 (1971).
- [2] Cezairliyan, A., M. S. Morse, H. A. Berman, and C. W. Beckett, High-speed (subsecond) measurement of heat capacity, electrical resistivity, and thermal radiation properties of molybdenum in the range 1900 to 2800 K, J. Res. Nat. Bur. Stand. (U.S.) 74A (Phys. and Chem.), 65 (1970).
- [3] Foley, G. M., High-speed optical pyrometer, Rev. Sci. Instr. 41, 827 (1970).
- [4] International Practical Temperature Scale of 1968, Metrologia 5, 35 (1969).
- [5] Tietz, T. E. and J. W. Wilson, Behavior and properties of refractory metals, Stanford University Press, California (1965), p. 28.
- [6] Jaeger, F. M., and W. A. Veenstra. The exact measurement of the specific heats of solid substances at high temperatures, VI, the specific heats of vanadium, niobium, tantalum, and molybdenum. Rec. Trav. Chim. 53, 677 (1934).
- [7] Lowenthal, G. C., The specific heat of metals between 1200 K and 2400 K, Australian J. Phys. 16, 47 (1963).
- [8] Kraftmakher, Ya. A., Vacancy formation in niobium. Solid State (USSR), 5, 696 (1963).
- [9] Conway, J. B., and R. A. Hein, "Enthalpy Measurements of solid materials to 2400 C by means of a drop Technique" in Advances in Thermophysical properties at extreme temperatures and pressures, S. Gratch, ed. (ASME, New York, 1965), p. 131.
- [10] Kirillin, V. A., A. E. Sheindlin, V. Ya. Chekhovskoi, and I. A. Zhukova, Experimental determination of the enthalpy of niobium in the temperature range 600 to 2600 K, High Temperature, 3, 357 (1965).
- [11] Reimann, A. L., Some high-temperature properties of niobium, Phil. Mag. 22, 34 (1936).
- [12] Tye, R. P., Preliminary measurements on the thermal and electrical conductivities of molybdenum, niobium, tantalum, and tungsten, J. Less-Common Metals, 3, 13 (1961).

- [13] Gebhardt, E., W. Durrschnabel, and G. Horz, J. Nucl. Mat. 18, 119 (1966).
- [14] Neimark, B. E., and L. K. Voronin, Thermal conductivity, specific electrical resistivity, and total emissivity of refractory metals at high temperatures, High Temperature, 6, 999 (1968).
- [15] Cost, J. R., Emissivities of niobium and niobium-nitrogen solids solutions, Trans. Metall. Soc. AIME 224, 634 (1962).
- [16] Petrov, V. A., V. Ya. Chekhovskoi, and A. E. Sheindlin, Experimental determination of the degree of blackness of niobium at temperatures of 1200 to 2500 K, High Temperature, 1, 416 (1963).
- [17] Gordon, A. R., and G. F. Muchnik, Determination of the emissivity of niobium as a function of the roughness of the surface, High Temperature, 2, 505 (1964).
- [18] Horz, G., W. Durrschnabel, and E. Gebhardt, Hemispherical total emittance of niobium, J. Nucl. Mat. 17, 277 (1965).
- [19] Whitney, L. V., The temperature scales of columbium, thorium, rhodium and molybdenum at 0.667 μ , Phys. Rev. 48, 458 (1935).
- [20] Khrustalev, B. A., I. P. Kolchenogova, and A. M. Rakov, Spectral coefficients of tantalum, molybdenum and niobium radiation, High Temperature, 1, 13 (1963).
- [21] Cezairliyan, A., J. L. McClure, and C. W. Beckett, High-speed (subsecond) measurement of heat capacity, electrical resistivity, and thermal radiation properties of tantalum in the range 1900 to 3200 K, J. Res. Nat. Bur. Stand. (U.S.) 75A (Phys. and Chem.) 1 (1971).
- [22] Cezairliyan, A., and J. L. McClure, High-speed (subsecond) measurement of heat capacity, electrical resistivity, and thermal radiation properties of tungsten in the range 2000 to 3600 K, J. Res. Nat. Bur. Stand. (U.S.), 75A (Phys. and Chem.), in press.
- [23] Hultgren, R., R. L. Orr, P. D. Anderson, and K. K. Kelly, Selected Values of Thermodynamic Properties of Metals and Alloys, John Wiley, New York (1963).

Chapter 4

DEPARTURE OF EMITTANCE - RESISTIVITY RELATION FROM THEORETICAL PREDICTIONS FOR REFRACTORY METALS AT HIGH TEMPERATURES

Ared Cezairliyan
National Bureau of Standards
Washington, D.C. 20234

Based on the free electron theory of metals and Maxwell's electromagnetic theory of radiation, a relation between thermal radiation emitted by a metal and its electrical resistivity was obtained by Aschkinass [1]. This was further modified and refined by other investigators [2,3]. The general relation expressing hemispherical total emittance, ϵ , as a function of electrical resistivity, ρ , is

$$\epsilon = \sum_{i=1}^n (-1)^{i+1} C_i (\rho T/c_2)^{i/2} \quad (1)$$

where T is temperature in K, c_2 is the second radiation constant and C_i are constants obtained in the derivation. For simplicity, ϵ will be referred to as emittance.

Different investigators have used different number of terms (ranging from one to four) in the above equation. Equation (1) for $n = 4$, given by Davisson and Weeks [3], is

$$\epsilon = 0.8992(\rho T/c_2)^{1/2} - 0.9047(\rho T/c_2) + 1.149(\rho T/c_2)^{3/2} - 1.245(\rho T/c_2)^2 \quad (2)$$

In this study the validity of Eq. (2) is checked using the results on four refractory metals, niobium, molybdenum, tantalum, and tungsten above 2000 K. Emittance and electrical resistivity were measured simultaneously by a transient technique. This technique is based on resistive self-heating of the specimen, by the passage of high currents through it, from room temperature to near its melting point in less than one second, and measuring the pertinent experimental quantities (voltage, current, and temperature) with millisecond resolution. Data taken during the heating period and the initial cooling period following the heating period are used to determine emittance as well as electrical resistivity. The details on the measurements are given in other publications [4,5,6,7].

Computed emittances, using $c_2 = 1.4388 \text{ cm K}$ in Eq. (2), in terms of measured resistivities were compared with experimentally obtained emittances. Emittance and electrical resistivity values were corrected for dimensions at the specimen temperature using thermal expansion results on niobium [8,9], molybdenum [8,9,10,11], tantalum [10,12], and tungsten [12,13]. The results on the refractory metals are shown in Fig. 1 in terms of the quantity ϵ_m/ϵ , where ϵ_m and ϵ are measured and computed emittances, respectively. It may be seen that, in general, the difference between experimental and theoretical results decreases with increasing temperature.

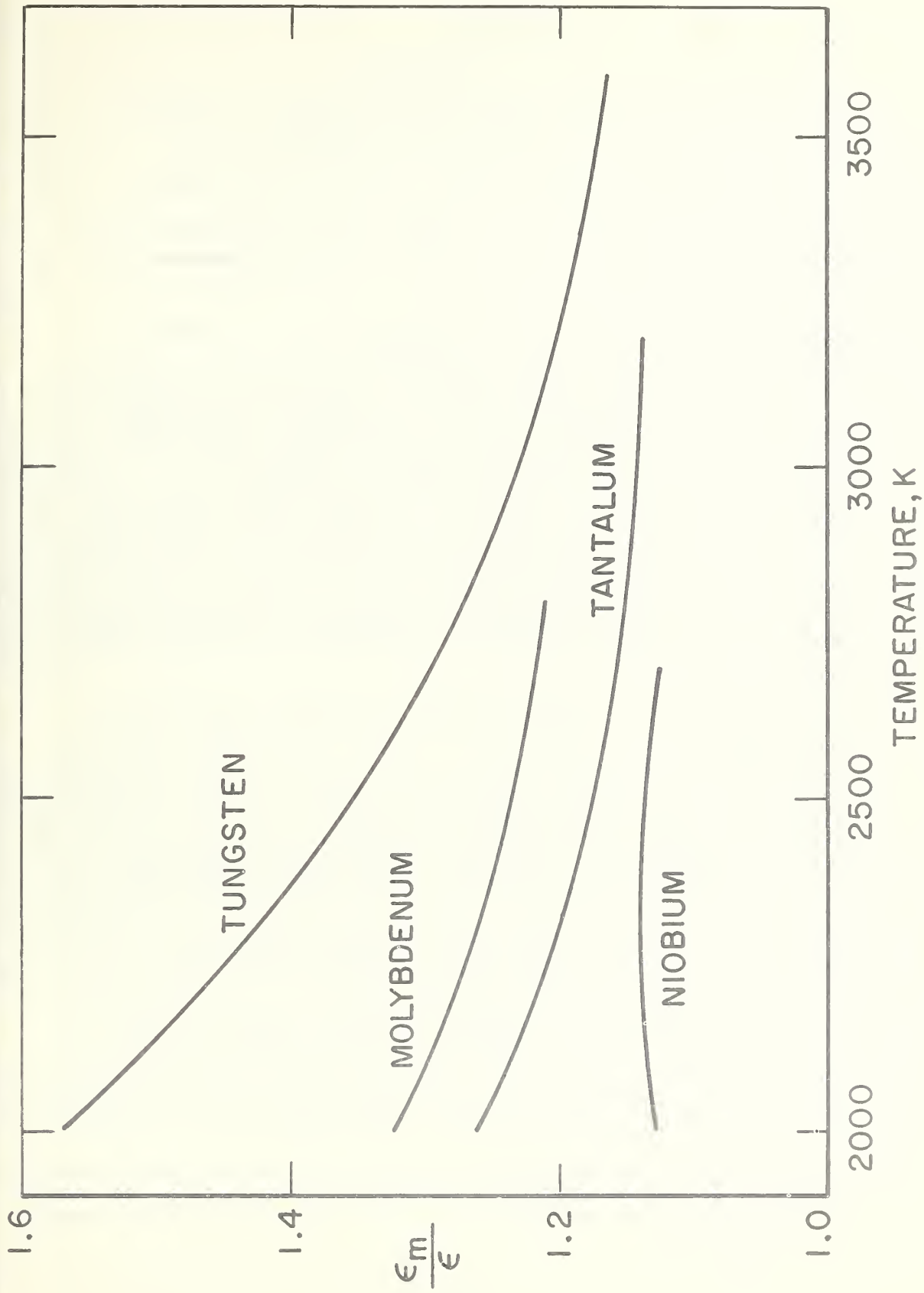


Figure 1. Variation of the ratio of measured emittance (ϵ_m) to computed emittance (ϵ) as a function of temperature for niobium, molybdenum, tantalum, and tungsten.

References

1. Aschkinass, E., Ann. d. Phys. 17, 960 (1905).
2. Foote, P. D., Bull. Nat. Bur. Stand. (U.S.) 11, 607 (1915).
3. Davisson, C., and J. R. Weeks, J. Opt. Soc. Am. 8, 581 (1924).
4. Cezairliyan, A., J. Res. Nat. Bur. Stand. (U.S.), 75A (Phys. and Chem.), in press.
5. Cezairliyan, A., M. S. Morse, H. A. Berman, and C. W. Beckett, J. Res. Nat. Bur. Stand. (U.S.) 74A (Phys. and Chem.), 65 (1970).
6. Cezairliyan, A., J. L. McClure, and C. W. Beckett, J. Res. Nat. Bur. Stand. (U.S.), 75A (Phys. and Chem.), 1 (1971).
7. Cezairliyan, A., and J. L. McClure, J. Res. Nat. Bur. Stand. (U.S.), 75A (Phys. and Chem), 283 (1971).
8. Edwards, J. W., R. Speiser, and H. L. Johnston, J. Appl. Phys. 22, 424 (1951).
9. Amonenko, V. M., P. N. V'yugov, and V. S. Gumenyuk, High Temp. 2, 22 (1964).
10. Worthing, A. G., Phys. Rev. 28, 190 (1926).
11. Rasor, N. S., and J. D. McClelland, J. Phys. Chem. Solids, 15, 17 (1960).
12. V'yugov, P. N., and V. S. Gumenyuk, High Temp. 3, 879 (1965).
13. Forsythe, W. E., and A. G. Worthing, Astrophy. J. 61, 146 (1925).

Chapter 5

THE RELATIVE ENTHALPY AND HEAT CAPACITY OF MOLYBDENUM METAL FROM 1170 TO 2100 K

By

Shigeru Ishihara and Thomas B. Douglas

Abstract

The enthalpy of two samples of molybdenum metal at least 99.8% pure (one triply zone-refined) was recently measured relative to 298 K at eleven temperatures from 1170 to 2100 K using a precise dropping-type method, and showed on simple smoothing a standard deviation of about 0.2%. Check measurements on synthetic sapphire (standard-sample Al_2O_3) were made at 1170 and 1700 K, and agreed excellently with earlier precise NBS data. The smoothed enthalpy and corresponding heat-capacity values for molybdenum are compared with the results of 17 previously published sets of results in the same temperature range. Subsequent planned measurements on this metal will complete the data for the whole temperature range 273 K to approximately 2500 K. Errors are estimated.

I. Introduction

The recent experimental results on molybdenum metal reported in this chapter for the first time were obtained as part of an NBS-sponsored program and primarily for the purpose of establishing suitable samples of this metal as a high-temperature heat-capacity standard. These results are included in this report because they are of equal importance in the AFOSR-sponsored program currently devoted to thermodynamic research on the high-melting-point metals and their Aerospace-important compounds: molybdenum metal is a key material in this class, but many of its previously published heat capacities disagree seriously at the higher temperatures.

The relative enthalpy of pure Al_2O_3 (as a standard reference material) was recently measured at the Bureau from 273 to 2250 K [1]¹. Two widely different dropping-type apparatuses were used over the respective temperature ranges 273 - 1173 K and 1173 - 2250 K. The results show almost perfect continuity at 1173 K (as well as at 273 K with earlier precise NBS adiabatic-

¹Numbers in brackets denote literature references at the end of this chapter.

calorimetry results from 15 to 380 K on a comparable sample), with estimated accuracies of enthalpy (relative to room temperature) of ± 0.1 and $\pm 0.2\%$ in these two respective higher temperature ranges. As recognized by many people, a metallic standard also is desirable; molybdenum was chosen because of its high melting point (2890 K), freedom from transitions, and availability in high purity. The measurements over the range 1170 - 2100 K have been completed, and are reported here. After the results on molybdenum to still higher temperatures (up to approximately 2500 K) have been obtained, a comparison will be available with those (1900 - 2800 K) by a widely different method, a precise millisecond pulse-heating method developed at NBS in the AFOSR-sponsored program [21].

The enthalpy or heat capacity of molybdenum has been measured by many other workers (by several, to within 100 K of the melting point), and later in this chapter we compare 17 sets of these results with ours. Although some workers have made no claim to even moderately good accuracy, the wide disagreements among the others on molybdenum (by as much as a factor of 1.5 for the heat capacity at 2500 K! [21]) are not easy to explain or rationalize. In an effort to achieve a much higher order of reliability of our results, we have paid particular attention to what are probably the most serious sources of error in such measurements (sample-temperature measurement, and sensitivity of the enthalpy and heat capacity of this metal to low-atomic-weight impurities). Details relevant to these sources of error are discussed in later sections of the chapter.

II. Samples

The enthalpy measurements were made on rods of three different samples of molybdenum--subsequently distinguished as A, B and C--of two different types. Samples A and B were really different specimens of the same sample, one previously drawn and annealed, and presently stocked by the Office of Standard Reference Materials of the Bureau. Sample C was 3-pass electron-beam zone-refined polycrystalline material machined to 0.35" diameter and obtained from Materials Research Corporation, of Orangeburg, N.Y., who classified it as of "grade 1" and stated a purity of 99.992%. Details of analyzing and treating the three samples prior to the enthalpy measurements are as follows.

Qualitative Spectrochemical Analyses -- All three samples were analyzed separately, and the results are given in Table 1A. (In the case of Sample C, the purest sample, special care was taken to remove all surface contamination, consume the sample completely in the arc excitation, and use a high-purity reference sample of molybdenum.) This technique omits the important nonmetals, but indicated a total metallic impurity of less than 0.02% for Samples A and B, and a still smaller figure for Sample C which is consistent with the supplier's claimed purity stated above.

Spark-Source Mass Spectrometry -- Two rods from the lot from which Samples A and B were taken were first etched in nitric acid, washed in distilled water, then boiled in distilled water to clean the surface. These specimens were then presparked to identify and remove any remaining surface contamination. The mass-spectra metric results are given in Table 1B. Note the near-completeness of the coverage of elements, and particularly the low levels of those low-atomic-weight elements analyzed for (to which the enthalpy and heat capacity of molybdenum, as calculated from the data, are particularly sensitive, as discussed in Section V). This analytical technique showed a total impurity of 0.02% by weight of the elements detected, and set a total upper limit of (an additional) 0.02% by weight to the elements (except F, Ne, Na, and Ti) partially masked by major interference.

Electronic Characterization -- This technique was applied to specimens typical of Samples A and B only. The specimens were cleaned with ethyl alcohol, then heavily electroetched in an electrolyte of sulfuric acid and methyl alcohol to remove surface contamination. For this technique adequate prior annealing of the specimens was important. Annealing for one hour at 1000°C (slow cool) proved inadequate, but the adopted conditions (two anneals, the second for two hours at 1200°C with slow cooling) was judged sufficient. The resistance ratio (273 K to 4 K) was then found to be 70. This ratio was interpreted assuming the residual resistance (at 4 K) to be due to equal atomic concentrations of the likely metallic contaminants W, Ta, Nb, and Zr; on this hypothetical basis the total impurity was calculated to be 0.2 weight % (0.1 atomic %). Note that these levels of impurity far exceed those found by the spectrochemical and mass-spectrometric analyses detailed above. The cause of the disagreement is not known.

Sample Annealing Prior to Enthalpy Measurements -- After etching with HNO_3 , then with HCl, with subsequent treatment with boiling water, Sample A was annealed for two hours at 1200°C in 10 cm pressure of argon. (After this etching, the surface was found to discolor in moist air but without detectable weight gain; nevertheless, moisture was excluded thereafter as a precaution.) Sample B was not deliberately annealed, although the first enthalpy measurement on it was made only after it had been held in the furnace at about 1425°C for about 40 minutes, and these conditions may have effected its annealing; at least, a repetition of this heating did not change its enthalpy detectably (see Table 2). Sample C was neither etched nor annealed; it had not been subjected to mechanical stress since its zone refinement, so that annealing was believed unnecessary.

An inspection of the data (Table 2, Section IV) will show that despite the apparent greater purity of Sample C, Sample A was chosen as the principal one. There were several reasons for this decision. Since the primary aim was to establish calorimetric values for an easily accessible standard material, an important factor was that the molybdenum represented by Samples A and B is more readily available and less costly than the zone-refined

Table 1A

Qualitative spectrochemical analyses of the molybdenum samples,
in weight %^a

Element	Sample A (1/8" rod)	Sample B (1/4" rod)	Sample C (triple-zone-refined; 1/2" rod)
	(weight %)	(weight %)	(weight %)
Al	.001 - .01	.001 - .01	-?
Ca	<.001	<.001	<.0001
Cu	<.001	<.001	<.0001
Fe	.001 - .01	.001 - .01	<.0001
Mg	<.001	<.001	<.0001
Mo	>10	>10	major constituent
Si	<.001	<.001	<.001
W	-	-	-?

^aAg, As, Au, B, Ba, Be, Bi, Cd, Ce, Co, Cr, Ga, Ge, Hf, Hg, In, Ir, K, La, Mn, Na, Nb, Ni, Os, P, Pb, Pd, Pt, Rh, Ru, Sb, Sc, Sn, Sr, Ta, Te, Th, Tl, U, V, W, Y, Zn, and Zr also were analyzed for but not detected. ("-" in the above table means the same.) The estimated limit of detection of an alkali metal is 0.005%.

Table 1B

Mass-spectrometric analysis of a representative specimen
of Samples A and B, in ppm by weight^b

Elements Measured				Elements Showing Interference			
Element	ppm	Element	ppm	Element	ppm	Element	ppm
Ag	1	Sb	0.5	Ar	<20	N	<10
Al	7	Si	40	Au	<10	Nb	< 3
As	2	V	0.4	B	< 0.1	Ni	<20
Ca	9	W	56	Ba	< 1	O	<30
Cr	12	Zn	0.26	C	< 3	Os	< 6
Cu	15			Cd	< 8	Pd	< 6
Fe	40			Cl	< 0.1	Pt	< 4
Ga	0.1			Co	< 7	Re	< 1
K	20			Cs	< 0.2	Rh	< 0.2
Mn	2			In	< 0.5	S	< 1
Mo	(matrix)			Ir	< 3	Sc	< 0.3
P	0.6			Li	< 0.3	Sn	<30
Rb	0.3			Mg	<31	Ta	<25

^bH and He were not analyzed for, and interference was complete for F, Ne, Na, and Ti. In addition to the elements listed in the table, the following were reported as not detected and to be considered as present below stated amounts (all less than 1 ppm each; e.g., Be, <0.01 ppm): Ac, Be, Bi, Br, Ce, Dy, Er, Eu, Ge, Gd, Hf, Hg, Ho, I, Kr, La, Lu, Nd, Pa, Pb, Pm, Po, Pr, Pu, Ra, Ru, Se, Sm, Sr, Tb, Tc, Te, Th, Tl, Tm, U, Xe, Y, Yb, and Zr.

(Sample C). (The only disadvantage of Sample B over A was its more compact shape, requiring longer times to reach temperature equilibrium in the calorimetric apparatus.) Additional facts weighing against the choice of Sample C are that it is believed to be less homogeneous in impurities, and also its characterization thus far is much less complete, as indicated earlier in this section.

III. Calorimetric Apparatus and Method

The apparatus used for the present work is essentially the same as the one used for earlier work and is described in ref. [32]. Materials studied with this high temperature enthalpy apparatus include graphite [32], aluminum oxide [33], tungsten [34], beryllium aluminate ($\text{BeO} \cdot \text{Al}_2\text{O}_3$) [35], pyrolytic graphite [36], and SRM 720 synthetic sapphire (Al_2O_3) [1].

This "drop" type apparatus consists of four major parts: one, an induction heating furnace to heat the specimen to the desired temperature; two, an automatic optical pyrometer to measure and control the temperature of the furnace and sample; three, an adiabatic receiving type calorimeter to measure the heat transfer from an encapsulated sample; and four, a semi-automatic lifting device to uniformly accelerate and decelerate the capsule suspended on a tungsten wire.

A capsule (empty or containing a specimen) at the furnace temperature is lifted into the calorimeter at a uniform acceleration of 9.1 meter/sec² with an elapsed time of around 600 milliseconds. The shutter and shields are closed in the same way for each lift. The rise in the calorimeter temperature is measured with an absolute copper resistance thermometer which has been compared with a NBS calibrated platinum resistance thermometer. Knowing the heat equivalent of the calorimeter enables us to determine the enthalpy change of the capsule and contents. One experimental point consists of enthalpy measurements of two lifts, one on an empty capsule and another on the same capsule with a molybdenum sample. The difference is the enthalpy change of the molybdenum specimen after applying a small correction for the change in final calorimeter temperatures near 298.15 K. This is true if the temperature of the capsule, radiation losses, flight time, and shutter and shield closures are the same for both lifts during the 0.1 second interval the capsule is in the cold zone at the time of the transfer.

The induction heated furnace is powered by a 7-1/2 kilowatt oscillator operating at 385 kHz with a water cooled copper working coil in a shape of a solenoid with shorter spacings near the ends to decrease the gradient of the induction field near the furnace core, where the capsule hangs during the heating operation. One-half centimeter from the bottom of the capsule is a diaphragm with an eighth inch hole through which the automatic optical pyrometer sights in the bottom of the capsule for temperature measurement and control. Placed on the axis of the working

coil and along the center of the quartz tube is a hollow graphite susceptor which couples with field and serves as the heating element. Concentric layers of carbon black, 25 μ particle size, and fine silicon carbide powder are used for thermal insulation inside the quartz tube because they do not appreciably couple with the working coil up to 2300 K. After thoroughly degassing the furnace parts by heating to 2800 K, the furnace is operated in a 1 cm³/sec flow of argon at 10 cm pressure.

An exploratory graphite probe the size of our capsule was used to measure the axial temperature gradient along the graphite core. This showed that the temperature along the axis is uniform to $\pm 2\text{-}1/2$ K for 20 centimeters from the bottom of the capsule at 2300 K after two hours furnace warm-up time. With sufficient warm-up time the temperature variation was found to be too small to determine with a visual pyrometer. This test plus other experimental tests--including variation of flight time, capsule material, sample size, suspension wire size, and pyrometer target, e.g. sighting on the diaphragm, with no change in test results--give us confidence that the temperature at the capsule bottom is the same as the temperature of the specimen, as well as we can determine.

The automatic optical pyrometer developed by Leeds and Northrup Company and used in our work is an instrument of high precision and sensitivity for measuring the brightness temperature of objects or substances between 1175 and 2800 K. A fast response photomultiplier alternately sees the target image and a filament image of an internally mounted standard lamp and automatically adjusts the reference lamp until the photomultiplier output level for both is the same. The apparatus has been modified many times to incorporate the many improvements that have been made on the instrument later. It requires a target size of somewhat less than one-eighth inch diameter at a distance of twenty inches and a means to measure the output current of the standard reference lamp. This instrument has been periodically calibrated by the radiation pyrometry section of NBS. The uncertainty of this instrument is now estimated to be ± 0.9 K at 1200 K, ± 0.8 K at 1350 K, ± 0.8 K at 1500 K, ± 1.3 K at 1675 K, and ± 3.0 K at 2475 K. Since the furnace temperature measurement is an important parameter in this enthalpy apparatus, extra effort and frequent checks have been exercised to see that the conditions of the environment during the use of the pyrometer simulate those during its calibration, and that the system is optically clean.

The adiabatic calorimeter used for this work was designed and developed by E. D. West in 1962 and the final modification was made in late 1966. Its heat equivalent is around 2900 joules per degree K and operates in the range 25 to 65°C. The apparatus has been repeatedly checked (8 times since the last modification) by electrical calibration and the standard deviation of the accumulated calibration data points

from a smoothed curve representation is estimated to be $\pm 0.004\%$ for a temperature interval of five degrees. The electrical energy supplied to the calorimeter for calibration is determined by the voltage, current, and heating interval on a heater element in the calorimeter, and is corrected for the leak rate which is small and almost constant. All instruments used in absolute measurements of EMF, resistance, time, and temperature have been periodically calibrated through the services available here at the NBS.

Briefly, the adiabatic calorimeter consists of two concentric cylinders, one made of nickel and the other of copper, in contact with each other with a ring 45 mm diameter and 8 mm thick. This introduces a time constant of about five minutes and reduces the temperature control problems associated with the surrounding adiabatic shield with moderate or high rate of heating. Surrounding the adiabatic shield is a guard jacket controlled at temperatures slightly below the temperature of the adiabatic shield. The leak rate is thus kept small and almost constant throughout the temperature range of the calorimeter. The absolute copper thermometer and differential thermometers, also copper, are wound around the copper cylinder and epoxied on for good thermal contact.

The lifting device used in this work is an operational amplifier designed to generate a signal to uniformly accelerate the hot capsule from the furnace to the calorimeter. This is accomplished by electronic double integration of a constant voltage source. Thus, the tension in the wire is smooth and the time of flight is constant for a given setting. A solid state interval timer is used to monitor the flight time of the capsule and the time intervals do not vary by more than ± 2 milliseconds out of 600.

IV. Enthalpy Data and Empirical Equations for Relative Enthalpy and Heat Capacity of Molybdenum

A chronological sequence of random furnace temperatures has been determined by the table of random numbers selected by a computer. This method was employed so as not to introduce a bias to the measurements due to the changing condition of furnace insulation or the gradual change in the automatic optical pyrometer. A day's run usually consists of four lifts, two empty and two filled with molybdenum sample. The last lift usually duplicates the first lift of the day, thus the agreement of the results is an indication that the warm up time of the furnace was sufficient to settle the gradients along the furnace core. There is usually a small but insignificant difference in the results between the two lifts and this small correction, nevertheless, has been applied as a drift correction and has somewhat improved the precision of the enthalpy data.

The weight of Sample A was constant to ± 0.06 mg below 2000 K, which is about the limit of the balance detection. An observed increase of 0.30 mg ($.004\%$) at 2000 K and 0.40 mg ($.005\%$) at 2100 K was too small to apply a correction. (The assumption was made that the pickup is due to

carbon from the susceptor.) Samples B and C, which were not subjected to these high temperatures, did not change weight.

A small correction for the difference in the final calorimeter temperature from the reference temperature, 298.15 K, is necessary. The difference for the 2100 K run amounted to a maximum of 17-1/2 K and 2% of the net heat measured for that furnace temperature. These corrections were applied using the heat capacity evaluations from references [30, 37, 38] and are believed to be accurate to at least 5%, thus contributing an error to the corrected enthalpy of the sample no greater than 0.1%.

The results of the enthalpy measurements on molybdenum are tabulated in table 2. Each data point represents the result of two lifts, one on the empty capsule and another on a filled capsule. The empty capsule represents 54.4%, 54.2%, and 54.3% of the gross heat measured for the molybdenum filled capsule at 1175, 1600, and 2100 K respectively. The capsule itself was machined from a molybdenum rod claimed to be of 99.95% purity.

Two convenient empirical equations (each with only 4 or 5 disposable constants) have been selected to represent the enthalpy data relative to 298.15 K. The enthalpy values obtained from either equation differ from each other by less than 0.03% throughout the observed temperature range (well within the precision of our measurements). Values of heat capacities derived from either equation will differ by less than 0.25% up through 1900 K. At 2000 K and 2100 K the difference is 0.39% and 0.86% respectively.

$$H_T - H_{298.15} = A + BT + CT^2 + D \exp(-E/T), \text{ j/M} \quad (1)$$

for 1175 < T < 2100, K

where,

$$A = -6.18063 (10^3)$$
$$B = 21.6641$$
$$C = 3.24129 (10^{-3})$$
$$D = 1590 (10^3)$$
$$E = 16,000$$

The coefficients A, B, C, and D were determined by the least squares relative fit method for a selected value of E = 16,000. The sum of the squares of the relative deviations for values of E = 10,000 to E = 22,000 is essentially the same, hence E = 16,000 is taken to be "typical" of the sets of equation that can be used.

Table 2

Individual enthalpy measurements on molybdenum

Temperature T (IPITS-68, K)	Date of run (all in 1971)	Sample	Heat from sample to calorimeter at 298.15K (observed) (joules)	$H_T - H_{298.15}$ (observed) ^a (joules/mole)	Deviation from Eq (1) (%)
1170.4	May 3	A	2021.15	23635	+0.08
		C	3431.71	23585	- .14
1198.6	10	A	2090.62	24447	+ .00
	10	A	2089.30	24431	- .06
1299.1	7	A	2346.46	27439	- .01
		A	2347.79	27454	+ .05
	June 4	A	2342.19	27470	+ .11
		B	2348.05	27457	+ .06
1399.6	April 7	A	2610.01	30522	+ .05
		A	2609.50	30516	+ .03
1499.0	29	A	2874.85	33617	+ .01
	29	A	2876.27	33634	+ .06
	June 1	B	2864.41	33592	- .06
1601.6	April 5	A	3151.20	36850	- .15
		A	3149.64	36832	- .20
1699.1	2	A	3422.29	40021	- .24
		C	5823.24	40021	- .24
1699.2	May 24	B	3427.65	40201	+ .20
		B	3424.81	40168	+ .12
1800.7	5	A	3732.22	43643	+ .19
		A	3732.76	43649	+ .21
1899.6	April 22	A	4020.16	47010	- .13
		C	6828.85	46988	- .06
2001.2	9	A	4334.30	50684	- .01
		A	4337.44	50721	+ .06
2102.4	May 19	A	4657.48	54463	- .04
		A	4657.67	54465	- .03

^aMo: 1 mole = 95.94 g; density = 10.2 g/cm³. The sample mass was redetermined in each run.

The second equation is as follows, and is in a form often more convenient for computations not using a computer.

$$H_T - H_{298.15} = F(T - 298.15) + (G/2)(T^2 - 298.15^2) + (H/3)(T^3 - 298.15^3), \text{ j/M} \quad (2)$$

for $1175 < T < 2100, \text{ K}$

where,

$$F = 25.4998$$

$$G = -2.13386 (10^{-4})$$

$$H = 2.88650 (10^{-6})$$

The estimated standard deviation of the observed points for both equations (1) and (2) is 0.13%. No attempt has been made to join smoothly the ends of the equations (1) and (2) at 1175 nor at 2100 K with results reported by previous investigators. The spread in observed points by various investigators as shown in figures 1 and 2 shows that more accurate data are needed both from room temperature to 1175 K and also to higher temperatures (above 2100 K).

As an overall check on the apparatus, one measurement of $H_{1173.2} - H_{298.15}$ and one of $H_{1702.2} - H_{298.15}$ were made on a SRM-720 sample of synthetic sapphire after most of the measurements of Table 2 had been completed. The values obtained were 99,841.5 and 169,454 j/mole, respectively. The former value differs by 0.01% from a determination made on this material by another more precise method [1, 39]. The latter value differs by 0.06% from previous determinations using our apparatus [1].

All furnace temperature is based on the International Practical Temperature Scale of 1968. Table 3C was prepared so that the readers, if they wish, can readily convert our values to the basis of the IPTS⁴⁸ scale, on which scale the preponderance of the investigators have reported their work on molybdenum.

Table 3A

Heat capacity and enthalpy of molybdenum^a

T (IPTS-1968, K)	C _p ^o (Joules/mole-K)	H _T ^o -H _{298.15} ^o (Joules/mole)
1173.15	29.29	23697
1200	29.47	24486
1250	29.81	25968
1300	30.16	27468
1337.58	30.42	28606
1350	30.52	28984
1400	30.88	30519
1450	31.26	32073
1500	31.65	33646
1550	32.06	35238
1600	32.49	36852
1650	32.93	38487
1700	33.40	40146
1750	33.90	41828
1800	34.42	43536
1850	34.96	45270
1900	35.53	47032
1950	36.13	48824
2000	36.76	50646
2050	37.42	52500
2100	38.11	54389

^a1 mole = 95.94 grams [31]

$$H_{298.15}^{\circ} - H_{273.15}^{\circ} = 594 \text{ joules/mole [30]}$$

This table was calculated from Eq (1).

Table 3B

Heat capacity and enthalpy of molybdenum^b

T (IPTS-1968, K)	C_p° (Cal/Mole-K)	$H_T^\circ - H_{298.15}^\circ$ (Cal/Mole)
1173.15	7.00	5664
1200	7.04	5852
1250	7.13	6207
1300	7.21	6565
1337.58	7.27	6837
1350	7.29	6927
1400	7.38	7294
1450	7.47	7666
1500	7.56	8041
1550	7.66	8422
1600	7.76	8808
1650	7.87	9199
1700	7.98	9595
1750	8.10	9997
1800	8.23	10405
1850	8.36	10820
1900	8.49	11241
1950	8.64	11669
2000	8.79	12105
2050	8.94	12548
2100	9.11	12999

^b1 cal = 4.1840 joules

1 mole = 95.94 grams [31]

 $H_{298.15}^\circ - H_{273.15}^\circ = 142 \text{ cal/mole [30]}$

This table is identical to Table 3A but in calorie units.

Table 3C

Corrections for molybdenum to convert to IPTS-48
and IPTS-68 scales. (See ref. [24])

Temp IPTS-68 or 48 (K)	Delta C_p (C_p) ₄₈ - (C_p) ₆₈ (joules/mole-K)	Delta H (H) ₄₈ - (H) ₆₈ (joules/mole)
1100	0.086	21.4
1150	.089	25.8
1200	.092	30.3
1250	.095	35.0
1300	.098	39.8
1350	.059	44.3
1400	.062	47.3
1450	.065	50.4
1500	.069	53.7
1550	.072	57.2
1600	.076	60.8
1650	.080	64.6
1700	.085	68.6
1750	.089	72.8
1800	.095	77.3
1850	.100	81.9
1900	.106	86.8
1950	.113	91.9
2000	.119	97.3
2050	.127	103.0
2100	.134	109.0

V. Comparison with Previous Investigators and Compilers

The high practical importance of the high-temperature thermal properties of molybdenum metal is reflected in the large number of experimenters who have reported measurements of its enthalpy or heat capacity. Table 4 summarizes, in approximately chronological order, all these investigations that we have found who report values in the temperature range of the present work (1170 - 2100 K). Most of this work employed either drop-type calorimetry (which measures relative enthalpy directly) or pulse-heating calorimetry (which measures the heat capacity). An exception is the work of Lowenthal, which used a.c. heating of the sample, and derived the heat capacity from its observed temperature fluctuations.

Figures 1 and 2 show a graphical comparison of our values with those of the earlier investigators. In Fig. 1 the base line represents our smooth values of enthalpy relative to 298.15 K as given by Eq (1) (Section IV), and the points represent the percentage deviations from this base of the individual unsmoothed values, including ours (all adjusted to 298.15 K whenever necessary). (Curves are given only in those cases where only smoothed values were reported.) Figure 2 shows total heat capacity vs temperature; the solid curve represents our smoothed values as given by the derivative of Eq (1), and the points are unsmoothed values, including ours. When the measurements were of enthalpy, the plotted values are simply $\Delta H / \Delta T$ from the unsmoothed enthalpies for pairs of successive temperatures (the curvature corrections are negligible in this case), with the following exception. The enthalpy values at relatively close temperatures were first averaged so as to make each interval ΔT as close to 100 K as practical, in order to afford a fairer comparison of precision from one investigator to another.

Figure 1 shows that the enthalpies of most of the other observers are generally lower than ours. The closer balance between positive and negative deviations of heat capacity (Fig. 2) is due partly to the fact that this graph, unlike Fig. 1, includes those observers who did not measure enthalpy but only heat capacity. In Fig. 2 the majority of points lie within $\pm 5\%$ of our curve, and almost all lie within $\pm 10\%$. The deviations from our results of the smoothed values of enthalpy and heat capacity adopted by three sets of well-known recent compilers are shown in Table 5. Since these adopted values are based on much of the work (except the more recent) represented in Figs. 1 and 2, they reflect some of the same trends. Nevertheless, Figs. 1 and 2 are actually more revealing: they show graphically the wide spread among some individual observers, and at the same time they suggest that in some cases poor agreement is largely attributable to poor precision.

VI. Discussion of Errors

The relatively good precision of our enthalpy measurements is shown in the last column of Table 2 and in Fig. 1, and the small degree to which the precision limits the reliability of our results (including our claim

Table 4

Outline of reported measurements of the enthalpy or heat capacity
of molybdenum metal above 1000 K

Authors	Reference	Year	Method	Temp. Range (K)	Remarks
Wüst <u>et al.</u>	[2]	1918	Drop	273 - 1773	--
Jaeger & Veenstra	[3]	1934	Drop	565 - 1828	--
Jaeger & Veenstra	[4]	1934	Drop	273 - 1673	Only smoothed values reported.
Redfield & Hill	[5]	1951	Drop	481 - 1359	Enthalpy error, <4%(estimated).
Kothen	[7]	1952	Drop	1103 - 2623	--
Lucks & Deem	[6]	1956	Drop	306 - 1882	Arc-melted Mo. Agreed on H of Al ₂ O ₃ with NBS: ±0.3%(mean). 300 - 1100 K.
Fieldhouse <u>et al.</u>	[8]	1956	--	804 - 1898	--
Rasor & McClelland	[12]	1960	Pulse heating	1100 - 2800	Mo arc-melted. 0.35% impurity reported.
Lehman	[14]	1960	Pulse heating	300 - 2800	Estimated error, 1-2.5% (C _p)
Kirillin <u>et al.</u>	[9,10]	1961	Drop	972-2610	0.05% impurity (spectrochem.)
Lazareva <u>et al.</u>	[11]	1961	Drop	1154 - 2462	0.02% impurity stated.
Taylor & Finch	[16,28]	1961, 1964	Pulse heating	200 - 2860	Estimated C _p error: <4%<2400K, <7%>2400K.
Pool <u>et al.</u>	[13]	1962	--	300 - 1300	--
Rudlin <u>et al.</u>	[17]	1962	Pulse heating	1550 - 2175	Estimated accuracy, ±10% (C _p).
Lowenthal	[15]	1963	T oscillations, a.c. heating	1288 - 2015	Estimated: 0.07% impurity, 0.5-1.5% C _p error.
Conway <u>et al.</u>	[22]	1964	--	1267 - 2628	--
Kirillin <u>et al.</u>	[18]	1968	Drop	1453 - 2834	--
Chekhovski & Petrov	[29]	1968	Drop	?	--
Chekhovski <u>et al.</u>	[20]	1970	Drop	2094 - 2869	Sample suspended in furnace by levitation.
Cezairliyan <u>et al.</u>	[21]	1971	Pulse heating	1900 - 2800	<0.05% impurity (spectrochem.), 2-3% C _p error estimated.
Ishihara & Douglas	This report	1971	Drop	1170 - 2102	3 high-purity samples

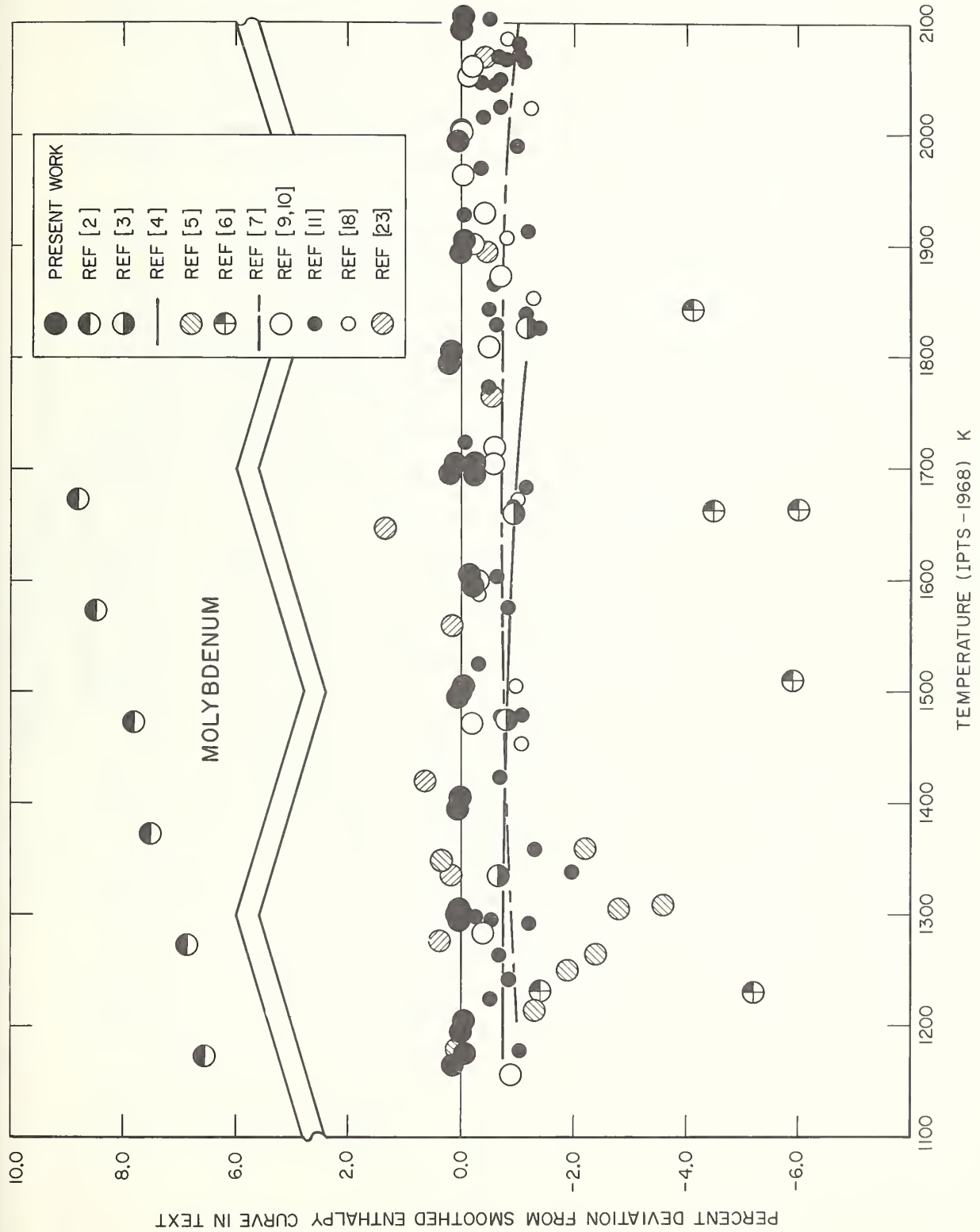


Figure 1. Comparison of molybdenum $H_T - H_{T=298.15}$ values of various investigators

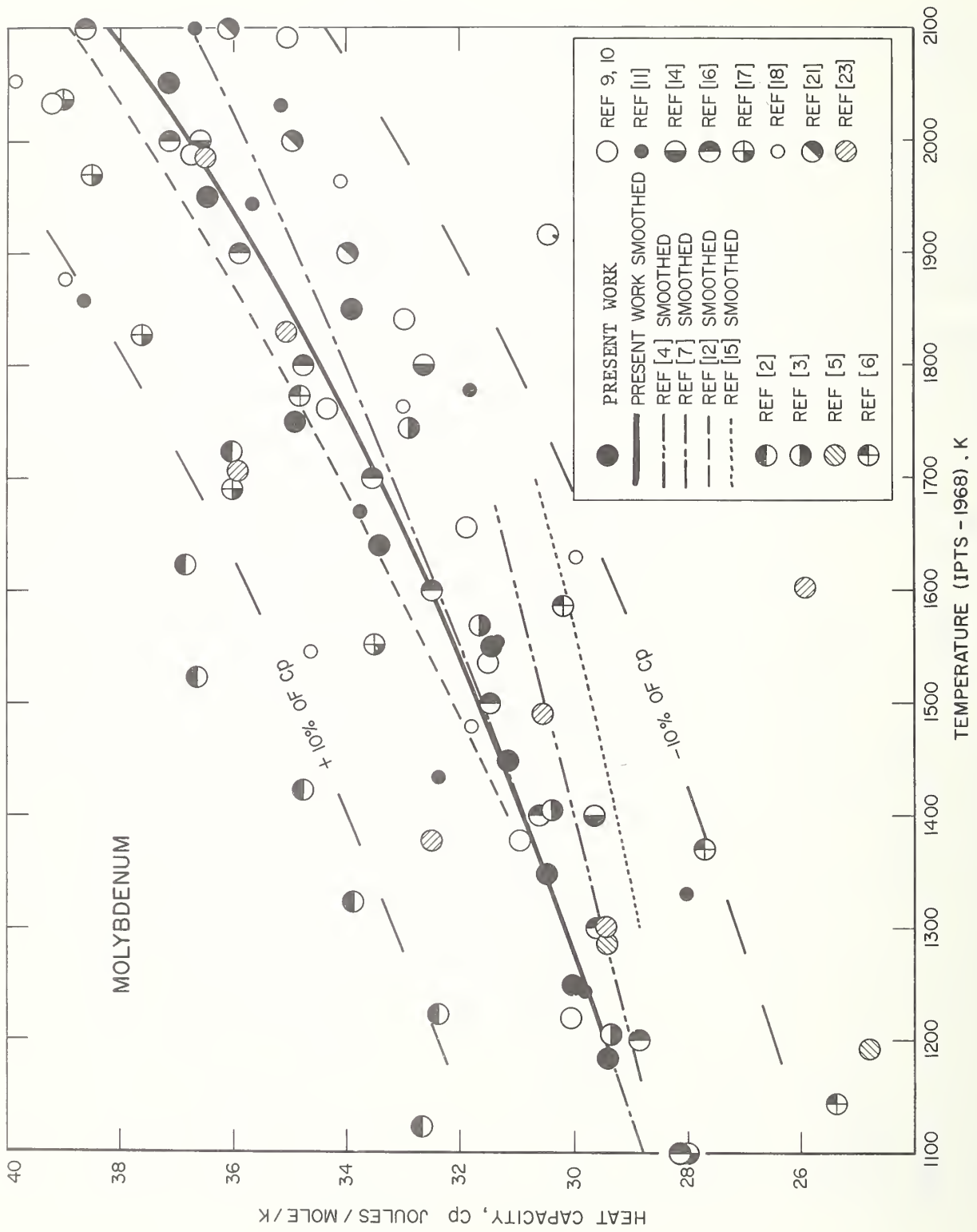


Figure 2. Comparison of molybdenum heat-capacity values of various investigators.

Table 5

Percentage deviation of the values of enthalpy and heat capacity of molybdenum adopted by various compilers from those of the present work (Eq 1)

Temperature T (K)	Enthalpy, $H_T - H_{298.15}$		Heat Capacity, C_p			
	Kelley [26] (%)	Hultgren et al. [25] (%)	JANAF [27] (%)	Kelley [26] (%)	Hultgren et al. [25] (%)	JANAF [27] (%)
1200	-1.2	-1.0	-0.6		+0.2	-2.0
1300	-1.0	-0.9	-0.7	+1.0	+0.3	-2.0
1400	-0.8	-0.7	-0.8	+0.7	+0.6	-1.7
1500	-0.7	-0.6	-0.9	+0.9	+0.5	-1.4
1600	-0.5	-0.5	-0.9	+0.9	+0.2	-1.3
1700	-0.4	-0.5	-1.0	0.0	-0.3	-1.2
1800	-0.4	-0.5	-1.0	-1.2	-1.0	-1.3
1900	-0.6	-0.6	-1.0	-2.6	-2.0	-1.6
2000	-0.7	-0.7	-1.1	-3.6	-3.3	-2.0
2100	-1.0	-1.2	-1.1			-2.6

that Eq (1) or (2) suitably represents the data) can be readily judged. As usual, the estimation of systematic errors is difficult, but in view of the main purpose of the work stated in the Introduction -- to arrive at definitive values -- an attempt should be made. We can do so more completely after the measurements on molybdenum are made in the adjoining temperature ranges 273 - 1170 K and 2100 - 2500 K, and after the samples have been finally analyzed and the most critical instruments recalibrated. Meanwhile, the following error analysis considers the contribution of all important presently known sources of error to our measurements.

In the present type of measurements, the sample-mass determination and energy measurement (the calorimetry, and accounting for the heat lost by the sample during its transfer to the calorimeter) are of course fundamental, and capable of introducing serious error. However, in our work these errors are believed to be relatively negligible, and we limit ourselves to considering the two sources of error in enthalpy measurement at high temperatures believed to be predominant -- (1) the effects of the sample impurities, and (2) the errors in measuring the average temperature of the sample in the furnace.

(1) Effects of sample impurities -- Impurities (if not adequately corrected for) may introduce error in two ways: (a) by making the sample one or more phases whose average heat capacity per unit mass differs from that of the pure nominal material (molybdenum), and (b) by generating phase changes with appreciable latent heats. The simplest way to estimate the order of magnitude of the error from (a) is to make the roughly valid assumption that all the impurity elements have the same atomic heat capacities as molybdenum, so that if one were to replace all the impurities atom for atom by molybdenum, the percentage change in sample mass should measure roughly the percentage change in both enthalpy and heat capacity. The effect on this basis is illustrated by the use of the comprehensive Table 1B: the "elements measured" indicate a net error of +0.02%, and the upper limits of the "elements showing interference", an additional +0.03%, or a total error of +0.05%. (Hydrogen, which was not analyzed for, could produce the greatest error: e.g., 0.01% by weight in molybdenum would produce an error of the order of +1%. It is believed likely, however, that hydrogen was at a much lower level.) As noted in Section II, the "electronic characterization" of Samples A and B was interpreted as indicating an order of magnitude greater impurity level (0.2% by weight) than did the other two analytical techniques, but the impurities and their amounts postulated in this interpretation (see Section II) would on the above basis introduce a total error of only +0.01%, owing to their high atomic weights.

Some impurities are capable of introducing much greater error of Type (b) (latent heats of extraneous phase changes), whose magnitude cannot really be estimated without specific knowledge as to what the phase changes are. It seems likely, however, that for a substance like molybdenum which when pure is believed to undergo no transitions, samples with as little impurities as ours would display phase heterogeneity in only very narrow

temperature ranges, with no thermal effects (except those of Type (a) discussed above) at other temperatures. By representing our smoothed data by a strictly monotonic function [Eq (1) or (2)], any such "transistory" effect should have been essentially eliminated.

We conclude from the above that the errors introduced into our enthalpies and heat capacities of molybdenum by the impurities were many times smaller than those caused by temperature errors (see below).

(2) Effects of temperature errors -- If the systematic error in measuring the average temperature of the sample in the furnace, and its variation with temperature, could be determined reliably, the corresponding effects on the calculated values of enthalpy and heat capacity could then be evaluated straightforwardly.

An approximation often made is that the error (expressed in K -- i.e., °K) in pyrometrically determined temperatures such as those of our data is approximately proportional to the square of the absolute temperature. The estimated pyrometric uncertainties listed in Section III approximately obey that temperature dependence, and interpolate to an uncertainty of 2.5 K at 2300 K. To this should be added the additional error in realizing the average temperature of the sample. On the basis of an earlier determination of the temperature profile of the furnace core at 2300 K, we made with simplifying assumptions a rough calculation which indicated that near 2300 K the temperature of the bottom of the sample container (which is what the pyrometer measures) may be as much as 0.5 K different from the average temperature of the sample. Assuming a total error of 3K at 2300 K, and of the same sign and proportional to the square of the temperature at other temperatures, the smoothed results of our measurements (as given by Eq (2), e.g.) indicate a corresponding error in the $H_T - H_{298.15}$ varying from 0.1% at 1200 K to 0.15% at 2000 K, and an error in C_p varying from 0.15% at 1200 K to 0.3% at 2000 K. (Some additional error in C_p near the ends of the temperature range investigated results when, as here, C_p is determined by differentiation of an empirical function representing the measured enthalpy.)

Some of the error in using a pyrometer may be a function of the pyrometer current. Hence, when in proceeding to successively higher temperatures a point is reached where a stronger filter (calibrated) is interposed and the adjusted pyrometer then abruptly drops to a much lower current, it is worthwhile to examine a regularly varying property to see whether a discontinuity in the measured values appears at that temperature. Our first such occurrence was between 1500 and 1600 K; however, the apparent discontinuity in our unsmoothed values for the enthalpy of molybdenum appears to be no greater than 0.1% if indeed it is outside the precision (see Fig. 1). (Our second such occurrence was between 2000 and 2100 K; but because of the marked curvature of the heat capacity of molybdenum in that temperature region and our lack of data at more than one temperature using the stronger filter, any search for an enthalpy discontinuity in that case would be unreliable.)

As stated in Section IV, the enthalpy of standard-sample aluminum oxide was measured once at 1170 K and once at 1700 K near the end of the present series of measurements on molybdenum. The agreement with the highly consistent earlier results (to 0.05% or better) is evidence that the pyrometry did not appreciably deteriorate during the measurements on molybdenum.

To summarize, we have no evidence thus far to believe that the errors in the smoothed values of enthalpy and heat capacity of molybdenum reported in this chapter are likely to exceed 0.5 and 1%, respectively, up to about 2000 K.

Although the error in sample-temperature measurements certainly seems to be the most serious one in measurements of this kind, and it is safe to guess that many investigators have seriously underestimated their systematic temperature errors, one is justified in wondering whether a substantial part of the large disagreement among the many investigators of the enthalpy and heat capacity of molybdenum is due to a real difference between some samples of the pure annealed metal. Our data on molybdenum include an enthalpy measurement on a sample with a very different history (Sample C, triple-zone-refined) at each of the temperatures 1170, 1699, and 1900 K. The agreement within 0.2% between Samples A and C at these three temperatures is some evidence, however circumstantial, that the massive annealed metal has reproducible enthalpies and heat capacities.

Several investigators have fitted their data for the enthalpy and heat capacity of molybdenum at high temperatures with the inclusion of a simple exponential term whose argument can be interpreted as the energy of some reversible process in the metal (e.g., vacancy formation and migration, but so far not satisfactorily identified -- see, e.g., Ref. [21]). Without pretending to throw any light on this interesting subject, we merely point out that our precise data (though not extending above 2100 K yet) were fit almost equally well by values of the constant E in Eq (1) varying from 0.9 to 1.9 eV. This range encompasses most of the values arrived at by others, and our arbitrary choice of 1.4 eV in Eq (1) (equivalent to $E = 16,000$ K) thus has no quantitative physical significance.

VII. Acknowledgements

The following professional staff of the National Bureau of Standards made substantial contributions to the work reported in this chapter. With the help of one of us (S.I.), E. D. West (NBS, Boulder) earlier designed and constructed the calorimetric apparatus. R. E. Michaelis (Office of Standard Reference Materials) furnished Samples A and B, and coordinated their various characterizations. The spectrochemical analyses were performed

by Virginia C. Stewart (Samples A and B) and Martha M. Darr (Sample C); the mass spectrometry, by C. W. Mueller and P. J. Paulsen; and the electronic characterization and its interpretation, by V. A. Deason and R. L. Powell (NBS, Boulder). E. Lewis, Jr. carried out the pyrometer calibrations; and D. A. Ditmars and M. L. Reilly provided a computer code and many of the bibliographic sources.

VIII. References

- [1] Certificate of Standard Reference Material 720, Synthetic Sapphire (Al_2O_3), Office of Standard Reference Materials, National Bureau of Standards, Washington, D. C. 20234 (Aug. 26, 1970).
- [2] F. Wüst, A. Meuthen, and R. Durrer, *Forsch. Gebiete Ingenieurw.* 204, 1-59 (1918).
- [3] F. M. Jaeger and W. A. Veenstra, *Rec. Trav. Chim.* 53, 677-687 (1934).
- [4] F. M. Jaeger and W. A. Veenstra, *Proc. Acad. Sci. Amsterdam* 37, 61-76 (1934).
- [5] T. A. Redfield and J. H. Hill, U. S. Atomic Energy Comm.; ORNL-1087, 1-9 (1951).
- [6] C. F. Lucks and H. W. Deem, WADC Tech. Rept. 55-496, 43 (1956).
- [7] C. W. Kothen, Dissertation, Ohio State Univ., Columbus, O. (1952).
- [8] I. B. Fieldhouse, J. C. Hedge, J. I. Lang, A. N. Takata, and T. E. Waterman, WADC Tech. Rept. 55-495 (1956).
- [9] V. A. Kirillin, A. E. Sheindlin, and V. Ya. Chekhovskoi, *Dokl. Akad. Nauk. SSSR* 139, 645-647 (1961) (English transl. pp. 557-559).
- [10] V. A. Kirillin, A. E. Sheindlin, and V. Ya. Chekhovskoi, *Int. J. Heat, Mass Transfer* 5, 1-9 (1962).
- [11] L. S. Lazareva, P. B. Kantor, and V. V. Kandyba, *Fiz. Met. i Metall* 11, 628-629 (1961) (English: *Phys. Metals and Metallog.* 11, 133-134 (1961)).
- [12] N. S. Rasor and J. D. McClelland, *J. Phys. Chem. Solids* 15, 17-26 (1960).
- [13] M. J. Pool, R. W. Sullivan, and C. E. Lundin, Quarterly Status Rept. No. 9, Contract AF 19(604)-7222, U. of Denver, Denver Research Inst., Denver, Colo. (1962).
- [14] G. W. Lehman, WADD Tech. Rept. 60-581 (1960) (19 pp).

- [15] G. C. Lowenthal, Aust. J. Phys. 16, 47-67 (1963).
- [16] R. E. Taylor and R. A. Finch, Atomics International NAA-SR-6034 (1961) (32 pp).
- [17] R. L. Rudkin, W. J. Parker, and R. J. Jenkins, Temp. Meas. Control Sci. Ind., Vol 3, part 2, 523-534 (1962).
- [18] V. A. Kirillin, A. E. Sheindlin, V. Ya. Chekhovskoy, and V. A. Petrov, ASME, Proc. 4th Symp. Thermophys. Prop., pp. 54-57, U. of Md., College Park, Md. (J. R. Moszynski, ed.) (1968).
- [19] A. E. Sheindlin, V. Ya. Chekhovskoi, and E. E. Shpil'rain, High Temp.-High Press. 2, 1-15 (1970).
- [20] V. Ya. Chekhovskoi, A. E. Sheindlin, and B. Ya. Berezin, High Temp.-High Press. 2, 301-307 (1970).
- [21] A. Cezairliyan, M. S. Morse, H. A. Berman, and C. W. Beckett, J. Research NBS 74A, 65-92 (1970).
- [22] J. B. Conway, R. A. Hein, R. M. Fincel, Jr., and A. C. Losekamp, Rept. TM 64-2-8, General Electric Co., NSP (1964).
- [23] M. Hoch, High Temp.-High Press. 1, 531-542 (1969).
- [24] T. B. Douglas, J. Research NBS 73A, 451-470 (1969).
- [25] R. Hultgren, R. L. Orr, P. D. Anderson, and K. K. Kelley, "Selected Values of Thermodynamic Properties of Metals and Alloys," Univ. of Calif., Berkeley, Calif. (table for Mo: March 1965).
- [26] K. K. Kelley, U. S. Bur. Mines Bull. 584, p. 125 (1960).
- [27] JANAF Thermochemical Tables (table for Mo: Dec. 31, 1966).
- [28] R. E. Taylor and R. A. Finch, J. Less-Common Metals 6, 283-294 (1964).
- [29] V. Ya. Chekhovski and V. A. Petrov, Teplofiz. Vysokikh Temperatur 6, 752 (1968).
- [30] M. L. Reilly and G. T. Furukawa, "Critical Analysis of the Heat Capacity Data of the Literature and Evaluation of Thermodynamic Properties of Cr, Mo, and W from 0 to 300 K," NSRDS-NBS (to be published).
- [31] Chemical and Engineering News, p. 43 (Nov. 26, 1961).

- [32] D. C. Ginnings, "Precision Measurement and Calibration on Heat," NBS special publication 300 ,6, 220 (1970).
- [33] NBS Report 9028, U. S. Air Force Order No. OAR 65-8, 71 (Jan, 1966).
- [34] NBS Report 9803, U. S. Air Force, OSR Order No. ISSA-67-6, 80 (Jan, 1968).
- [35] NBS Report 9601, U. S. Air Force Order No. ISSA-67-6, 55 (July, 1967)
- [36] NBS Technical Note 494, ARPA-NBS Program, p. 18 (Sept., 1969).
- [37] K. F. Starret and W. E. Wallace, J. Am. Chem. Soc. 80, 3176 (1958).
- [38] G. T. Furukawa, private communication.
- [39] D. A. Ditmars and T. B. Douglas, J. Res. NBS 75A, 5 (Sept.-Oct. 1971)

THE HEAT OF FORMATION OF $\text{MoF}_6(\ell)$ BY
SOLUTION CALORIMETRY; ANALYSIS OF PRELIMINARY EXPERIMENTS

R. L. Nuttall, K. L. Churney, M. V. Kilday

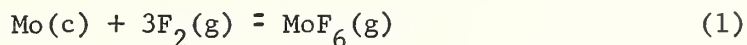
Introduction

This laboratory is currently engaged in a program to determine the heats of formation of the lower fluorides (and the oxy-fluorides) of molybdenum. Since it was deemed unlikely that the compound currently of interest, $\text{MoF}_5(\text{c})$, could be formed in reasonable quantities by direct reaction of $\text{F}_2(\text{g})$ with $\text{Mo}(\text{c})$, two other reaction schemes are being used which involve either $\text{MoF}_6(\text{g})$ or $\text{MoF}_6(\ell)$. The first, the method of choice, is the reaction of $\text{MoF}_5(\text{c})$ with $\text{F}_2(\text{g})$ to form $\text{MoF}_6(\text{g})$. Because the available quantity of $\text{MoF}_5(\text{c})$ and the heat of reaction ^{1/} were expected to be small, a second, more sensitive, scheme was deemed necessary either as a check or as an alternative route. The method selected was the heat of solution of $\text{MoF}_6(\ell)$ in base and $\text{MoF}_5(\text{c})$ in base containing an oxidant based on the apparent success of this method with $\text{MoCl}_5(\text{c})$ [3], for example. Both methods require an accurate value for the heat of formation of $\text{MoF}_6(\ell)$ or $\text{MoF}_6(\text{g})$. Unfortunately, the heat of formation of $\text{MoF}_6(\text{g})$ derived by

^{1/}
-24 ± 15 kcal per mol $\text{MoF}_5(\text{c})$ based on an estimated heat of formation of $\text{MoF}_5(\text{c})$ [1] and the heat of formation of $\text{MoF}_6(\text{g})$ [2].

solution calorimetry differs from that determined by direct combination of the elements.

Settle et al [2] obtained -372.35 ± 0.22 kcal/mol for the reaction



by burning molybdenum sheet suspended on a nickel rod in 14-15 atm of $\text{F}_2(\text{g})$ in a nickel combustion bomb. Correction for unburned molybdenum ($\leq 4\%$ of initial sample weight) could be made unambiguously and accurately. While the corrections for the formation of $\text{MoF}_5(\text{c})$ (typically $0.10 \pm 0.05\%$ of molybdenum burned), $\text{NiF}_2(\text{c})$ formed due to corrosion, and impurities in the original sample were somewhat uncertain, all made relatively small contributions to the resulting value of $\Delta H_f^\circ [\text{MoF}_6(\text{g})]$ (0.003%, 0.059%, and 0.087% on the average, respectively). Recalculation of the latter two corrections using newer selected values for heats of formation (see [2,4]) yielded a value of -372.29 kcal [5] for reaction (1).

The only other determination of the heat of formation of $\text{MoF}_6(\ell)$ was made by Myers and Brady [6] by measuring the heats of solution of $\text{MoF}_6(\ell)$ and $\text{MoO}_3(\text{c})$ in 0.531 N aqueous NaOH and of NaF(c) in 0.531 N aqueous NaOH containing molybdate. These authors calculated their results according to the reaction scheme given by eq (2)

$$\text{MoF}_6(\ell) + 8\text{NaOH(soln)} = \text{Na}_2\text{MoO}_4(\text{soln}) + 6\text{NaF(c)} + 4\text{H}_2\text{O(soln)} \quad (2)$$

to obtain -388.6 ± 4 kcal for the heat of formation of $\text{MoF}_6(\ell)$. Recalculation of their results using newer selected values [2,4] of the heat of formation $[\text{NaOH} \cdot 515\text{H}_2\text{O}](\text{soln})$, $\text{MoO}_3(\text{c})$, and NaF(c) yields a value of -393.2 kcal mol⁻¹. Using the selected value of

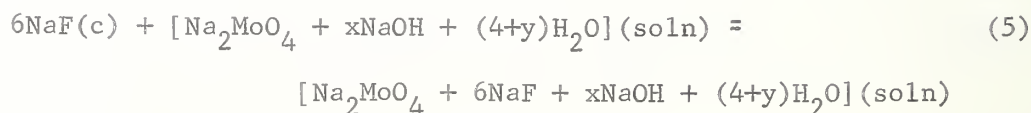
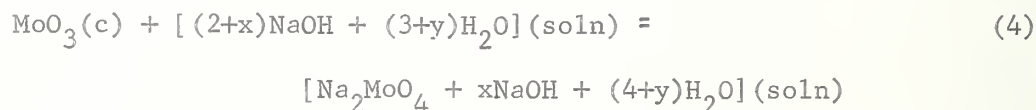
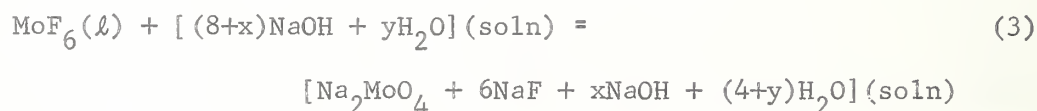
6.66 kcal/mol for the heat of vaporization of $\text{MoF}_6(\ell)$ [5] (based on the measurements of Ruff and Ascher [7], Cady and Hargreaves [8], and Osborne et al [9]), one obtains -386.6 ± 4 kcal for reaction (1). The uncertainty in this result greatly exceeds any error due to the failure of Myers and Brady to maintain rigid stoichiometry. The result is 14.3 ± 4 kcal more negative than that obtained by Settle et al.

Because of this discrepancy and particularly because solution calorimetry involving $\text{MoF}_6(\ell)$ is also to be used to determine the heat of formation of $\text{MoF}_5(\text{c})$, it was considered necessary to repeat the measurements of Myers and Brady. We considered it more likely that the error lay in their work than in that of Settle et al.

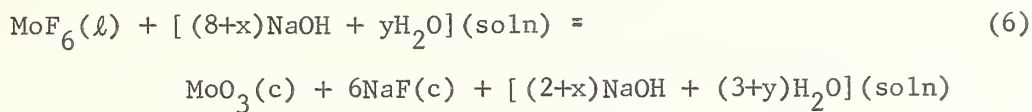
In the following three sections an outline of the reaction scheme for the solution experiments is given, a brief summary of experimental method, and a short summary and discussion of results.

Reaction Scheme of Solution Experiments

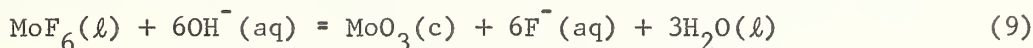
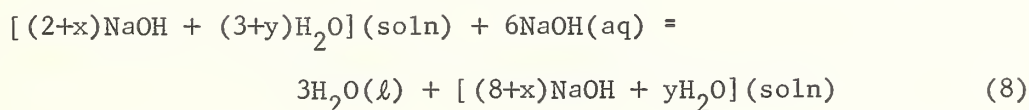
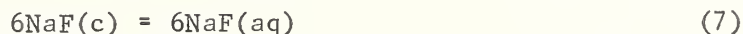
The actual reaction scheme used by Myers and Brady involves the following three reactions:



If rigid stoichiometry is maintained so the value of x and y are the same for all reactions, one obtains for the sum of reactions (3) - (4) - (5):



Reaction (6) can be simplified by adding reactions (7) and (8) to give (9)



Thus, the heat of reaction (9), ΔH_9 , is given by

$$\Delta H_9 = \Delta H_6 + \Delta H_7 + \Delta H_8$$

where ΔH_6 is determined experimentally and is equal to

$$\Delta H_6 = \Delta H_3 - \Delta H_4 - \Delta H_5$$

The heat of formation of $\text{MoF}_6(l)$, $\Delta H_f^\circ[\text{MoF}_6(l)]$, would then be given by the heats of formation of the other species in reaction (9) and ΔH_9 :

$$\begin{aligned} \Delta H_f^\circ[\text{MoF}_6(l)] = & \Delta H_f^\circ[\text{MoO}_3(c)] + 3\Delta H_f^\circ[\text{H}_2\text{O}(l)] + 6\Delta H_f^\circ[\text{F}^-(aq)] \\ & - 6\Delta H_f^\circ[\text{OH}^-(aq)] - \Delta H_9 \end{aligned}$$

Apart from experimental uncertainties, the uncertainty in the assumed value for heat of formation of $\text{F}^-(aq)$ will cause the

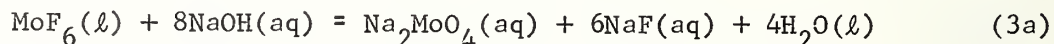
largest systematic error in the heat of formation of $\text{MoF}_6(\ell)$.

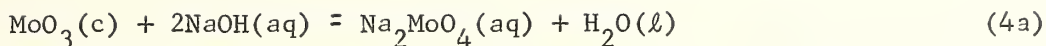
The advantage of carrying out reactions (3) through (5) with rigid stoichiometry is that it eliminates any need for non-existent heat of dilution data for basic molybdate solutions with and without fluoride. Further, the correction terms, ΔH_7 and ΔH_8 , added to ΔH_6 are small and unambiguous. The value selected by Parker [10] for $\Delta H_7/6$, is $+0.218 \pm 0.010$ kcal/mol. (The selection was based upon very few experimental measurements of the integral heat of solution and estimated of heats of dilution). The value of ΔH_8 when $y \gg 3$ is given by

$$\Delta H_8 = 6 \left[1 - \frac{(1+x/2)}{y} \right] \phi_L(y) + 3 \frac{(3+x)}{y} \bar{L}_2(y)$$

where $\phi_L(y)$ and $\bar{L}_2(y)$ are the relative apparent molal enthalpy and relative partial molal enthalpy of solute, respectively, of $[\text{NaOH} + y\text{H}_2\text{O}](\text{soln})$. The maximum value of $\Delta H_8/6$ when $y > 100$ (molality less than 1.5) and $x \ll y$ is $0.112 \text{ kcal mol}^{-1}$.

Neither the experiments carried out by Brady and Myers nor our preliminary work comply with the rigid stoichiometry required to write reaction (6). Further, intercomparison of our preliminary work with that of Myers and Brady and other workers is more informative if done on reactions (3) through (5) separately. Thus, we will consider the heat of reactions (3) through (5) individually. Reactions (3) and (4) will be corrected, if possible, by estimates for dilution effects to yield the corresponding heats of reaction at infinite dilution ^{for} reactions (3a) and (4a), respectively.





Comparison of our limited work (single experiment) and the experiment of Myers and Brady for reactions similar to reaction (5) are compared to the selected value of ΔH_7 to shed light on the difference in dilution heat effects of basic molybdate solutions with and without fluoride.

Experimental Procedure

For the preliminary experiments described here CP grade MoO_3 and NaF were used without further purification. The MoF_6 was purchased from Ozark-Mohoning Company and was purified by trap-to-trap distillation in an all-metal system. The MoF_6 was then transferred by distillation into Kel-F (polychlorotrifluoroethylene) bulbs for introduction into the calorimeter. These bulbs were made from 1/2-inch lengths of 3/8-inch I.D. tubing by sealing on end, windows of 0.005-inch film and a 1/8-inch tube sidearm. The bulbs were filled through the sidearm which was then sealed off.

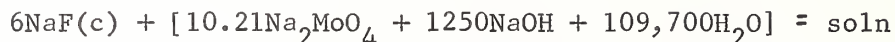
The calorimeter is a precise adiabatic calorimeter which has been described previously [11], [12]. The interior of the calorimeter vessel is all platinum. For the $\text{MoF}_6(\ell)$ solution experiments, the sample holder was replaced by a Monel holder for the Kel-F bulbs. A Monel cutter was used to cut out the end windows for starting the solution reaction.

The energy equivalent of the calorimeter was determined using electrical heating before and again after each solution experiment.

Analysis of Results

A) Heat of Solution of NaF(c)

We have carried out a single experiment corresponding to the reaction



for which we obtain $\Delta H(25.0\text{C}) = +1.33 \text{ kcal}$. Myers and Brady [6] studied the approximate reaction



for which they obtained $\Delta H(25.0\text{C}) = +0.54 \text{ kcal}$. The selected value for ΔH_7 [10], is $+1.308 \pm 0.06 \text{ kcal}$. Because of the larger ratios of moles of NaOH and Na_2MoO_4 to moles NaF(c) in our experiment than in Myers and Brady, one would expect our result to be in closer agreement with ΔH_7 .

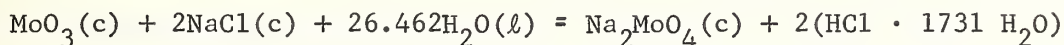
B) Heat of solution of MoO₃(c)

Three experiments were carried out for the heat of solution of $\text{MoO}_3(\text{c})$ according to reaction (3) at an average temperature of 24.9 C which are summarized below along with the results of Myers and Brady (M.B.)

Run	Normality of NaOH	$\frac{\text{Moles NaOH}}{\text{Moles MoO}_3}$	$\frac{\text{Moles H}_2\text{O}}{\text{Moles NaOH}}$	$-\Delta H_4$ (kcal)
1	0.706	50.8	78.7	18.69
2	0.706	120.1	78.7	18.56
3	0.643	124.4	86.4	<u>18.69</u>
				18.65±0.08
M.B.	0.1075	24.9	515	17.6

The value for ΔH_{4a} of reaction (4a) based on Parker's selection [2] is -18.80 kcal/mol . This value is based on the heats of solution of

Graham and Hepler [13] of the same number of moles of $\text{MoO}_3(\text{c})$ and $\text{Na}_2\text{MoO}_4(\text{c})$ in 0.531 N NaOH and $\text{Na}_2\text{MoO}_4(\text{c})$ in very dilute base and water and the work of Koehler et al [14] who studied the following reaction by solution calorimetry.



Recalculation of both results in accordance with newer selected auxiliary data yields ΔH_{4a} for the heat of formation of $\text{MoO}_3(\text{c})$ minus that of $\text{Na}_2\text{MoO}_4(\text{c})$ of -172.72 ± 0.07 kcal and -172.98 ± 0.11 kcal from Graham et al and Koehler et al, respectively. Parker selected [5] a value of -172.81 kcal/mol to which we assign an uncertainty of ± 0.12 kcal. Use of the value of $\Delta H_{\infty}^{\circ}$ of $\text{Na}_2\text{MoO}_4(\text{c})$ of -2.4 kcal selected by Hepler et al [13] and selected values of the heat of formation of $\text{NaOH}(\text{aq})$ and $\text{H}_2\text{O}(\ell)$ yields the value selected for ΔH_{4a} .

Recalculation of the results of Graham and Hepler for the heat of solution of $\text{Na}_2\text{MoO}_4(\text{c})$ in very dilute base water or assuming that Φ_L for $\text{Na}_2\text{MoO}_4(\text{aq})$ is the same as for $\text{Na}_2\text{SO}_4(\text{aq})$ yielded a value of $\Delta H_{\infty}^{\circ} = -2.41 \pm 0.05$ (av. dev.) kcal. Use of this value and the pairs of experiments reported by Grahams et al [13] for $\text{MoO}_3(\text{c})$ and $\text{Na}_2\text{MoO}_4(\text{c})$ yielded a separate check of Parker's selection as well as a correction to infinite dilution for the heat of solution of $\text{MoO}_3(\text{c})$ as shown below

Run	$\frac{\text{Moles NaOH}}{\text{Moles MoO}_3(\text{c})}$	$\frac{\text{Moles H}_2\text{O}}{\text{Moles MoO}_3(\text{c})}$	ΔH_3 kcal	Corr. to ∞ kcal	ΔH_{3a}^* kcal
1	111.2	104.5	-18.52	-0.50	-19.02
2	205.2	104.5	-18.70	-0.21	-18.91
3	247.7	52.23	-18.75	-0.22	-18.97
4	160.4	104.5	-18.69	-0.31	-19.00
5	192.2	104.5	-18.66	-0.15	-18.81

* The sum of columns 4, the observed value, and 5, the dilution correction.

The average ΔH_{3a} is -18.94 ± 0.07 (av. dev.) kcal with an estimated uncertainty of ± 0.15 kcal as compared with -18.81 kcal selected by Parker (which has a comparable uncertainty). Comparison of this table with our preliminary results suggest the heat of dilution to infinite dilution is of the order of -0.2 kcal to yield an estimated value from our results of -18.85 ± 0.15 kcal for reaction (3a). It seems apparent that the result obtained by Myers and Brady is too positive particularly if it is compared with the results of Koehler et al [14] for the heat of solution of $\text{MoO}_3(\text{c})$ in a solution of the approximate composition $18[\text{NaOH} \cdot 278\text{H}_2\text{O}]$ of -18.450 ± 0.030 kcal.

C) Heat of Solution of $\text{MoF}_6(\ell)$

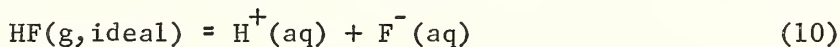
Three measurements of the heats of solution of $\text{MoF}_6(\ell)$ were carried out for reaction (3) at 24.69 ± 0.05 C, one at 25.55 C, and another at 29.62 C as summarized below for reaction (3) along with results of Myers and Brady (M.B.).

Run	Normality of NaOH	Moles NaOH Moles $\text{MoF}_6(\ell)$	Moles H_2O Moles NaOH	Temperature (C)	$-\Delta H_3$ (kcal)
1	.643	162.0	86.4	29.62	165.1
2	.643	172.8	86.4	24.67	168.0
3	.643	203.4	86.4	24.63	170.7
4	.643	120.2	86.4	24.78	168.2
5	.706	88.9	78.7	25.55	171.8
M.B.	.531	513	515	25.0	154.7

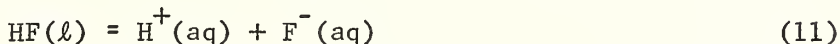
The value for ΔH_{3a} of reaction (3a) based on the selected values [2,4] of heats of formation is -170.05 kcal. The heat of formation of

MoO₄⁻(aq) is based on comments in section B and the heat of formation of MoO₃(c) selected by Parker [5] of -178.08 kcal to which we assign an uncertainty of 0.08 kcal. The latter value is based on the work of Staskiewicz et al [15] (-177.99* ± 0.10 kcal) and Mah [16] (178.15* ± 0.11 kcal) rather than the earlier work of Delepine [17] (-167 kcal), Mixer [18] (-185 kcal), Moose and Parr [19] (-175.6 kcal) or Neumann et al [20] (-180.4 kcal). The selected value for the heat of formation of MoF₆(l) is the recalculated value of the results of Settle et al [1].

The selected value for the heat of formation of F⁻(aq) [4], -79.50 kcal, has been the subject of considerable controversy. A brief summary of the problem as of 1969 is given by Armstrong [21] and in 1971 by Vanderzee and Rodenburg [22]. The latter determined a value of -14.72 ± 0.10 kcal mol⁻¹ for the reaction at 25 C.



This value supports the value selected by Parker [10] of -14.70 kcal/mol. Recently, Smith et al [23] determined a value of -7.691 ± 0.030 kcal mol⁻¹ for the reaction at 25 C



Using the value of 7.231 ± 0.025 kcal mol⁻¹ for the heat of vaporization of HF(l) to HF(g, ideal) in its standard state determined by Vanderzee and Rodenburg [24], one obtains from the previous work of Vanderzee and Rodenburg on reaction (10) an alternative value for reaction (11) of -7.49 ± 0.10 kcal mol⁻¹. Recently, Settle et al [25] have completed a study of the heat of formation of HF(l) for which

* Recalculated

they obtain $-72.57 \pm 0.09 \text{ kcal mol}^{-1}$. In conjunction with the two more recent values for the heat of reaction (11), this yields values for the heat of formation of $\text{F}^{-}(\text{aq})$ of $-80.26 \pm 0.09 \text{ kcal mol}^{-1}$ (Smith et al) and $-80.06 \pm 0.14 \text{ kcal mol}^{-1}$ (Vanderzee and Rodenburg). The corresponding value of ΔH_{3a} for these values of the heat of formation of $\text{F}^{-}(\text{aq})$ would be -174.61 kcal and -173.41 kcal , respectively.

Estimating the dilution correction that must be added to our experimental values of ΔH_3 to obtain ΔH_{3a} to be at most of the order of -1 kcal , it appears that our preliminary results are not consistent with the more recent determinations of the heat of formation of $\text{F}^{-}(\text{aq})$. Nevertheless, our results do support a conclusion that the value for ΔH_3 determined by Myers and Brady is far too positive.

References

- [1] Settle, J. L., Feder, M., Hubbard, W. N., J. Phys. Chem. 5, 1337 (1961).
- [2] Wagman, D. D., Evans, W. H., Parker, V. B., Halow, I., Bailey, S. M., Schumm, R. H., Nat. Bur. Std. (U.S.) Tech Note 270-4 (1969).
- [3] Shchukarev, S. A., Vasil'kova, I. V., Sharupin, R. N., Vestnik Leningrad Univ. 14, No. 4, Ser. Fiz. i Khim., No. 1, 73-77 (1959).
- [4] Wagman, D. D., Evans, W. H., Parker, V. B., Halow, I., Bailey, S. M., Schumm, R. H., Nat. Bur. Std. (U.S.) Tech. Note 270-3 (1968).
- [5] Parker, V. B., Private Communication, Nat. Bur. Std. (U.S.), See Ref. [2].
- [6] Myers, O. E., Brady, A. P., J. Phys. Chem. 64, 591 (1960).
- [7] Ruff, O., Ascher, E., Z. Anorg. Chem. 196, 413 (1931).
- [8] Cady, G. H., Hargreaves, G. B., J. Chem. Soc. 1563 (1961).
- [9] Osborne, D. W., Schreiner, F., Malm, J. G., Selig, H., Rochester, L., J. Chem. Phys. 44, 2802 (1966).
- [10] Parker, V. P., Thermal Properties of Aqueous Uni-valent Electrolytes. National Standard Reference Data Series-NBS 2. U. S. Govt. Printing Office; Washington, D. C. 1965.
- [11] Kilday, M. V., Prosen, E. J., NBS Rept. 8306 (1964).
- [12] Kilday, M. V., Prosen, E. J., Wagman, D. D., NBS Rept. 10004 (1969).
- [13] Graham, R. L., Hepler, L. C., J. Amer. Chem. Soc. 78, 4846 (1956).

- [14] Koehler, M. F.; Pankratz, L. B.; Barany, R.; U. S. Bur. Mines Rept. Invest. 5973 (13p) 1962.
- [15] Staskiewicz, B. A.; Tucker, J. R.; Snyder, P. E.; J. Amer. Chem. Soc. 77, 2987 (1955).
- [16] Mah, A. D., J. Phys. Chem. 61, 1573 (1957).
- [17] Delepine, M., Bull. Soc. Chim. 29, 1166 (1903).
- [18] Mixter, W. G., Amer. J. Sci. 29, 488 (1910).
- [19] Moose, J. E.; Parr, S. W.; J. Amer. Chem. Soc. 46, 2656 (1924).
- [20] Neumann, B.; Kroger, C.; Kunz, H.; Z. anorg. und Allgem. Chem. 218, 379 (1934).
- [21] Armstrong, G. T., AFOSR Scientific Report AFOSR 69-2154 TR, NBS Report 10074, July 1 (1969).
- [22] Vanderzee, C. E.; Rodenburg, W. W.; J. Chem. Thermodynamics 3, 267 (1971).
- [23] Smith, P. N.; Johnson, G. K.; Hubbard, W. N.; Private Communication, Argonne Nat. Lab., March 1970.
- [24] Vanderzee, C. E.; Rodenburg, W. W.; J. Chem. Thermodynamics 2, 461 (1970).
- [25] Settle, J. L., Hubbard, Johnson, G. K.; Greenberg, E.; Private Communication, Argonne Nat. Lab., July 1970.

Chapter 7

PROVISIONAL RESULTS ON THE PREPARATION, MELTING, AND VAPORIZATION OF MoF₅

Ralph F. Krause, Jr.

Abstract

A sample of MoF₅ was prepared from the reaction of MoF₆ vapor with powdered Mo near 150°C, purified by simple vacuum distillation near 90°C, and collected as a viscous golden-yellow liquid which crystallized after a few days. A temperature-time melting curve of the light yellow solid gave a freezing-point-lowering of 0.22 kelvin, which was estimated to correspond to a cryoscopic impurity of 0.15 mol %, and a melting point for the pure substance of 45.67°C, which is much lower than a published value of 67°C. Several entrainment measurements on the sample at 60 and 90°C showed that the partial pressure of MoF₅ vapor, if assumed monomeric, was 26 to 34% of a direct vapor pressure measurement, the only published work, and that the vapor contained from 7 to 24 mol % MoF₆, whose presence indicates disproportionation of the sample. The entrainment value of the MoF₅ pressure decreased with subsequent flows which corresponds to a build-up in the liquid sample of a soluble impurity such as MoF₄. Deliberate enhancement of the carrier gas with MoF₆ vapor restored a maximum value which is in line with a sample of zero impurity. Composition of the gaseous and condensed phases are still in doubt and further analyses are needed. Since there is evidence that the sample reacts somewhat with pyrex, future plans involve vaporization in monel.

Literature Survey

The fluorides of molybdenum have been a part of some recent reviews. Ferguson¹ has discussed the chemistry of the anhydrous halides and oxyhalides of chromium, molybdenum, and tungsten. Canterford, Colton, and O'Donnell² have attempted to systematize the physical and chemical properties of the hexa- and pentafluorides of the second and third row transition elements.

Although molybdenum can have in theory a valency from 0 to 6 and the hexa-, penta-, tetra-, and trifluorides have been reported in the literature, only the thermodynamic properties of the hexafluoride have been well-characterized. Several investigators, the most recent of which are Claassen, Goodman, Holloway, and Selig³ have measured both the infrared and Raman spectra of MoF₆(g). Osborne, Schreiner, Malm, Selig, and Rochester⁴ have measured the low-temperature heat capacity, triple point, heat of fusion, vapor pressure, and heat of vaporization. Using fluorine bomb calorimetry, Settle, Feder, and Hubbard⁵ have measured the heat of formation of MoF₆.

In contrast, work on MoF₅ has just begun. Fifty years after the original preparation⁶ of MoF₆, Peacock⁷ was the first to prepare MoF₅ by reacting F₂(g) with Mo(CO)₆ at -75°C. The product was heated to 170°C; the yellow distillate of MoF₅ and the green residue of MoF₄ were identified by chemical analysis as shown in Table 1. Using this preparation, Cady

Table 1
Chemical Analyses of Some Molybdenum Fluorides

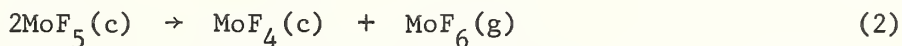
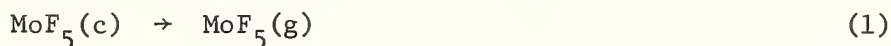
Comp'd	Investigator	Ref.	%Mo	%F
MoF ₃	Emeleus & Gutman ⁿ	12	62.2	36.1
	LaValle <i>et. al.</i> Theoretical	14	62.8 62.9 (62.73)	35.7 (37.27)
MoF ₄	Peacock Theoretical	7	56.3 (55.80)	43.2 (44.20)
	Peacock Edward <i>et. al.</i> Ouellette <i>et. al.</i> Churney (this work) Theoretical	7 10 11 17	49.9 50.4 50.19 50.14 ^a 50.47 ^a 50.37 ^a 50.45 ^a (50.25)	50.5 (49.75)
MoF ₆	Churney (this work)	17	45.79 45.79 45.91 (45.70)	 (54.30)
	Theoretical		(51.05)	(40.44)
MoOF ₄	Theoretical		(56.79)	(33.74)
MoOF ₃	Theoretical			

^aThese values involve a blank correction based on the high results of presumed pure MoF₆.

and Hargreaves⁸ measured directly the vapor pressure of MoF₅(ℓ) from 70 to 160°C with a pyrex diaphragm gauge as a null device; they also reported the disproportionation of MoF₅ at 165°C to form MoF₆ and involatile MoF₄, for whose identity no analytical results were given. Also reporting no analytical results, O'Donnell and Stewart⁹ combined MoF₆ and PF₃ in a glass vacuum system fitted with brass valves and found the only products to be MoF₅ and PF₅. Edwards, Peacock, and Small¹⁰ reported yet another method of preparation and the crystalline structure of MoF₅. They passed sublimed MoF₆ over Mo powder in a nickel tube at 300 - 400°C and purified the product by trap-to-trap distillation at 65°C in a glass vacuum system. Finally, Ouellette, Ratcliffe, and Sharp¹¹ modified this last method by heating a metal reaction vessel to 60°C and determined the infrared and Raman spectra of crystalline and liquid MoF₅.

The purity of MoF₅ from the above preparations is open to question. On the basis of a chemical analysis for Mo alone, an observed value of 0.2% greater than theoretical for MoF₅ as shown in Table 1 could possibly be an indication for as much as 25 mol % MoOF₄ in the sample. In a related example the evidence for purity and crystalline structure of MoF₃ is conflicting. Emeleus and Gutmann¹² prepared a non-hygroscopic dark-pink powder on heating the tribromide in HF; then Gutmann and Jack¹³ determined a cubic ReO₃-type structure by x-ray powder diffraction. Later LaValle, Steele, Wilkinson, and Yakel¹⁴ reduced MoF₅ with Mo powder and found their tan product to have the rhombohedral VF₃-type structure. Yet both samples were believed to be MoF₃ as Table 1 indicates.

If disproportionation of MoF₅ were to occur in addition to simple vaporization as shown by eqs 1 and 2,



another interpretation of Cady and Hargreaves' vapor pressure data⁸, which they represented as

$$\log P(\text{torr}) = 8.58 - 2772/T(\text{K}) \quad (3)$$

should be that

$$P = P_1 + P_2 \quad (4)$$

in which P_1 is the partial pressure of $\text{MoF}_5(\text{g})$ in eq 1 and P_2 is the partial pressure of $\text{MoF}_6(\text{g})$ in eq 2. Eqs 1 and 2 represent a binary system that is univariant. If MoF_4 is soluble in liquid MoF_5 , either the case in which the concentration of MoF_4 is near zero or perhaps Raoult's law could be applied. The terms P_1 and P_2 are related to the thermodynamic properties of eqs 1 and 2 respectively by

$$P_i = \exp [\Delta S_i^\circ/R - \Delta H_i^\circ/RT] \quad (5)$$

The inverse temperature derivative of eq 4 leads to

$$-R[dP/d(1/T)] = \Delta H_1^\circ P_1 + \Delta H_2^\circ P_2 \quad (6)$$

If we let T be 383 K, which comes from the average inverse temperature of Cady and Hargreaves' data, and assume values of ΔS_1° and ΔS_2° , values of P_1/P , ΔH_1° , and ΔH_2° may be generated from eqs 4, 5, and 6. Using the estimation methods of Kubaschewski and Evans¹⁵, values of ΔS_1° and ΔS_2° at 383 K were taken as 30.7 and 15.5 eu respectively; however, since the most uncertain estimate is the entropy of $\text{MoF}_5(\text{c})$ at 298 K, this served as a convenient parameter for the calculation by an iterative method of the results shown in Table 2. Here it seems plausible indeed that appreci-

Table 2

Estimate^a of the Change in Enthalpy of Eqs 1 and 2,
Using the Data of Cady and Hargreaves (ref 8)

$S^\circ(\text{eu})$ $\text{MoF}_5(\text{c})$ 298 K	$P_1/(P_1+P_2)$ % 383 K	ΔH_1° kcal 383 K	ΔH_2° kcal 383 K
35	40	15.9	10.5
36	51	15.3	9.9
37 ^b	61	14.8	9.3
38	70	14.3	8.8
39	79	13.9	8.2
40	87	13.4	7.7

^a Assumed values of ΔS_1° and ΔS_2° which are related to S° in this table were used along with eqs 4, 5 and 6. Subscripts refer to eqs 1 and 2.

^b This corresponds to values of ΔS_1° and ΔS_2° as 30.7 and 15.5 eu, respectively. See text.

able disproportionation occurs along with simple vaporization over the temperature range of Cady and Hargreaves' vapor pressure data.

Preparation

A sample of MoF_5 was prepared from the reaction of triple-distilled MoF_6 vapor with powdered Mo in a previously evacuated monel tube near 150°C . In order to remove any possible HF, vapor from the commercial source of MoF_6 was treated with a column of NaF, which was prepared by heating NaHF_2 to 350°C in a helium flow (eventually discharged through soda-lime). More volatile impurities like F_2 were removed by pumping on the first distillate of MoF_6 which was held in a dry-ice slurry. As the reader will see later, the cryoscopic impurity of a sample of MoF_6 which was similarly treated was 0.031 mol %. The commercial supplier of the powdered Mo (200 mesh) had reduced it in hydrogen and assayed it at 99.90%; a general spectrographic analysis is currently underway. Stainless-steel valves with teflon-packed stem and seat connected the reaction tube to the source of MoF_6 and to a series of three previously evacuated and baked pyrex U-tubes. After a few minutes of reaction a batch of about 1 g of product was condensed at room temperature in the first pyrex tube while the excess MoF_6 was withdrawn over a period of several hours to a liquid nitrogen trap in the brass and copper vacuum system (10^{-5} torr). When a few batches of the viscous golden-yellow liquid had accumulated, it was purified by simple vacuum-distillation near 90°C . The distillate was collected in the second U-tube and allowed to drain into another vessel for subsequent analysis while the third tube was kept in a dry-ice slurry. The remaining residue, which was about 5% of the original, became brownish-yellow.

Since purification of MoF_5 seemed difficult, reliance on the purity of reactants was tempting. Both MoF_5 and MoF_6 are very reactive with moisture. When a sample of MoF_5 was accidentally exposed to moist air, its surface turned green; this leads one to question the nature of Peacock's⁷ green MoF_4 . On one occasion the series of three pyrex U-tubes exploded in the fume hood after it had been detached from the vacuum

system. Thereafter any fluoride sample was disposed of by drawing over it a large quantity of water with an aspirator. If a pyrex tube under vacuum is not baked in a Bunsen flame beforehand, its surface turns blue and is etched on exposure to these fluorides. Although MoF_6 appeared to be stable for many days in a properly prepared pyrex tube at room temperature, white needle-like crystals which melt near 95°C have been observed to form in pyrex which was kept near 100°C . Sealing pyrex previously exposed to MoF_5 turned the glass bluish-black. Edwards *et. al.*¹⁰ believed the most likely impurity to be MoOF_4 which Cady and Hargreaves⁸ found to have at 100°C a vapor pressure about 2.5 times that of their MoF_5 measurement. Using a common derivation¹⁶ for simple batch distillation of an ideal binary solution, one finds that an initial fraction of distillate which contains about 65 mol % of the original mixture must be discarded to reduce the more volatile component in the residue from 0.5 mol % to 0.1 mol %. Clearly fractional distillation would be more appropriate than the trap-to-trap process used by Edwards *et. al.* In this work this impurity was hopefully reduced by discarding the first two batches from the reaction tube because the surface of powdered Mo seemed a likely source of oxygen.

Churney¹⁷ analyzed a weighed sample of MoF_5 which was prepared as above and sealed under vacuum in a pyrex vessel with a break seal. The sample was dissolved in water, made alkaline with 2N KOH, and oxidized to Mo(VI) by aqueous hydrogen peroxide. Using the 8-hydroxyquinoline gravimetric method¹⁸, he determined % Mo which as shown in Table 1 involves a blank correction. He checked his method by several analyses of presumed pure MoF_6 , which was also supplied in a pyrex ampoule. The average deviation above theoretical of % Mo in the MoF_6 served as the blank correction. The high results are explicable on the basis of entrapped silica in the fine fritted glass crucibles. Since analysis of Mo above is ambiguous, plans are afoot to determine F by a null-point potentiometric method¹⁹.

Melting and Purity

The melting point is a most important physical property from the standpoint of identification and purity of a given compound. Taylor and Rossini²⁰ have described a method for determining, from appropriate temperature-time melting curves, the melting point T_m of a given substance, and within certain wide limits, the melting point T_o of that substance for zero impurity. This method applies to a liquid-soluble and solid-insoluble impurity and assumes that its mol fraction N_s in the sample is small in which case

$$N_s = (T_o - T_m) \Delta S_m^\circ / RT_m \quad (7)$$

Since samples of MoF_5 and MoF_6 were of necessity small and had to be handled in a vacuum system, a miniature melting point tube was constructed of three concentric pyrex tubes (of diameters 4, 8, and 28 mm). The smallest tube held a chromel-alumel thermocouple, the sample was sealed in the middle tube, and the third tube was evacuated and submerged in a stirred water bath which was controlled constant to 0.005 kelvin during an experiment. The 1.7 ml sample (11 cm long and 1 mm wall) required several days to crystallize. Since stirring was not possible, the impurity was assumed to diffuse uniformly in the liquid phase during the 30 to 60 min. of melting. The rate of melting was constant to the extent that the difference between the bath temperature T_b and the sample temperature T was from 20 to 40 times greater than the melting range; so the melting curve was assumed as a rectangular hyperbola upon three selected points of which a geometrical construction yielded T_m and T_o . These points were selected from that portion of the melting curve which extended over 1/4 to 1/2 of the material melted and satisfied a test for the assumed nature of the curve such that $(z-z_r)/(T-T_r)$, in which z is the time and z_r is an arbitrary reference, appeared linear with $(z-z_r)$. The results of melting MoF_6 are shown in Table 3 and agree very well with the calorimetric value of Osborne *et. al.*⁴. The last line was believed to give a better value than the two preceding because a copper core the length of the sample served as the thermocouple junction.

Table 3

Observed Melting Data on Samples of MoF₅ and MoF₆

Sample ^a	Investigator	Ref	Bath temp. °C	Sample ^b mp °C	mp lowering kelvin	Cryoscopic impurity mol %
MoF ₅	Peacock	7		64		
	Cady & Hargreaves	8		67		
	This work		49.4	46.4		
			49.35	45.51	0.16	0.11 ^c
			48.42	45.45	0.22	0.15 ^c
MoF ₆	Osborne <u>et. al.</u>	4		17.58	0.00516	0.0032
	This work		15.62	17.43	0.18	0.11
			19.68	17.35	0.18	0.11
			19.63	17.55	0.050	0.031

^aLines 4 and 5 refer to the same sample; similarly lines 7 and 8 refer to another. The sample holder for lines 5 and 9 used a copper core the length of the sample.

^bThe mp for zero impurity is the sum of columns 5 and 6.

^cThese values are based on an estimated heat of fusion of 1400 cal per MoF₅.

The results of MoF₅ were quite surprising compared to those of the other investigators^{7,8}. An error that is possibly related to lack of stirring is shown in Table 3. The experiment of line 4 which required 15.6 min. to melt half the sample indicated a lower $(T_o - T_m)$ than that of line 5 which required 28.0 min., but the former was without a copper core. The error of some solid solution is suspected because MoF₅ has a small heat of fusion, which will be discussed later. To explain the large discrepancy, however, one may wonder if MoF₅ can form a metastable solid as sulfur does. Another explanation is that an eutectic is formed as Meyer, Oosterom, and Van Oeveren²¹ offered in an analogous case. They found a eutectic of NbCl₅-NbOCl₃ (5.6 mol %) which melted 3.5 kelvin below pure NbCl₅ and mixtures with NbOCl₃ greater than 5.6 mol % whose mp were observed greatly increased.

An estimate of the entropy of fusion is required to calculate from eq 7 the cryoscopic impurity of MoF₅. The fraction of sample melted is expressed as

$$f = (T_o - T_m)/(T_o - T) \quad (8)$$

and the heat balance during melting may be approximated as

$$k(T_b - T)dt = n(\Delta H_m^\circ)df + CdT \quad (9)$$

in which k is the heat transfer constant, n is the moles of sample, and C is the heat capacity of sample and container. The ratio k/C was evaluated by integrating eq 9 for the special case of $f = 1$. Differentiating eq 8, substituting in eq 9, and integrating the result by partial fractions gives ΔH_m° . Using an estimated value of C and points from the melting curve of the experiment in line 5 of Table 3, gave an estimate of 1400 cal/mol for $\Delta H_m^\circ(\text{MoF}_5)$.

The heat transfer coefficient k was evaluated independently from a consideration of the heat transfer characteristics of the mp tube. Longitudinal heat conduction from the bath to the sample was estimated by integrating

$$d^2T/dx^2 = m(T - T_b) \quad (10)$$

in which m is a constant, and was found as 10% of the radiant heat transfer from the isothermal bath to the enclosed sample holder. Their sum was 10% greater than that observed from the melting curve. Perhaps the major contribution to this difference is an error in the assumed value of C . Finally the temperature difference between the thermocouple junction and the sample was estimated, by integrating an expression similar to eq 10, as 0.015 kelvin.

Vaporization by Entrainment

The details of an entrainment measurement similar to what was performed here was described in an earlier paper²². In general a flow of helium, which was dried in a molecular sieve to about 1.5 ppm, was passed over a sample of MoF_5 in a pyrex vapor cell at a given temperature, which was provided by a stirred oil bath controlled constant to 0.005 kelvin. The sample distillate was condensed by a dry-ice slurry downstream and weighed in a sealed pyrex tube, and the quantity of carrier gas was measured in a tank. Saturation of the carrier gas was closely approximated by using the guidelines

of Merten and Bell²³ for an appropriate geometry of the vapor cell and flow of the gas mixture. An empirical test for saturation, however, has yet to be made.

The preliminary results of the entrainment measurements are shown in Table 4. The partial pressure of MoF₅ was calculated from eq 11 as if the vapor were monomeric.

$$P_1 = (n_1/n_{\text{total}}) P_{\text{total}} \quad (11)$$

Table 4
Preliminary Results of Vaporizing a Sample of MoF₅
by Entrainment

Expt. ^a	T K	Gas Flow ml/sec	w(MoF ₅) distil- late,mg	P(MoF ₅) of sample torr	P(MoF ₆) of sample torr	P(MoF ₆) ^c added torr	N(MoF ₆) mol %
1	333.0	0.799	88.7	0.468	0.151		24
2		1.008	251.7	0.459	b		
3		0.650	156.0	0.442	0.065		13
4	362.8	1.172	501.0	b	0.4479		
5		1.173	422.9	2.883	0.4476		13
6		1.271	477.0	2.755	0.207		7
7	333.0	1.037	191.6	0.465		0.087	15.8
8	362.8	0.814	297.7	3.010		0.509	14.5

^aThe series 1, 2, and 3 and the series 5 and 6 give the results of successive flows without altering the sample between runs. On the other hand the sample was pre-treated before runs 1, 4, 5, 7, and 8 with MoF₆ after which any excess was evacuated.

^bThese condensates were accidentally destroyed before weighing.

^cHere the carrier gas was deliberately enhanced with MoF₆ before reaching the sample.

Experiments 1 through 6 indicate that MoF₅ vaporizes simply and disproportionates. Before each experiment the sample at room temperature was connected to the vacuum system for several hours with no visible transfer of MoF₅. At the conclusion of a flow the distillate of MoF₅ was warmed to room temperature while connected to the vacuum system and any MoF₆ was added to that

condensed further downstream by liquid nitrogen. These distillates were identified roughly by their physical properties. In the series (1, 2, and 3) and the series (5 and 6) successive flows of helium were passed over the sample which was not altered between runs by a treatment with MoF₆ vapor. The liquid residue appeared darker brownish-yellow as the observed partial pressure of MoF₅ decreased; this corresponds to an increase of a soluble impurity such as MoF₄. Upon treating this dark residue with MoF₆ vapor, after which any excess was evacuated at room temperature, the residue was transformed to a light yellow crystal again.

The last two experiments in Table 4 involve a flow of helium which was deliberately enhanced with MoF₆ vapor. This vapor was generated by a constant temperature bath, in which methanol was circulated through an external dry ice slurry and which was controlled to 0.01 kelvin for more than 5 hours at -65°C. The partial pressure of MoF₆ was calculated from the data of Osborne et. al.⁴ At the end of these runs the residue continued to remain light yellow. The partial pressure of MoF₅ was found as 26 to 34% of Cady and Hargreaves' direct pressure measurement.

Tentative values of ΔH° and ΔS° of eq 1 at 348 K were calculated by eq 5 and the pressure data of experiments 7 and 8 as 15.0₄ kcal and 30.4₆ eu, respectively. Cady and Hargreaves' pressure data of eq 3 gives ΔH° and ΔS° of eq 1 at 383 K as 12.68 kcal and 26.1 eu respectively.

Since there is some evidence that MoF₅ and MoF₆ react somewhat with pyrex, future plans involve entrainment measurements in monel.

References

- [1] J. E. Fergusson, "Halide Chemistry of Chromium, Molybdenum, and Tungsten," Halogen Chemistry, vol 3, V. Gutmann (editor), Academic Press, London, 1967, p. 227.
- [2] J. H. Canterford, R. Colton, and T. A. O'Donnell, *Rev. Pure and Appl. Chem.*, 17, 123 (1967).
- [3] H. H. Claassen, G. L. Goodman, J. H. Holloway, and H. Selig, *J. Chem. Phys.*, 53, 341 (1970).
- [4] D. W. Osborne, F. Schreiner, J. G. Malm, H. Selig, and L. Rochester, *J. Chem. Phys.*, 44, 2802 (1966).
- [5] J. L. Settle, H. M. Feder, and W. N. Hubbard, *J. Phys. Chem.*, 65, 1337 (1961).
- [6] O. Ruff and F. Eisner, *Chem. Ber.*, 40, 2926 (1907).
- [7] R. D. Peacock, *Proc. Chem. Soc.*, 59 (1957).
- [8] G. H. Cady and G. B. Hargreaves, *J. Chem. Soc.*, 1568 (1961).
- [9] T. A. O'Donnell and D. F. Stewart, *J. Inorg. Nucl. Chem.*, 24, 309 (1962).
- [10] A. J. Edwards, R. D. Peacock, and R. W. H. Small, *J. Chem. Soc.*, 4486 (1962).
- [11] T. J. Ouellette, C. T. Ratcliffe, and D. W. A. Sharp, *J. Chem. Soc.*, 2351 (1969).
- [12] H. J. Emeleus and V. Gutmann, *J. Chem. Soc.*, 2979 (1949).
- [13] V. Gutmann and K. H. Jack, *Acta Cryst.* 4, 244 (1951).
- [14] D. E. LaValle, R. M. Steele, M. K. Wilkinson, and H. L. Yakel, Jr., *J. Amer. Chem. Soc.*, 82, 2433 (1960).
- [15] O. Kubaschewski and E. Evans, Metallurgical Thermochemistry, Pergamon Press, New York, 1958, pp. 180-197.
- [16] Chemical Engineers' Handbook, J. H. Perry (editor), McGraw-Hill Book Co., New York, 1950, p. 580.
- [17] K. L. Churney, private communication, Aug. 1971.

- [18] A. I. Vogel, Quantitative Inorganic Analysis, John Wiley and Sons, Inc., New York, 1961, pp. 506-508.
- [19] T. A. O'Donnell and D. F. Stewart, *Anal. Chem.*, 33, 337 (1961).
- [20] W. J. Taylor and F. D. Rossini, *J. Res. Nat. Bur. Stand.*, 32, 197 (1944).
- [21] G. Meyer, J. F. Oosterom, and W. J. Van Oeveren, *Rec. Trav. Chim. Pays-Bas*, 80, 502 (1961);
- [22] R. F. Krause, Jr. and T. B. Douglas, *J. Phys. Chem.*, 72, 475 (1968).
- [23] U. Merten and W. E. Bell, "The Transpiration Method," The Characterization of High-Temperature Vapors, J. L. Margrave (editor), John Wiley & Sons, New York, 1967, pp. 91-114.

Chapter 8

THE INFRARED SPECTRUM OF MATRIX ISOLATED NbF_5

Nicolo Acquista and Stanley Abramowitz
National Bureau of Standards
Washington, D. C. 20234

The infrared spectra of matrix isolated NbF_5 as well as some gas phase spectra have been observed. These spectra have been obtained using double boiler Knudsen cells. Interpretation of the spectra to yield the six infrared active frequencies of a C_{4v} monomeric structure for NbF_5 is advanced.

* This research was sponsored by the Air Force Office of Scientific Research, United States Air Force under AFOSR-ISSA-69-001.

The study of the spectra of the MF₅ molecules have shown these molecules to have either a D_{3h} (trigonal bipyramid) or C_{4v} structure. In several instances structures are different for the gaseous liquid and solid phases. Furthermore, for the group VA fluorides, PF₅ and AsF₅ have D_{3h} symmetry and SbF₅ has C_{4v} symmetry. This seems to indicate that the barrier to internal rotation may be low leading to an equilibrium between D_{3h} and C_{4v} structures. Indeed, for VF₅ there exists some evidence for such an interpretation of the observed infrared and Raman spectra. There are also polymers in the vapors of some of these species including a tetramer of C_{4v} symmetry. The x-ray diffraction patterns of NbF₅, TaF₅, SbF₅, etc. have been interpreted on the assumption of a tetrameric C_{4v} structural unit for the crystalline species. We have investigated the infrared spectra of the matrix isolated vapors above solid NbF₅. By employing double boiler techniques we have been able to obtain the spectra of the matrix isolated monomer.

There is no complete infrared spectrum of NbF₅. Blanchard [1] studied gaseous NbF₅ in the infrared region using NaCl and KBr optics at several temperatures up to 142°C and observed three strong bands above 500 cm⁻¹. On the basis of his temperature studies he assigned the bands to fundamental of monomeric NbF₅. In order to make a partial vibrational assignment he assumed NbF₅ gas to have a trigonal bipyramidal structure (D_{3h}). Other pentahalides of the 5th group are known to have this symmetry [2]. The vibrational representation of an XY₅, D_{3h} molecule is 2a₁' + 2a₂" + 3e' + e" with the a₂" and e' modes infrared active and the a₁', e' and e" modes Raman active. For a C_{4v} molecule the vibrational representation is 3a₁ + 2b₁ + b₂ + 3e₂ (a₁ and e infrared active; a₁, b₁, b₂ and e Raman active). Using the observed vibration rotation band contours Blanchard assigned the infrared bands at 740, 688 and 510 cm⁻¹ to ν₅(e'), ν₃(a₂") and ν₄(a₂") respectively.

The Raman spectrum of liquid NbF₅ was observed at several temperatures by Selig et al [3]. They concluded in contrast to VF₅ that there was no evidence for polymerization in the liquid. The observed spectral intensity changes with temperature in liquid VF₅ were interpreted as indicating the presence of polymer, while the absence of these changes in the Raman spectrum of liquid NbF₅ to the absence of polymer.

The Raman spectrum of liquid NbF₅ is very simple, consisting of 4 strong lines and 3 weak features. The bands observed at 767 and 683 cm⁻¹ are highly polarized relative to the others. These lines are assigned to ν₁(a₁') and ν₂(a₁') respectively. The other strong features at 253 and 226 cm⁻¹ and the weaker features were unpolarized. The selection rules for D_{3h} point group call for six Raman active bands of which two should be polarized. As a complete infrared spectrum was lacking, the other lines were not assigned. Selig et al considered the observed infrared band at 688 cm⁻¹ assigned to ν₃(a₂") by Blanchard as an accidental coincidence.

Beattie et al [4] observed the Raman and infrared spectra of the liquid and solid NbF_5 . Their conclusions, different from Selig, were that a cis-fluorine bridged tetrameric structure exists in the liquid and solid phases. They also carried out force field calculations for this species in condensed phases. These calculations show the expected distribution of vibrational frequencies for this cis-fluorine-bridged tetrameric NbF_5 unit. Many coincidences of the observed vibrational features were predicted for this symmetry of the molecule.

Electron diffraction data [5] show NbF_5 vapor at 300 K consists of tetramers as in the solid, while at 475 K the vapor is mostly monomer with D_{3h} symmetry.

The electric deflection technique [6] has also been applied to NbF_5 vapor at 310 K. The conclusions from these experiments were that NbF_5 vapor behaves as a non-polar molecule and that a large concentration of monomer is present.

In view of the lack of a complete infrared spectrum and the uncertainty in its vibrational assignment, it appeared worthwhile to reinvestigate NbF_5 . In particular it was felt that the matrix isolation technique could be useful for observation of the infrared spectrum of monomeric NbF_5 .

Experimental

In the present work, the electron beam furnace, an Air-Products Cryotip operated at liquid hydrogen temperature and a Perkin-Elmer infrared spectrophotometer operated from $4000\text{--}50\text{ cm}^{-1}$ were used [7]. Stainless steel Knudsen single and double oven crucibles with one mm orifices were employed. The double oven cell consisted of two identical crucibles separated by a thin walled stainless steel tubing of $1/16$ " diameter. It was possible to change the distance between the crucibles. Our furnace conditions allowed the direct heating of the upper crucible; the lower was heated by conduction through the thin walled stainless steel connecting tubing. The larger the separation of the two crucibles the greater the temperature difference between the upper and lower crucibles. The use of stainless steel for the double oven with its relatively low thermal conductivity allowed temperature differences as great as 100°C to be maintained when the two crucibles were separated by 1.5 inches. The temperature of both crucibles was measured with a W 3% Re vs. W 25% Re thermocouple.

The NbF_5 , obtained from commercial sources, was used after prolonged outgassing. During deposition the lower crucible was maintained at $25\text{--}30^\circ\text{C}$ to give NbF_5 a vapor pressure in the range of 0.001 to 0.005 torr [8]. The flow of argon, the matrix gas used in all the experiments, was in range of 10 to 20 mmoles/hour. Estimates of the M/R in general are difficult to make. For a single boiler with knowledge of flow rates, the Knudsen formula

and the geometry of the system an estimate can be made. When a double boiler is used, the M/R is still more uncertain. If, for our system we estimate the M/R ratio to be about 500-1000 for a single boiler experiment, the ratio in the double boiler will be considerably greater. Nevertheless, most spectra were obtained in 30 minutes to one hour.

The gas phase spectrum of NbF_5 was observed using a 10 cm gas cell having a monel body. CsI windows were demountably attached through Viton O rings. This cell was heated to about 80°C in order to obtain a spectrum in the $400\text{--}800\text{ cm}^{-1}$ region. (Unfortunately, we were not able to observe a spectrum using a one meter cell because of the low vapor pressure of NbF_5 at room temperature coupled with the inconvenience of heating such a cell.) The NbF_5 reacts with the CsI windows. This reaction proceeds at a rate such that about 10-15 minutes is available to obtain a spectrum of gaseous NbF_5 . The spectra were calibrated by using absorption line of atmospheric water, ammonia, and CO_2 . The bands were measured to $\pm 1\text{ cm}^{-1}$.

Experimental Results

The gas phase spectrum of NbF_5 is shown in Figure 1. This spectrum was run on a 112 G equipped with a 40 l/mm grating and a suitable interference filter. From the observed contour of the doublet at 745.2 and 732.8 cm^{-1} we conclude that these are two different bands and are not as Blanchard concluded due to one vibration. Our conclusion was reached by considering the contours expected for various f constants using the B values calculated from the interatomic distances given by Romanov and Spiridanov [5]. The contour expected for a P-R separation of 12.4 cm^{-1} does not conform to the one observed [9]. Therefore, one concludes that there are three strong features in the Nb-F stretching region (745.2 , 732.8 and 689.7) which are assignable to the three infrared stretching modes of a C_{4v} molecule ($2a_1 + e$). The band which occurs at 513 cm^{-1} in an argon matrix was also observed in the gas phase. Unfortunately, the pressures needed for the observation of the far infrared spectrum required temperatures too high for our cell. At these high temperatures the NbF_5 reacted too rapidly with the CsI windows.

The infrared spectrum of NbF_5 vapors isolated in Ar matrices at liquid hydrogen temperatures is shown in Figures 2 and 3. This spectrum has two regions of strong and one of weak absorption. Bands appear at 740 , 729 , 686 and 513 cm^{-1} in Figure 2. The spectra in this region remained essentially the same whether single or double boiler effusion cells were used. The effusion temperature for the single oven was set to about 300 K. When the double oven was used, the lower crucible temperature was set to 300 K while the upper crucible temperature reached a temperature of about 400 K. At this temperature one should expect effusing vapor to contain a large proportion of monomer.

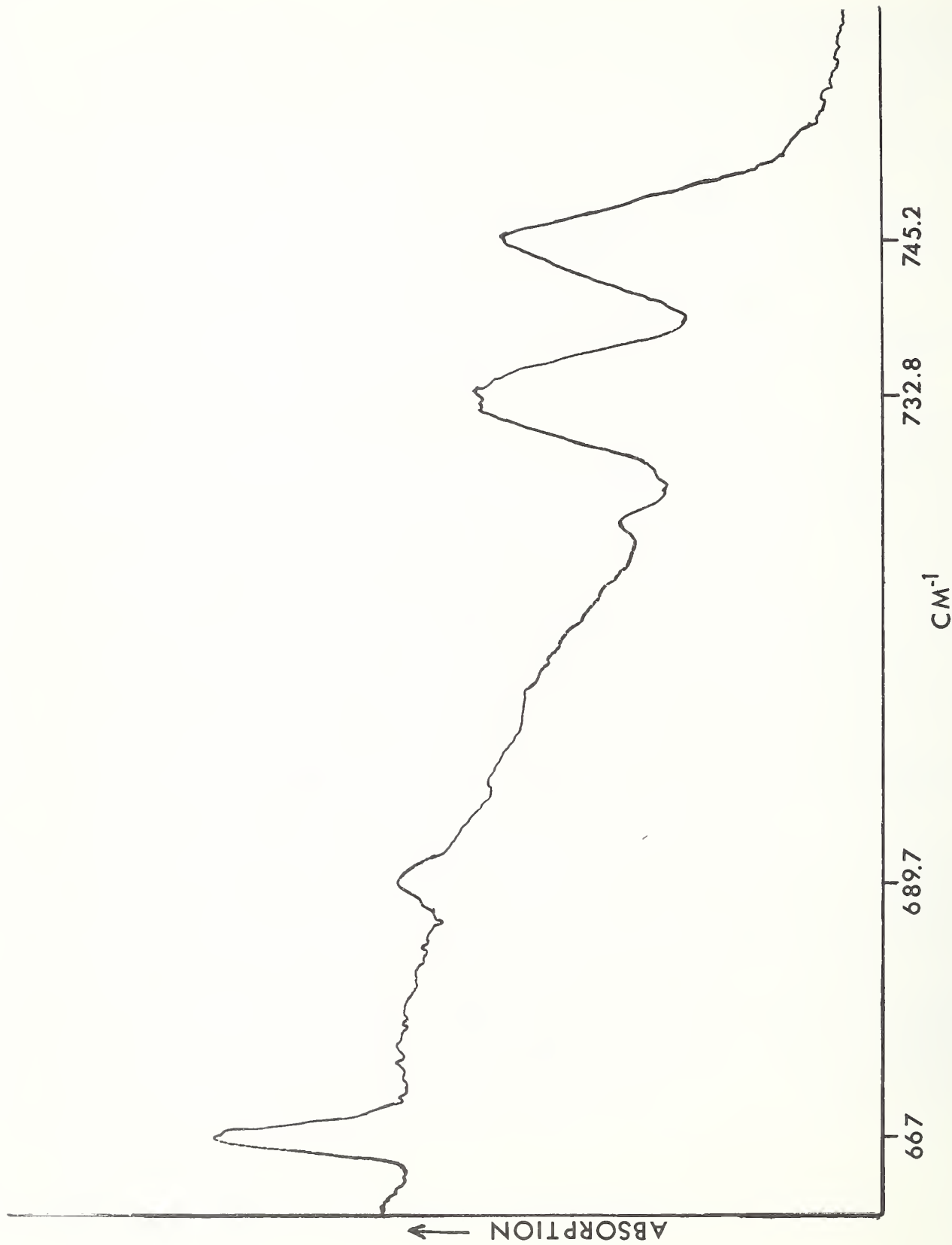


Figure 1

The Gas Phase Infrared Spectrum of NbF₅.
The band at 667 cm⁻¹ is due to atmospheric CO₂.

ABSORPTION

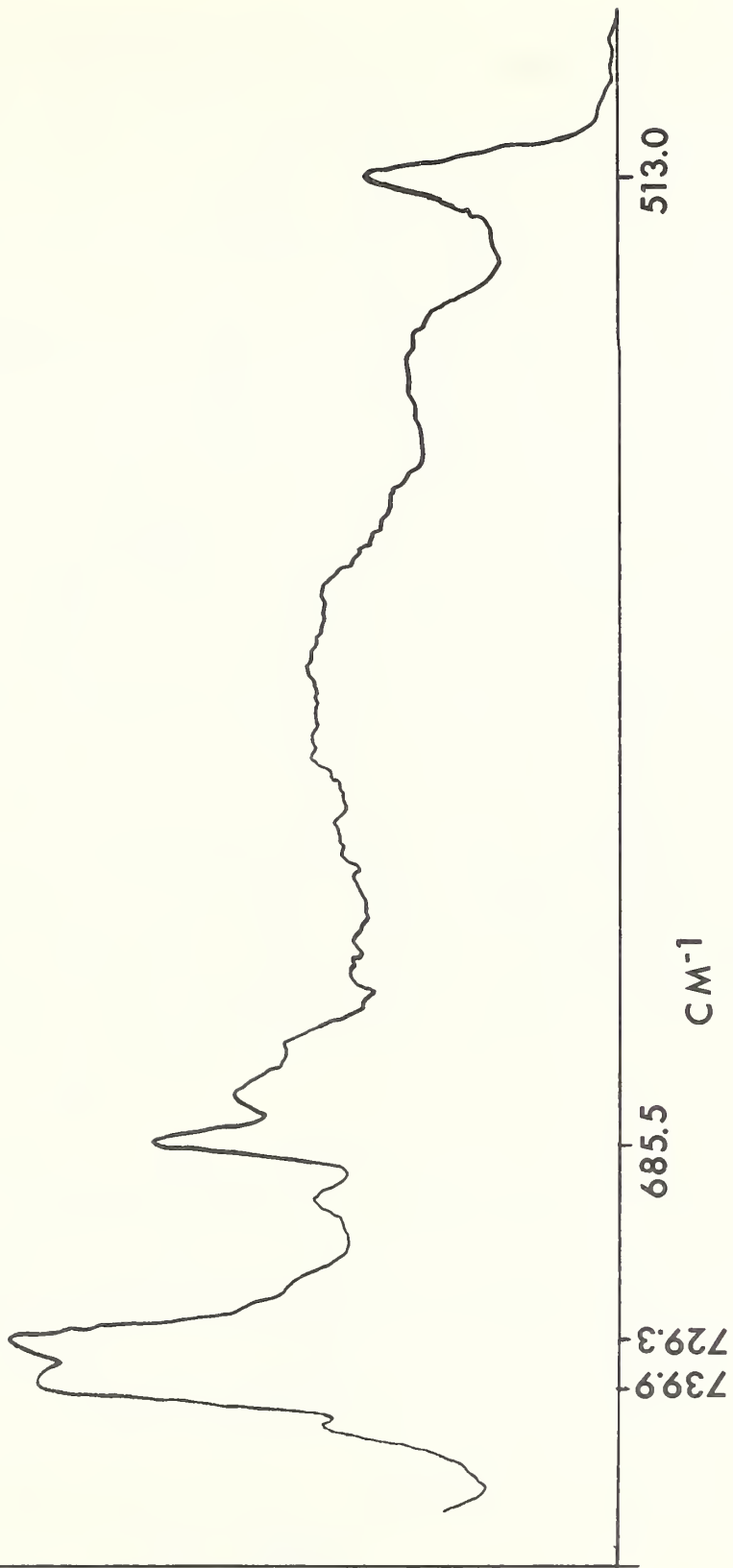


Figure 2
The Infrared Spectrum of
Matrix Isolated NbF₅.

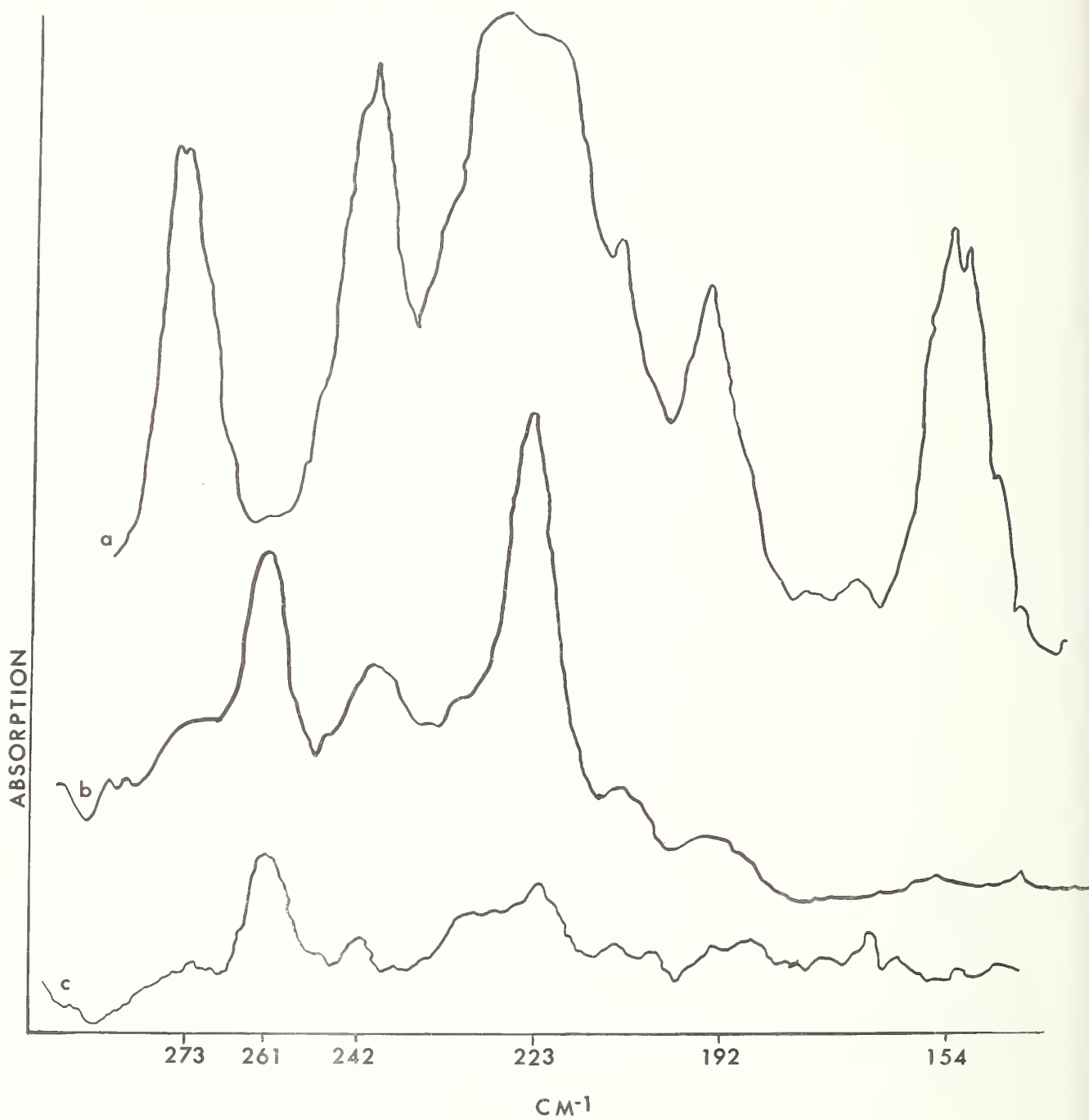


Figure 3
Infrared Spectra of Matrix Isolated NbF₅.
116

The gas phase infrared results shown in Figure 1 agree quite well with the matrix data. The matrix data support the conclusions that we are observing monomer in the temperature range of 370 to 410 K. Both sets of data are listed in Table I with our assignment of these bands. The above observation that the double boiler experiment in which monomer prevails yields essentially the same spectrum as the single boiler does not appear unusual. These high frequency vibrations which are assigned to the stretching modes are less likely to be perturbed when the monomer is condensed into polymers than the low frequency bands.

Figure 3 curve (a) shows the far infrared spectrum of NbF_5 in an argon matrix at liquid hydrogen temperatures from 300 to 130 cm^{-1} . The NbF_5 effused from a single boiler crucible at a temperature of 325 K. At this temperature the vapor consists primarily of polymer. The multiplicity of bands is an indication of their presence in the matrix. Bands occur at 271, 242, 222, 194 and 158 cm^{-1} . Curve (b) shows the same region of the spectrum when double boiler effusion is used. Here the double oven consisted of two crucibles separated by 1.5 inch. The temperature of lower crucible was 315 K, the upper 400 K. The character of the spectrum has changed. At 400 K the vapor is primarily monomeric. All the bands have been reduced in intensity and a new band appears at 261 cm^{-1} . The double oven effect is evident here. The polymer bands are still present but considerably weakened. Diffusion experiments in this region showed a disappearance of 261 cm^{-1} and a broadening, and slight increase of bands at 222 and 242 cm^{-1} .

A final double oven experiment was performed in which the 261 cm^{-1} band was more intense than the polymer (curve c) bands. When this had been accomplished, the far infrared was examined to about 50 cm^{-1} . An absorption band was observed at 103 cm^{-1} . This band was detected only when the monomer band was present. On the basis of the double oven and diffusion experiments both the bands were assigned to monomeric NbF_5 . These results are summarized in Table I, together with a proposed vibrational assignment. In the table are included the Raman bands found in the liquid by Selig et al.

Conclusion

The monomeric spectrum of NbF_5 has been observed and all six infrared active fundamentals have been assigned on the assumption of C_{4v} symmetry. The double oven experiments proved very effective in separating the monomer from the polymer bands. The assignment of this molecule is complete except for the Raman active b_1 and b_2 species. One would expect $\nu_4(b_1)$ and $\nu_5(b_1)$ to have frequencies of about 500 and 275 cm^{-1} respectively while $\nu_6(b_2)$ is expected to have a frequency of about 300 cm^{-1} . The fundamental frequencies assigned in this study are consistent with those of SbF_5 [10], BrF_5 , ClF_5 and IF_5 [11]. Unfortunately, for all these species no infrared spectra have been observed below 200 cm^{-1} . The lowest frequency of VF_5 [12], AsF_5 [13] and PF_5 [14,15] appear at 109, 138 and 179 cm^{-1} respectively. This is consistent with the observation of 103 cm^{-1} for the lowest frequency of NbF_5 .

Table I

Observed Bands and Vibrational Assignment for NbF₅

Matrix ^a	Gas ^a	Selig, Liquid ^b	Assignment
		767	
739.9	745.2		ν_1 (a)
729.3	732.8		ν_7 (e)
		726	
685.5	689.7		ν_2 (a)
		683	
513.0	497		ν_3 (a)
271			
		315	
261			ν_8 (e)
		253	
242			polymer
		226	
222			polymer
194			polymer
158			polymer
		136	
103			ν_9 (e)

^a this study

^b Reference 3

References

1. S. Blanchard, J. Chim. Phys. (1965), 919.
2. K. Nakamoto, Infrared Spectra of Inorganic and Coordination Compounds (John Wiley and Sons, Inc., New York, N. Y., 1970).
3. H. Selig, A. Reis and E. L. Gasner, J. Inorg. and Nucl. Chem. 30, 2087 (1968).
4. I. R. Beattie, K. M. S. Livingston, G. A. Ozin and D. J. Reynolds, J. Chem. Soc. (London) (A1969), 958.
5. G. V. Romanov and V. P. Spiridanov, Vestn. Mosk. Univ. Khim. 23, 761 (1968).
6. T. R. Dyke, A. A. Muentzer, W. Klemperer and W. E. Falconer, J. Chem. Phys. 53, 3382 (1970).
7. S. Abramowitz, N. Acquista and I. W. Levin, J. Res. NBS 72A, 487 (1968).
8. J. H. Junken, R. L. Fauen, Jr., E. J. Barber and H. A. Beinhardt, J. Am. Chem. Soc. 74, 3464 (1952).
9. R. V. Valentine, Ph.D. Thesis, Purdue University, 1957.
10. A. L. K. Aljibury and R. L. Redington, J. Chem. Phys. 52, 453 (1970).
11. G. M. Begun, W. H. Fletcher and D. F. Smith, J. Chem. Phys. 42, 2236 (1965).
12. H. Selig, J. H. Holloway, J. Tyson and H. H. Claasen, J. Chem. Phys. 53, 2559 (1970).
13. L. C. Hoskin and R. C. Lord, J. Chem. Phys. 46, 2402 (1967).
14. I. W. Levin, J. Chem. Phys. 50, 1031 (1969).
15. I. W. Levin, J. Mol. Spectroscopy 33, 61 (1970).

SURVEY OF THE SYSTEMS Mo-C, Ta-C and Nb-B WITH EMPHASIS ON
COMPOUNDS SUITABLE FOR ENTHALPY MEASUREMENT BY DROP CALORIMETRY,
INCLUDING A LITERATURE SURVEY OF ENTHALPY AND HEAT CAPACITY DATA
ON SELECTED COMPOUNDS FROM THESE SYSTEMS

David A. Ditmars

I. Introduction

Refractory metal carbides and borides, because of their extremely high melting points (some as high as 4000 K) and because of the stability of certain compounds of this class at elevated temperatures, are attractive prospects for construction materials in very-high-temperature applications. Thermodynamic data on well-characterized compounds of this class should be of use not only in design calculations but also in predicting the behavior of refractory metals themselves when exposed to corrosive environments. As part of the continuing NBS effort to improve or augment the thermal data on these carbides and borides, the literature has been surveyed for heat capacity and enthalpy investigations of stable compounds chosen from the systems Mo-C, Ta-C and Nb-B. In addition, efforts have been made to obtain compounds belonging to these systems, suitable for precise high-temperature enthalpy measurements. The results have given valuable insight into the difficulty of synthesizing refractory carbides and borides and in their adequate characterization.

II. Stable Phases Suitable for Calorimetric Measurement

A. Phase Diagrams--General Features

The phase diagrams for the refractory carbides and borides of this study are shown in figures 1, 2 and 3. These represent the latest information available on these systems and resulted from an extended experimental investigation [1]^a which employed x-ray, metallographic, DTA and standard chemical analytical techniques.

^aFigures in brackets indicate literature references listed at the end of this chapter.

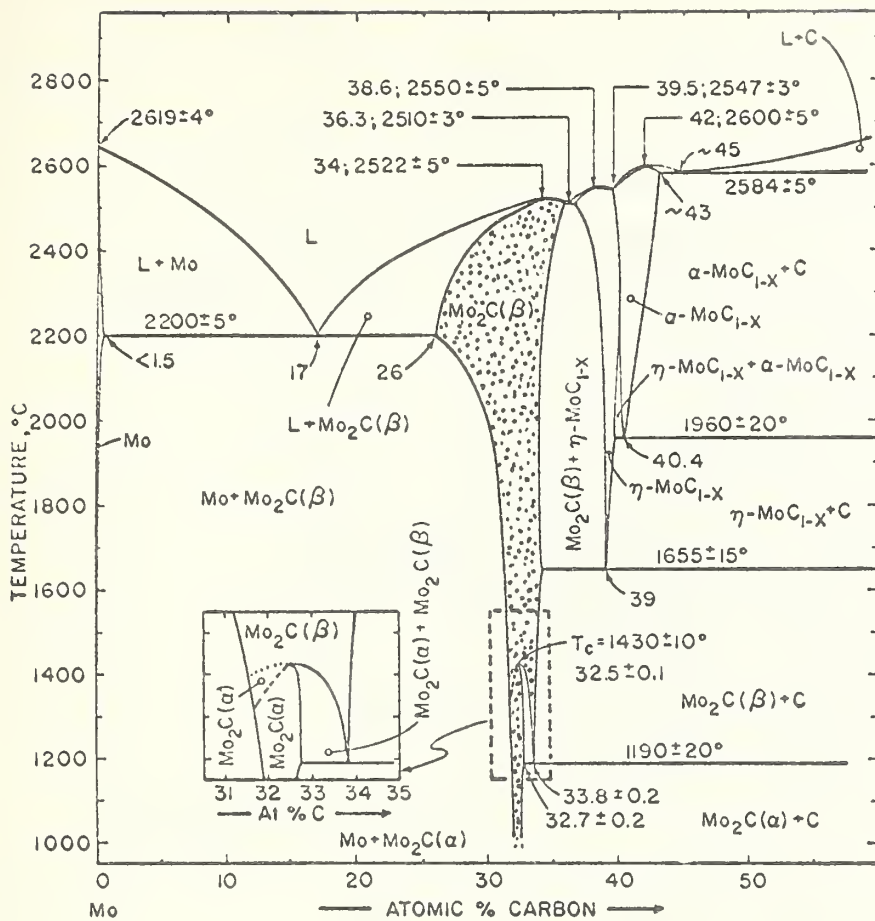


Figure 1. Phase diagram of the system Mo-C (ref.[1]).

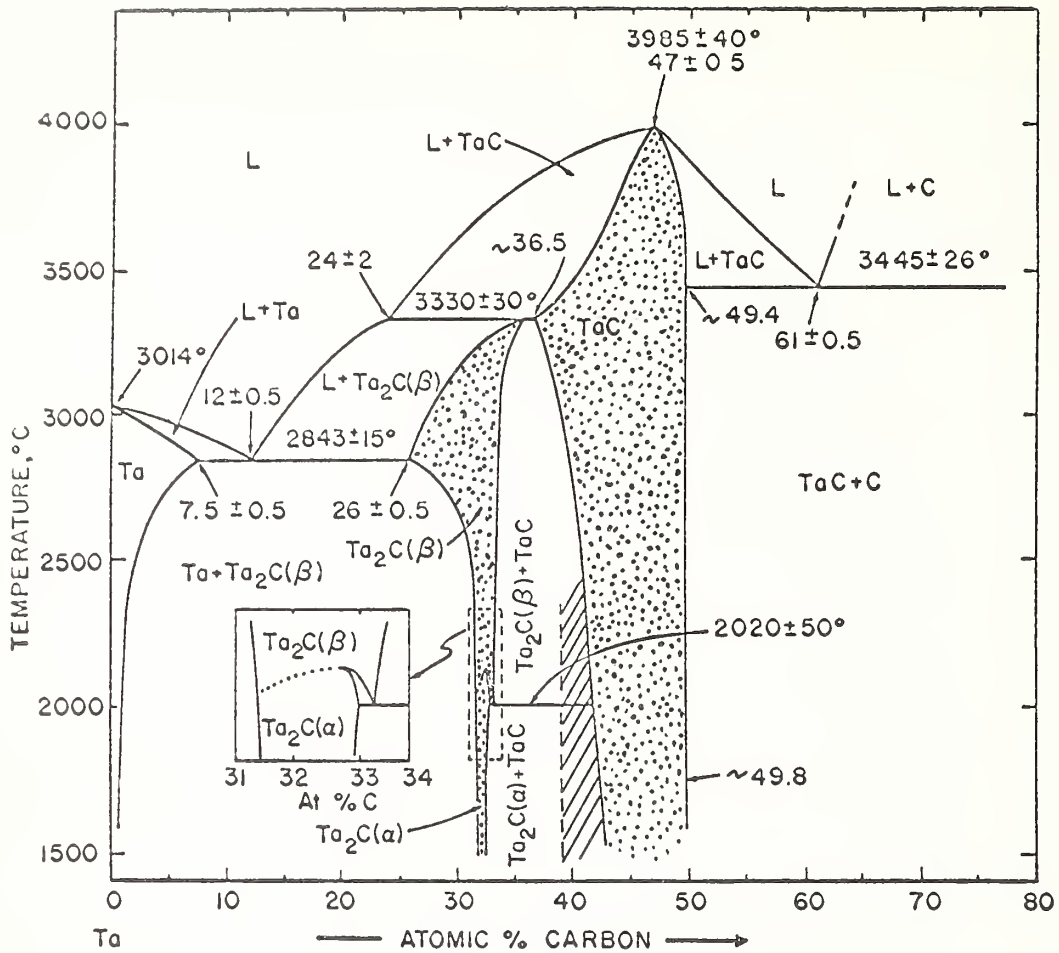


Figure 2. Phase diagram of the system Ta-C (ref.[1]).

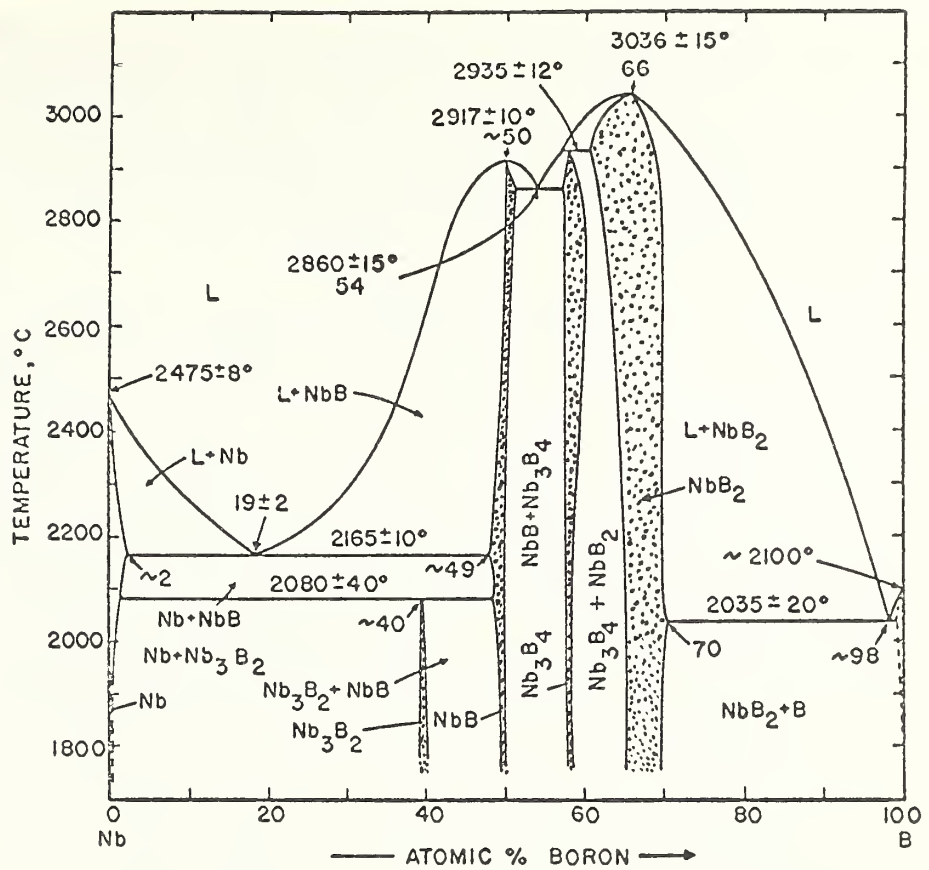


Figure 3. Phase diagram of the system Nb-B (ref.[1]).

The general features exhibited by all these systems which are especially pertinent to the present study are the formation of high-temperature phases unstable at lower temperatures (particularly in the Mo-C system) and the existence of solid phases stable over a wide range of temperatures extending to room temperature but with a variable range of homogeneity. These latter solid phases exist within the speckled areas in the phase diagrams.

Since the enthalpy measurements planned on these systems will be carried out with drop-type calorimeters (one, isothermal; one, adiabatic) in which the samples are suddenly quenched to the ice point from a temperature as high as 1173 K (isothermal calorimeter) or to room temperature from a temperature as high as 2600 K (adiabatic calorimeter), the study has been initiated with those compounds stable over these temperature ranges or with at most one polymorphic transition. With these guidelines in mind the following compounds were selected as potential candidates for study: Mo_2C , TaC , Ta_2C , NbB , NbB_2 , Nb_3B_2 and Nb_3B_4 . Note again that these are conventional formulae corresponding to compounds of ideal stoichiometry whereas in reality, both the metal and non-metal sublattices show a considerable tolerance for vacancies, giving rise to a continuous series of defect compounds [6]. For instance (see fig. 1), at 2000°C, the structure identified with " Mo_2C " can exist with any carbon concentration from ~ 30 to ~ 34 atomic percent.

Two of the difficulties which seriously limit the value of much of the existing thermal data on these compounds is that previous investigators have in many cases not recognized the importance of establishing the stoichiometry of the compounds they investigated, nor (in the case of Mo_2C) the considerable effect of this upon a recently identified order-disorder transition in this compound.^b The value of the thermal data to be obtained in this program will be further enhanced by the investigation of two or more compositions of some of the compounds. This will hopefully allow interpolation of the thermal properties of other compositions. The existence of variable and narrow

^b According to both Storms [4] and Rudy [2], Mo_2C , upon cooling to room temperature from above 1700 K, undergoes a transition from the (disordered) β phase to the (ordered) α phase. Furthermore, there exist critical cooling rates for this compound, dependent upon the carbon content, which if exceeded could result in "frozen-in" disorder. These same investigators have indicated that both the sample carbon content of the Mo_2C samples chosen for measurement in this program and the known cooling rates within the existing drop calorimetric apparatuses are such as to minimize the risk of the sample being in a non-equilibrium state within the calorimeters.

homogeneity ranges (especially in the system Nb-B) indicates that considerable difficulty can be expected in achieving high phase-purity for some of these compounds. This proved to be the case in one commercially available sample of "NbB" which x-ray analysis showed to be only 75 percent NbB with the remainder NbB_2 , Nb_3B_2 and an unknown fourth phase. Therefore, in selecting compounds for enthalpy measurements, priority has been given to those compounds having the widest homogeneity ranges (Mo_2C , TaC and NbB_2).

B. Methods of Synthesis and Sample Characterization

1. Synthesis

The synthesis of any one of these compounds can be a considerable problem in itself and involves a good measure of "trial and error". It is in general not possible to purchase these compounds "off the shelf" if one desires to obtain material of a chemical and phase purity adequate for meaningful thermodynamic investigations. Also, it is usually not possible to produce these carbides and borides by blindly heating mixtures containing the correct stoichiometric proportions of the metal and non-metal components, and assuming that the desired compound alone will result [2]. This is so, partly because the temperatures required to melt or react these substances (mostly in excess of 1500 K) are sufficiently high that selective vaporization of one of the components can alter the composition significantly, leading sometimes to the formation of undesired phases [2].

The favored method for synthesis of these compounds is by powder metallurgy. Arc-melting has also apparently been used successfully. In the former technique, high-purity powders of the elements involved are thoroughly mixed (sometimes with an excess of one or the other) with an organic binder and cold-pressed into pellets. The binder is driven off as the pellet is heated--usually to above 1500 K--to homogenize it. In the case of the Ta-C compounds, the pellet must then be reground and the powder heated to 1800 K several times [3]. X-ray patterns are customarily taken between each regrinding and heating to establish when the material has reached the desired phase purity.

In the case of Mo_2C , adjustment of this compound to a composition which will be stable and phase-pure at all temperatures down to room temperature can be achieved by taking advantage of the fact that Mo_2C vaporizes congruently near $MoC_{0.49}$ [4]. The sample is fabricated in nearly these proportions by the powder technique referred to above and then heated for several hours at 2400 K, driving off any excess component as well as dissolved oxygen.

2. Sample Characterization

Whereas the techniques of synthesis may vary with each of the compounds referred to above, the same methods of analysis are useful for all of them for proper characterization. Standard analytical techniques (mass spectrographic analysis, atomic absorption spectroscopy) can be employed to indicate the amounts of trace elements present. In addition, a separate analysis for oxygen is desirable. However, because of the high likelihood of phase impurities in these compounds, a "wet" chemical analysis for the major components will not suffice to complete the sample characterization. A number of techniques have been applied by workers to establish the phase purity of their samples; among them, nuclear magnetic resonance, x-ray diffraction, neutron diffraction, microscopic metallographic analysis and a combination of the last method with electron microprobe analysis. The first three methods cannot be considered as definitive methods if one is concerned with phases present in amounts below a few atomic percent. Metallographic examination is the most useful technique here and it is claimed [2] that properly applied, it can quantitatively detect as little as 0.1 percent of a foreign solid phase.

III. Literature

A. General References

The most valuable general references dealing with the chemistry, thermodynamics and phase behavior of refractory carbides and borides have been found to be the monographs of Storms [5] and Hausner and Bowman [6], the extensive report series of Rudy and co-workers [7,8,9,10,11,12] and the compendia of Schick [13], Hansen [14], Elliot [15] and Shunk [16].

A search of the literature has been made for reported enthalpy and specific heat data on the carbides and borides of interest to this program. In addition to consulting the general references listed above, Chemical Abstracts were covered through July 1971; Ceramic Abstracts, through December 1970 and the Bulletin(s) of Thermodynamics and Thermochemistry, through No. 13 (1970). The results of this search are tabulated in table 1.

Table 1

Reported Investigations of Enthalpy and Heat Capacity
of solid Mo₂C, TaC, Ta₂C, NbB, and NbB₂

<u>Compound</u>	<u>Year</u>	<u>Enthalpy</u> <u>Range</u> K	<u>Heat Capacity</u> <u>Range</u> K	<u>S</u> _{298.15} cal, mol ⁻¹ , K ⁻¹	<u>Ref.</u>
Mo ₂ C	1964	533-2200			[19]
	1966		52-296	15.73 ± .09	[17]
	1966	406-1403			[17]
	1968		21-300	15.74 ± .03	[18]
TaC	1940		55-295	10.11 ± 0.08	[20]
	1962	538-2761			[23]
	1963	1296-2843			[21]
	1963	1300-2100			[22]
	1965	476-1113			[24]
	1966	405-1700			[17]
	1967	324-985			[25]
	1968	1205-2163			[26]
	1968		1.5-18		[27]
Ta ₂ C	1968		1.5-18		[27]
NbB	1969		1.5-18		[28]
NbB ₂	1962	468-1102			[29]
	1963		5-350	8.91 ± .01	[30]
	1966		0.6-2.8		[31]

References

- [1] Rudy, E., AFML-TR-65-2, Part V, 1969.
- [2] Rudy, E., private communication, March 1971.
- [3] Bowman, A., private communication, March 1971.
- [4] Storms, E. K., private communication, March 1971.
- [5] Storms, E. K., The Refractory Carbides, Academic Press, 1967.
- [6] Hausner, H. H., and Bowman, M. G., Fundamentals of Refractory Compounds, Plenum Press, 1968.
- [7] Rudy, E., Windisch, ST., and Chang, Y. A., AFML-TR-65-2, Part I, Vol. I, March 1965 (Mo-C system).
- [8] Rudy, E., Windisch, ST., and Hoffman, J. R., AFML-TR-65-2, Part I, Vol. VI, January 1966 (Mo-C system).
- [9] Rudy, E., Windisch, ST., Stoicks, A. J., and Hoffman, J. R., AFML-TR-65-2, Part I, Vol. XI, April 1967 (Mo-C system).
- [10] Rudy, E., AFML-TR-65-2, Part V, 1969 (Mo-C, Ta-C, NbB systems).
- [11] Rudy, E., and Harmon, D. P., AFML-TR-65-2, Part I, Vol. V, January 1966 (Ta-C system).
- [12] Rudy, E., and Windisch, ST., AFML-TR-65-2, Part I, Vol. X, (May 1966) (Nb-B system).
- [13] Schick, H. L., Thermodynamics of Certain Refractory Compounds, Vols. I and II, Academic Press, 1966.
- [14] Hansen, M., Constitution of Binary Alloys, Second edition, McGraw-Hill, 1958.
- [15] Elliot, R. P., Constitution of Binary Alloys, First supplement, McGraw-Hill, 1965.
- [16] Shunk, F. A., Constitution of Binary Alloys, Second supplement, McGraw-Hill, 1969.

- [17] Pankratz, L. B., Weller, W. W., and King, E. G., Bureau of Mines Rept. Invest. 6861 (1966).
- [18] Paukov, I. E., Strelkov, P. G., and Filatkina, V. S., Russ. J. Phys. Chem. 42 (11), 1576 (1968).
- [19] Southern Research Institute, ASD-TDR-62-765 (1963).
- [20] Kelley, K. K., J. Am. Chem. Soc. 62, 818 (1940).
- [21] Levinson, L. S., J. Chem. Phys. 39 (6), 1550 (1963).
- [22] McDonald, R. A., Oetting, F. L., and Prophet, H., Interagency Chemical Rocket Propulsion Group, Working Group on Thermochemistry, Proc. first meeting, N.Y. (1963). CPIA Pub. No. 44 (U), p. 213 (Feb. 1964).
- [23] Neel, D. S., Pears, C. D., and Oglesby, S., WADD-TR60-924 (Feb. 1962).
- [24] Mezaki, R., Tilleux, E. W., Jambois, T. F., and Mangrave, J. L., Proc. Third Symposium on Thermophysical Properties, Purdue Univ., Lafayette, Ind., p. 138 (1965).
- [25] Chang, Y. A., Trans. AIME 239, 1685 (1967).
- [26] Bolgar, A. S., Guseva, E. A., Gorbatyuk, V. A., and Fesenko, V. V., Sov. Powd. Met. Metal Ceram., No. 4, 297 (1968).
- [27] Toth, L. E., AFOSR-68-0265 (Feb. 1968).
- [28] Tyan, Y. S., Toth, L. E., and Chang, Y. A., J. Phys. Chem. Solids 30, 785 (1969).
- [29] Mezaki, R., Tilleux, E. W., Barnes, D. W., and Margrave, J. L., Int. At. Energy Agency, Proc. Symp. on Thermod. of Nucl. Mat., Vienna, p. 775 (1962).
- [30] Westrum, E. F. Jr., and Clay, G. A., J. Phys. Chem. 67, 2385 (1963).
- [31] Ukei, K., and Kanda, E., Sci. Rep. Res. Inst. Tohoku Univ. Ser. A, Suppl. 18, 413 (1966).

Chapter 10

A HIGH-SPEED METHOD OF MEASURING THERMAL EXPANSION OF ELECTRICAL CONDUCTORS

Ared Cezairliyan
National Bureau of Standards
Washington, D.C. 20234

To avoid the difficulties involved in conventional steady-state methods of measuring thermal expansion of electrically conducting substances at temperatures above approximately 2000°K, a transient technique is developed. In this technique, the specimen can be pulse heated from room temperature to near its melting point in less than one second and pertinent experimental quantities can be measured with a time resolution of 0.4 ms and a full-scale signal resolution of one part in 8000.

The method is based on detecting the change in radiance coming from a constant radiation source as a result of the expansion of the specimen placed between the radiation source and a radiation detecting system. Aperture stop of the optical system (Figure 1) is defined by a diaphragm which has a rectangular opening (15.9 x 12.7 mm). The "effective" aperture of the system depends on the dimensions of the rectangular opening and the area of the portion of the specimen in line with the opening. As the specimen is pulse heated its dimensions increase which, in effect,

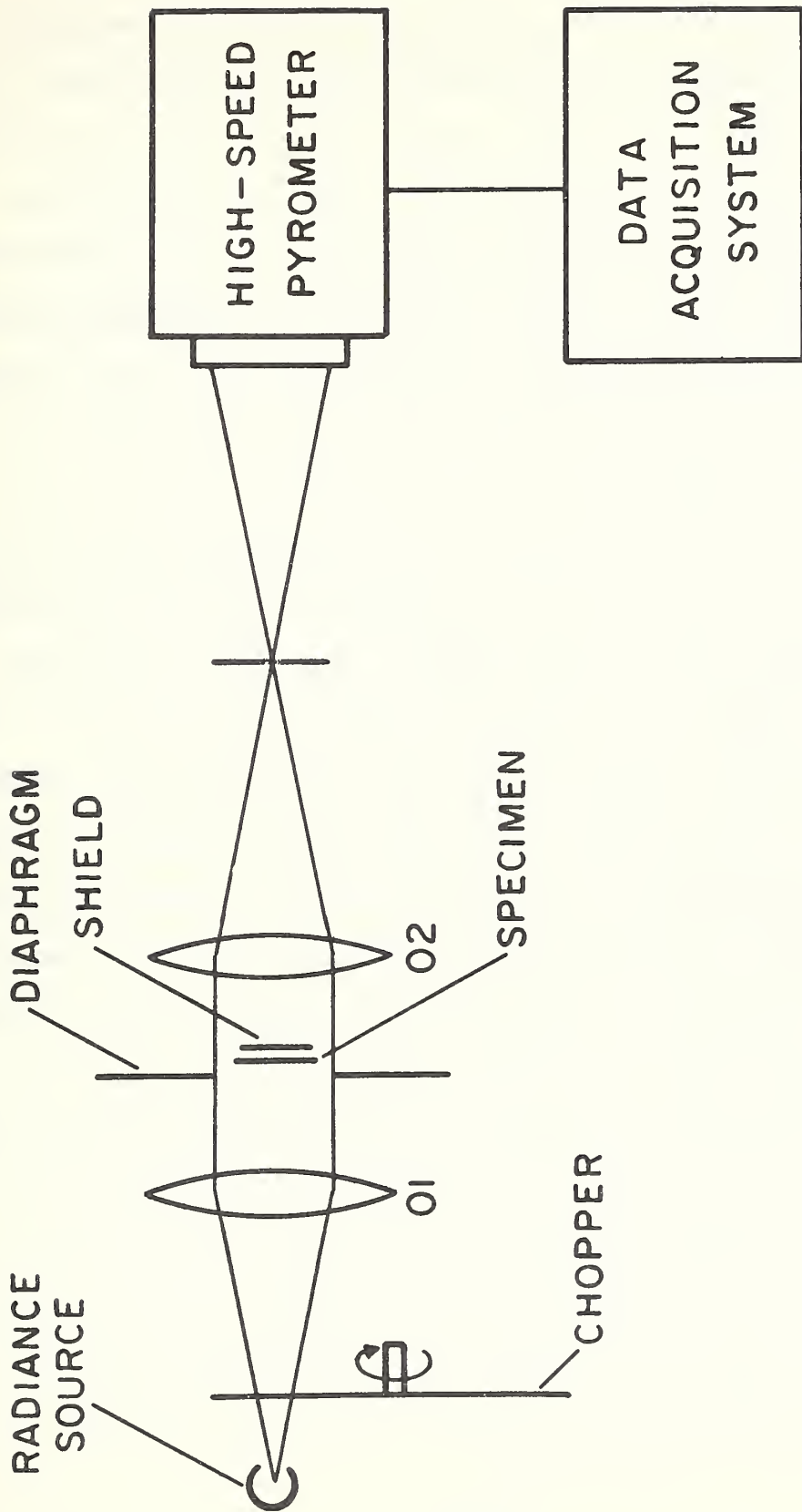


FIGURE 1. Optics of the high-speed thermal expansion measurement system.

reduce the "effective" aperture. To eliminate errors on final results due to radiation emitted by the specimen, radiance from the source is modulated at 600 Hz with a chopper. This allows the pyrometer to measure alternately (1) radiances from the radiation source and the specimen together, and (2) radiance from the specimen alone. Then, the difference between the two radiances is proportional to the dimensions of the specimen. Specimen radiance as seen by the pyrometer is minimized by placing a shield, which is slightly narrower than the specimen, between the specimen and the pyrometer.

This note describes the results of preliminary experiments designed to demonstrate the feasibility of the method. They were performed in the temperature range 300 to 700 K to allow the comparison of the results with those obtained by well-established steady-state methods.

The specimen was a platinum strip with the following nominal dimensions: length = 90 mm, width = 11 mm, and thickness = 0.03 mm. It was pulse heated by passing electric currents through it. During this time, current flowing through the specimen and potential difference across the mid-portion were measured. Potential leads were platinum wires (0.02 mm in diameter) spot welded to the strip approximately 30 mm apart. In addition, radiance from the radiation source attenuated by the expanding specimen was measured with a high-speed photoelectric pyrometer [1]. Recordings of experimental quantities were made with a high-speed digital data acquisition system [2]. Details of the electrical pulsing, control, and measuring circuits were described in an earlier publication [2].

Specimen temperature during the pulse heating period was determined from a knowledge of the resistance-temperature relationship for platinum [3].

The relation between variation of radiance with specimen expansion was determined by calibrating the optical system under steady-state conditions. This was accomplished by inserting obstructions of known cross-section in the optical path. A total of five cylindrical obstructions, ranging from 0.025 to 0.25 mm in diameter, were used. The results of radiance variation in terms of obstruction cross-section were fitted to a linear function using the least squares method, which gave a standard deviation of 0.06 percent.

Two pulse experiments were performed in which the platinum specimen was heated from room temperature to 700 K in approximately 120 ms. Thermal expansion results of each experiment were fitted to a third degree polynomial function using the least squares method, which gave a standard deviation of less than 0.1 percent. The results of the two experiments are in agreement within 2 percent. The averages of the results of the two experiments are approximately 3 percent lower than the recommended values for thermal expansion of platinum given by Kirby et al [4]. Estimates of errors indicate that the present results are accurate within 5 percent.

The results of preliminary experiments described above demonstrate the feasibility of measuring thermal expansion of electrical conductors by a transient technique. Because of the very short experiment duration, this technique is particularly attractive for measurements at high

temperatures (above 2000 K). Also, the fact that only the middle portion of the specimen is used for the measurements, uncertainties due to axial temperature gradients are greatly reduced.

At the present time, several refinements are being considered to improve the accuracy of the measurements. These are summarized in the following items:

- a. to reduce the effective aperture--this will increase the measurement sensitivity.
- b. to use specimens which are of tubular shape--this will eliminate uncertainties due to possible specimen misalignment and movement providing better symmetry.
- c. to measure specimen temperature directly with a high-speed pyrometer.
- d. to investigate the possibility of using a laser as the radiation source.

References

- [1] Foley, G. M., Rev. sci. Inst. 41, 827 (1970).
- [2] Cezairliyan, A., M. S. Morse, H. A. Berman, and C. W. Beckett, J. Res. Nat. Bur. Stand. (U.S.) 74A (Phys. and Chem.), 65 (1970).
- [3] Evans, J.P., National Bureau of Standards, private communication.
- [4] Kirby, R.K., T. A. Hahn, and B. D. Rothrock, "Thermal Expansion", American Institute of Physics Handbook, third edition, to be published.

Chapter 11

ROTATING OPTICAL ATTENUATOR FOR THE GENERATION OF SUBSECOND DURATION SAWTOOTH SHAPE RADIANCE PULSES

Ared Cezairliyan
National Bureau of Standards
Washington, D. C. 20234

Abstract

A rotating attenuator for the generation of subsecond duration sawtooth shape radiance pulses is described. The attenuator disk is in the form of a cam. The geometry of the opening of a diaphragm used as the aperture stop determines the shape of the radiance pulses. Radiance is determined from the measurements with a high-speed photoelectric pyrometer. Recording of signals is made with a high-speed digital data acquisition system. The combined measuring and recording systems have a full-scale signal resolution of approximately one part in 8000 and a time resolution of 0.4 ms. Two different diaphragms are used in this study yielding radiance pulses (20 to 150 ms long) with linear and quadratic rise. The standard deviation of the experimental points from the pertinent functions describing the radiance variation is less than 0.5 percent.

1. Introduction

Considerable amount of work has been done to develop various techniques to modulate radiance beams in the visible as well as in the ultraviolet and infrared regions. Most of these techniques were confined to generating either repetitive rectangular pulses, or short-duration fast-rise-time single pulses. A review of various methods for modulating radiance pulses was given by Jones [1]. Optical modulation techniques in the infrared region were discussed by Hudson [2].

Increasing interest in research in transient techniques for the measurement of properties of matter at high temperatures and related studies have necessitated the development of programable optical attenuators. Such attenuators are needed in order to simulate (using steady-state radiance sources) the rapid heating or cooling of the specimen and also to check dynamic characteristics of radiation detectors and of high-speed temperature measurement systems in general.

2. Method and Apparatus

In this study an optical system, including a rotating optical attenuator is described which is capable of generating repetitive sawtooth shape (either linear or quadratic) radiance pulses, ranging from 20 ms to several seconds in duration. The optical system is shown in figure 1. It consists of a radiance source (tungsten filament lamp), a rotating disk (cam with helical circumference), a special diaphragm, a high-speed pyrometer, and other pertinent optical components. The lenses 01 and 02 shown in figure 1 were 63 mm in diameter with $f = 2.5$. The circumference of the disk was machined in such a way that its radius r was proportional to the angle from a fixed reference point according to the following relation

$$r = r_0 - k\alpha \quad (1)$$

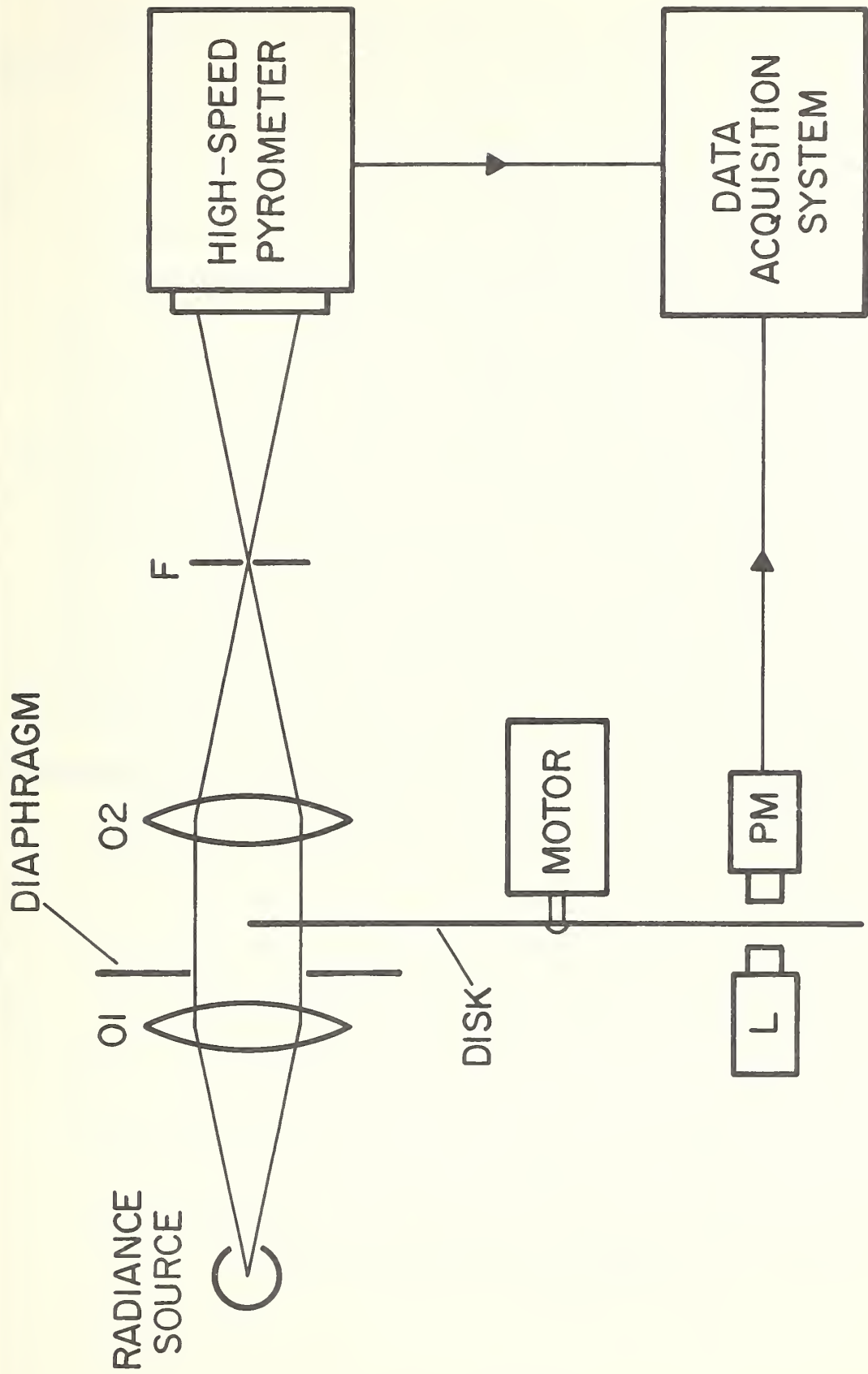


FIGURE 1. Functional diagram of the optical system for the generation of subsecond duration sawtooth shape radiance pulses.

where r_0 is the maximum radius, α the angle, and k , the proportionality constant. The maximum and minimum radii of the disk were 7 in. (177.8mm) and 6 in. (152.4 mm), respectively, yielding a maximum difference of 1 in. (25.4 mm). The thickness of the disk was 0.12 in. (3 mm).

The aperture stop of the optical system was defined by the circumference of the disk and the diaphragm placed in the collimated portion of the beam. As the disk rotated, the effective cross-sectional area of the beam changed, which, in turn, generated sawtooth shape pulses. The shape of the diaphragm opening determined the shape of the radiance pulse. For example, a rectangular opening as seen in figure 2 yields a pulse with linear rise, a triangular opening gives a pulse with quadratic rise. Rotation of the disk was synchronized with other measuring equipment with a signal obtained from a radiation detector. The radiation detector PM (figure 1) generated a signal each time a 0.2 mm in diameter hole H (figure 2) fabricated in the disk was in line with the detector and the light source L (figure 1). Relative radiance of the source after attenuation was measured with a high-speed photoelectric pyrometer [3]. The electrical signals from the pyrometer were recorded with a high-speed digital data acquisition system [4]. The combined measuring and recording system has a full-scale signal resolution of approximately one part in 8000 and a time resolution of 0.4 ms.

The photomultiplier in the pyrometer was alternately exposed to the radiance from the tungsten filament lamp and to the radiance from a reference lamp. This scheme eliminated errors that result from photomultiplier fatigue, etc.

Pulse shape as a function of time for various diaphragm geometries are derived in the following paragraphs.

Effective cross-sectional area of the light beam, when disk circumference is at point x on the diaphragm, may be expressed as

$$A_x = \int_0^x y \, dx \quad (2)$$

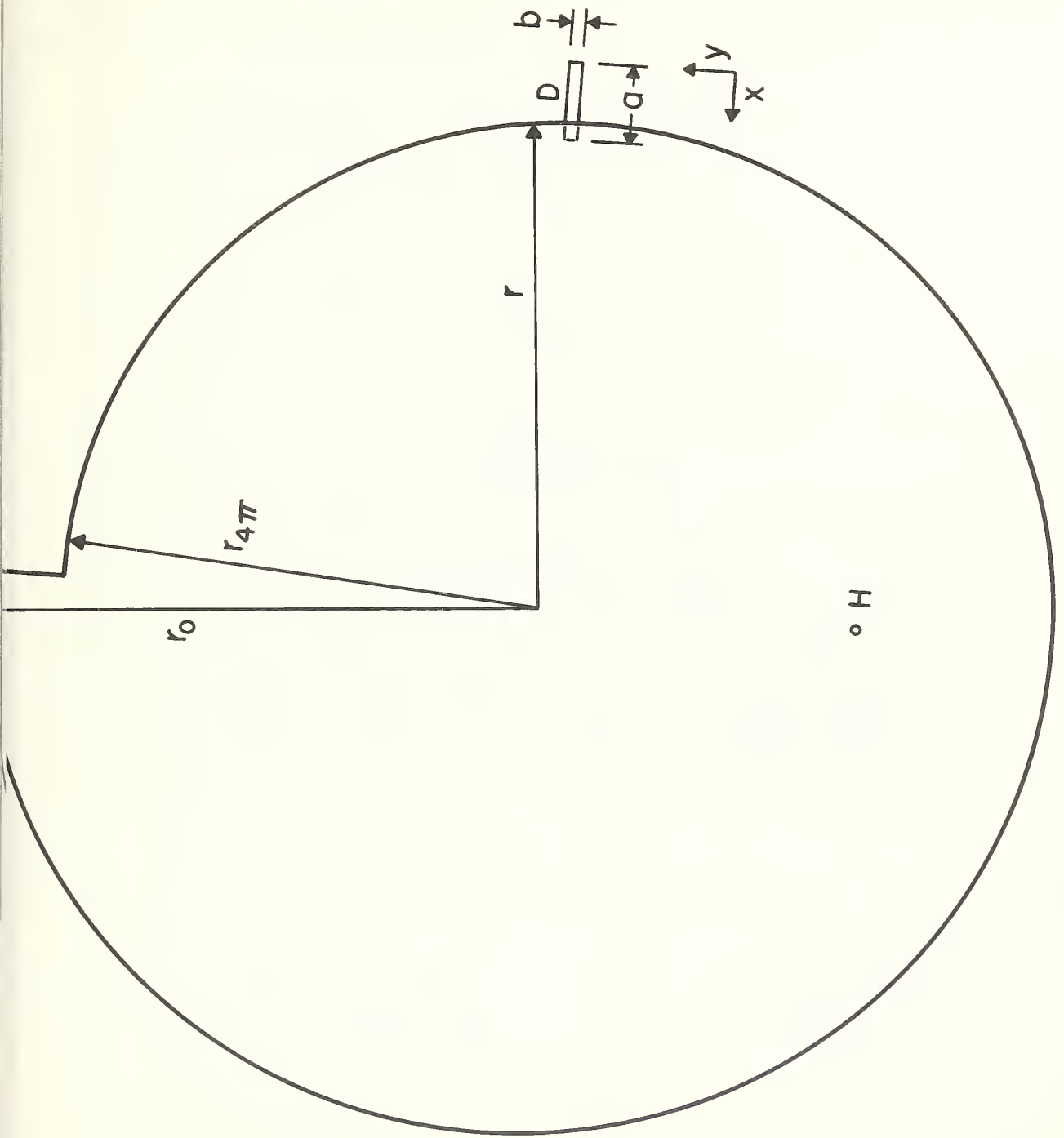


FIGURE 2. The attenuator disk and the diaphragm opening.

where $x = r_0 - r$ and y is the width (height) of the diaphragm at x (figure 2).

For rectangular geometry, $y = \text{constant} = a$, thus

$$A_x = ax \quad (3)$$

For triangular geometry, $y = bx$, thus

$$A_x = bx^2/2 \quad (4)$$

When the disk rotates at constant speed, angle of rotation is proportional to time t

$$a = k't \quad (5)$$

From Eq. (1) and the definition of x

$$x = r_0 - r = k\alpha \quad (6)$$

Combination of Eqs. (5) and (6) yields

$$x = kk't \quad (7)$$

Radiance L as seen by the pyrometer at a given instant is

$$L = k'' A \quad (8)$$

Combination of Eqs. (3), (4), (7), and (8) yields the following:

For rectangular geometry

$$L = Kt \quad (9)$$

For triangular geometry

$$L = K't^2 \quad (10)$$

where K and K' are combination of constants. Equations (9) and (10) represent radiances which are linear and quadratic functions of time, respectively.

3. Results

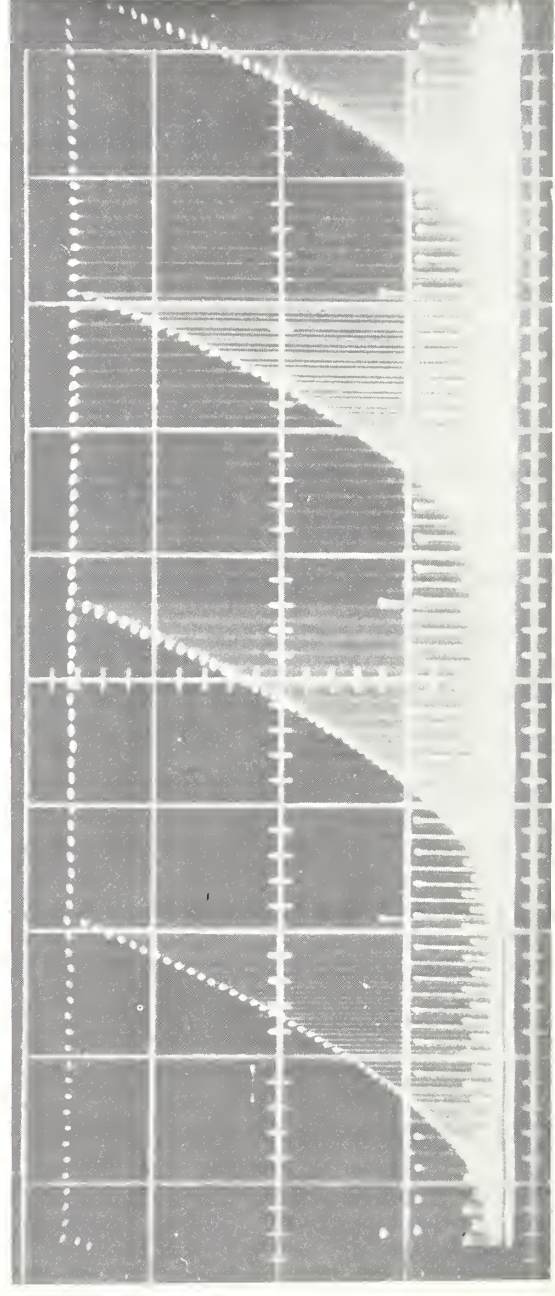
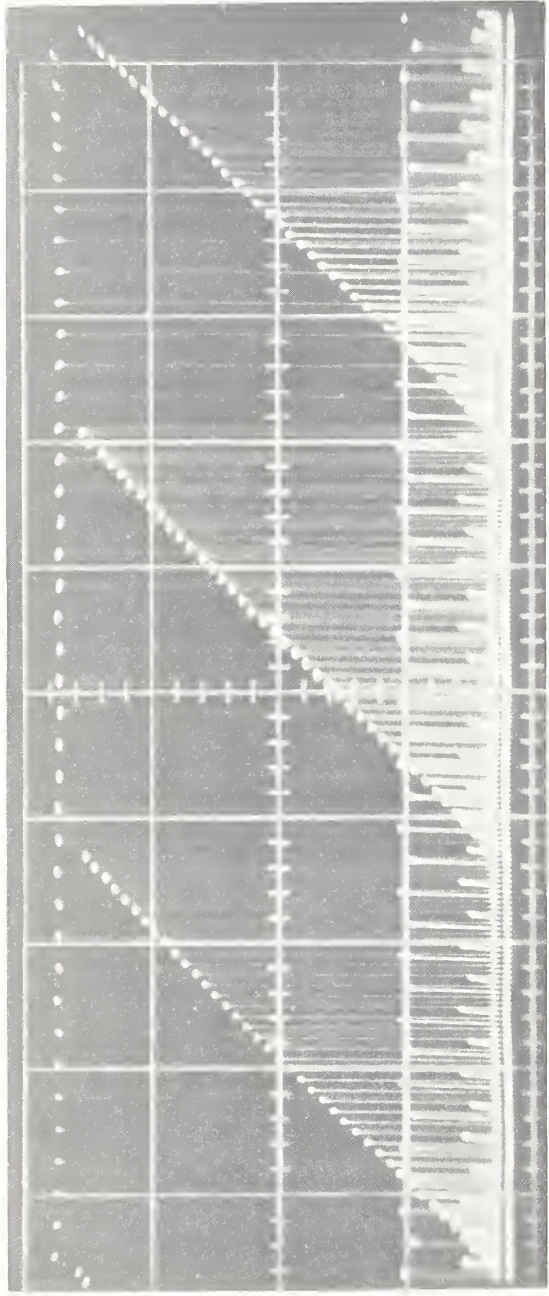
In order to assess the operational characteristics of the system, experiments were performed using diaphragms of rectangular and triangular openings. These experiments are summarized in the following paragraphs.

Linear Radiance Pulses: A total of fifteen experiments were conducted at five different attenuator speeds yielding radiance pulses (increasing linearly with time) in the range 20 to 150 ms. Additional four experiments were performed with the direction of rotation of the attenuator reversed. This scheme generated radiance pulses which decreased linearly with time.

Quadratic Radiance Pulses: A total of four experiments were conducted at two different attenuator speeds. An additional experiment was performed with the direction of rotation of the attenuator reversed.

Oscilloscope trace photographs of representative radiance pulses are shown in figure 3. The radiances as detected by the high-speed pyrometer and recorded with the digital data acquisition system were fitted to linear and quadratic functions, depending on the pulse shape, using the least squares method. The summary of the experimental parameters and the results are given in table 1. It may be seen that average standard deviation (individual point) of the results of both pulse shapes is approximately 0.6 percent corresponding to data covering a radiance ratio of over 10.

The above value for the standard deviation reflects departure from ideal behavior which may be due to several factors, such as random noise in radiance samples and in the pyrometer operation, non-uniformity in the lenses and in the optical alignment, non-uniformity in the attenuator circumference, variation in the attenuator speed, etc. In order to separate the contribution of the pyrometer and the random noise inherent in radiance measurements from the attenuator and the associated optical system,



RADIANCE

TIME

FIGURE 3. Oscilloscope trace photographs of linear (upper) and quadratic (lower) pulses. Horizontal scale: 10 ms (upper), 20 ms (lower) per major division. Vertical scale: arbitrary units. Dots forming the long horizontal lines

TABLE 1

Summary of Experimental Parameters and Results

em	Radiance Variation	Direction of Radiance Variation	Pulse Length (ms)	Number of Experiments	Number of Points per Experiment	Average Radiance Ratio	Average Standard Deviation (%)
1	Linear	Increasing	23	3	20	10.3	0.6
2	Linear	Increasing	30	3	26	12.1	0.7
3	Linear	Increasing	39	3	33	9.0	0.6
4	Linear	Increasing	59	3	50	11.8	0.5
5	Linear	Increasing	144	3	123	11.3	0.6
6	Linear	Decreasing	23	1	20	10.0	0.7
7	Linear	Decreasing	30	1	26	9.5	0.7
8	Linear	Decreasing	39	1	33	10.4	0.6
9	Linear	Decreasing	59	1	50	10.6	0.5
0	Quadratic	Increasing	60	3	39	11.0	0.6
1	Quadratic	Increasing	40	1	26	10.1	0.5
2	Quadratic	Decreasing	60	1	39	11.1	0.6

two separate experiments were conducted under steady-state conditions. In one of the experiments, the attenuator was positioned to provide the maximum opening of the diaphragm as seen by the pyrometer. Then the pyrometer response to the radiance source was recorded. The standard deviation of the results was 0.2 percent. A similar experiment was performed with the attenuator positioned to provide radiance equivalent to that of the lowest level used in the dynamic experiments. The standard deviation of the results of the pyrometer output was 0.8 percent. If one assumes an approximately linear variation of randomness between the two extremes, one arrives at a value of 0.5 percent for the standard deviation contributed by the pyrometer and radiance measurements in general. Thus, if it is assumed that total standard deviation is the square root of the sum of the squares of individual standard deviation, the standard deviation corresponding to the non-uniformities of the attenuator and the associated optical components becomes approximately 0.3 percent.

In order to ascertain the fact that the value obtained for the standard deviation was the result of random deviations in the data, the data on radiance was also fitted to functions of one and two higher degrees than the pertinent one. No improvement in the standard deviation was observed. This indicated that there was no detectable systematic curvature imposed on the proper function.

4. Conclusion

The results of the experiments described above have shown the feasibility of generating subsecond duration pulses of prescribed shapes (linear and quadratic) with a standard deviation of less than 0.5 percent over a radiance ratio of 10. The method allows one to insert appropriate diaphragm in the optical system to obtain radiance pulses of various shapes. For example, in addition to linear and quadratic, it is possible to generate pulses of cubic, exponential and other shapes.

The scheme of generating radiance pulses allows one to detect the linearity of radiation detectors under dynamic conditions, and also provides the experimenter with means of simulating high-speed heating or cooling experiments.

5. References

1. Jones, O. C., J. Sci. Instr., 41, 653 (1964).
2. Hudson, R. D., Infrared System Engineering, Wiley, New York (1969) p. 235.
3. Foley, G. M., Rev. Sci. Instr., to be published (1970).
4. Cezairliyan, A., M. S. Morse, H. A. Berman, and C. W. Beckett, J. Res. Nat. Bur. Stand. (U. S.), 74A (Phys. and Chem.) 65 (1970).

Chapter 12

OPTICAL METHODS OF MEASURING TRANSIENT HIGH TEMPERATURES

Ared Cezairliyan
National Bureau of Standards
Washington, D. C. 20234

Abstract

Various optical methods, primarily photoelectric and photographic, of measuring transient high temperatures are described. Emphasis is placed on techniques of measuring transient temperatures of solids above approximately 1500 K with subsecond (upper millisecond to upper microsecond) resolution. Advantages and limitations of the various methods are discussed and estimates of uncertainties are given. Application of the high-speed temperature measurement methods to various fields of investigations, including determination of thermo-physical properties, is presented.

1. Introduction

Increasing interest in high-speed studies of high-temperature phenomena and the utilization of transient techniques for the measurement of properties at high temperatures has necessitated the development of temperature measurement methods having high time resolution. Most well-established steady-state temperature measuring devices, such as thermocouples, resistance thermometers, conventional optical and automatic optical pyrometers, etc., are inadequate because of their relatively long response times. The definite advantages of non-contact methods in high temperature measurements suggest the selection of optical methods in developing high-speed high temperature measuring systems.

Although at present there is no commercially available instrument for high-speed temperature measurements, several prototype instruments have been developed in various laboratories for research purposes. However, most of these instruments were built for specific practical applications with little attention being given to the attainment of high precision and accuracy. Preliminary research has shown the potential of optical methods as means for high-speed measurement of high temperatures. Optical methods may be classified under the following general categories: photoelectric, photographic, and spectroscopic. Each method has certain advantages and the selection of an appropriate method for high-speed temperature measurements depends upon the specific application. Since the primary objective of this paper is to discuss techniques of measuring transient temperatures of solids at high temperatures, emphasis is placed on the photoelectric and photographic methods;

the spectroscopic methods are used for temperature measurements in gases. In view of the lack of accurate and versatile high-speed (millisecond and microsecond resolution) pyrometers, certain criteria and possible avenues for future research and development are also discussed in the last section of the paper.

2. General Considerations

A basic requirement in all high-speed optical temperature measurements is the availability of sufficient number of photons within the bandwidth of the detection system. Selection of a proper detection system to meet this requirement depends on a number of factors. Among these are: (1) level of temperature to be measured, (2) effective wavelength of radiance measurement, (3) spectral sensitivity of detectors, (4) time resolution, (5) characteristics of existing calibration facilities, and (6) special experimental requirements. Some of the above items are interrelated in such a way that the proper selection of a detection system must be based on optimization under a given set of conditions.

Calibration facilities for conventional pyrometry (visual or automatic) are developed for the red region in the vicinity of 650 nm. Therefore, it is advantageous to utilize this wavelength in high-speed pyrometry as much as possible. This can be done successfully for temperatures up to approximately 5000 K. Above 5000 K it may be desirable to shift the operation to shorter wavelengths because the peak of the Planck radiation function moves toward shorter wavelengths with increasing temperature. The selection of the wavelength to correspond to the peak in radiation at the average temperature of measurements provides

the detection system with the maximum number of photons. However, in most cases the peak of the radiation function for a given temperature does not correspond to the wavelength of the maximum response of the detector. Therefore, an optimization becomes necessary.

The high-speed temperature measurement methods described in the literature are based, in general, on the measurement or comparison of radiance of the specimen with that of a known reference. The detection systems used for the measurement or comparison of radiances are mainly photoelectric or photographic.

If the unknown radiance source is not a blackbody, measurements performed at one wavelength, in conjunction with a proper calibration, yield brightness temperature. To obtain true temperature, a knowledge of normal spectral emittance for the surface at the operating temperature is required. Accurate measurements of this property at high temperatures are difficult and results reported in the literature cannot be properly applied to a particular specimen due to strong dependence of normal spectral emittance on surface conditions. To avoid some of the above difficulties, a few investigators have developed techniques in which radiance measurements are performed at more than one wavelength. Such an approach eliminates, to a first approximation, a knowledge of the absolute value of normal spectral emittance. However, this method is wavelength sensitive, and thus its ultimate accuracy depends on the accuracy with which effective wavelengths can be determined.

In steady-state temperature measurements, detectors are used generally to match the radiance of the unknown with that of the reference. However, in high-speed measurements this approach cannot be used because of time limitations. In the latter case, the unknown temperature is usually determined by the interpolation of the unknown radiance from bracketing reference radiances. Accuracy of this approach depends, among other factors, on the linearity of the detectors. Linearity of photomultipliers is generally better than 1 percent over a radiance range of 3 decades, which is sufficient for most measurements. If properly exposed, processed, and interpreted, linearity of films may be 1 percent over a radiance range of 2 decades.

3. Photoelectric Methods

In most photoelectric methods, the unknown radiance is detected with a photocell or a photomultiplier corresponding to a bandwidth at a certain effective wavelength. The resultant electrical signal is recorded with an appropriate high-speed recording system.

The photocell or the photomultiplier is exposed to the unknown radiance continuously during the transient experiment and its output is recorded either with a high-speed chart recorder or an oscilloscope. The system is calibrated under steady-state conditions before or after an experiment by substituting a standard radiance source for the unknown. This scheme has the disadvantage that it assumes stability and reproducibility of the detector between calibration and transient experiments. Studies performed on photomultipliers indicate that this assumption is not completely justified; thus, measurements based on the above technique may be subject to considerable errors.

In the literature, a few investigators used this or similar techniques to measure temperatures in connection with either the studies of temperature variations in transient events, or property measurements utilizing transient techniques. These are summarized in the following paragraphs.

Use of a photomultiplier, in conjunction with proper optics and electronics, to measure temperature fluctuations of incandescent surfaces was described by Dehn¹. The time resolution was better than 1 μ s. Photomultiplier output was recorded with an oscilloscope. Reported measurement inaccuracy was approximately 10 percent, with a sensitivity of 2 K at 1100 K. The technique was used to measure temperature fluctuations of an oscillating magnetron.

The design of a photoelectric pyrometer intended for use in transient measurements of thermal properties at temperatures above 1300 K was described by Rasor and McClelland². This instrument could measure small temperature changes (6 K) with a response-time of less than 10 ms during pulse heating of the specimen. A photomultiplier having a S-1 surface was used as a detector, and its output was recorded with an oscillograph.

In an attempt to measure specific heat by a transient technique at temperatures above 1300 K, Cezairliyan³ used a photomultiplier (S-20 surface) with associated optics and electronics. Signals were recorded with an oscilloscope. The system measured radiance of the specimen as it was heated at the rate of 6600 Ks⁻¹.

For the transient measurement of specific heat of metals at high temperatures, Affortit and Lallement⁴ utilized a photomultiplier system, in addition to thermocouples, to measure the temperature of a heating specimen. Signals were recorded with an oscilloscope.

A high-speed ratio (multicolor) pyrometer, which operated on the principle of measuring sequentially radiance at three different wavelengths (700, 800, and 900 nm), was described by Hornbeck⁵. A single detector was used for all selected wavelengths. Signals were recorded with an oscilloscope. Reported measurement rate was over 1000 sets per second.

Another version of a high-speed multicolor pyrometer was described by Kottenstette⁶. This pyrometer also employed the method of measuring unknown radiance at three different wavelengths ranging approximately from 600 to 750 nm. A separate detector (silicon photovoltaic cell) for each wavelength was used. Detector response time was 5 μ s. Signals were recorded with an oscilloscope. The pyrometer's operating range was from 1500 to 4000 K with a reported inaccuracy of 3 percent at 4000 K.

In some experiments, it is important to determine rapidly temperature distribution over the specimen. A pyrometer, utilizing a photomultiplier, was designed by Sims and Place⁷ that could measure temperature distribution over an incandescent surface. The scanning was achieved by a rotating disk, which contained fifteen holes in the form of a spiral. The duration of a complete scan was approximately 0.1 s. Recording of signals was made with an oscilloscope. The reported inaccuracy was 4 K at 1400 K.

All of the above were preliminary attempts to measure temperature at high speeds by photoelectric methods. In all cases, the system was calibrated either before or after the experiment under steady-state conditions. This assumed that the behavior of the detectors and other related components were not altered between the calibration and the actual experiment. Since photomultipliers are highly unstable, the above approach cannot be used for accurate measurements. Foley⁸ developed a laboratory prototype of a pyrometer that eliminated the above uncertainties by incorporating a self-calibrating scheme during the experiment. The pyrometer permitted 1200 evaluations of the specimen temperature per second. A schematic diagram of the optical system of the pyrometer is shown in figure 1. An outline of the description of the method and operational characteristics of the pyrometer is given in the following paragraphs.

A chopper disk (shutter) in the pyrometer alternately passes precisely timed samples of radiance from the specimen (unknown) and from a reference source through an interference filter (wavelength 650 nm, bandwidth 10 nm) to a photomultiplier (S-20 surface). The reference source is a calibrated gas-filled tungsten lamp. Successive exposures to the reference pass through a sequence of three different calibrated optical attenuators, mounted on a rotating disk on the chopper motor shaft, resulting in a staircase of reference exposures, with approximately 50 percent attenuation between succeeding steps. The target may be as small as 0.2 mm in diameter at a range of 100 mm.

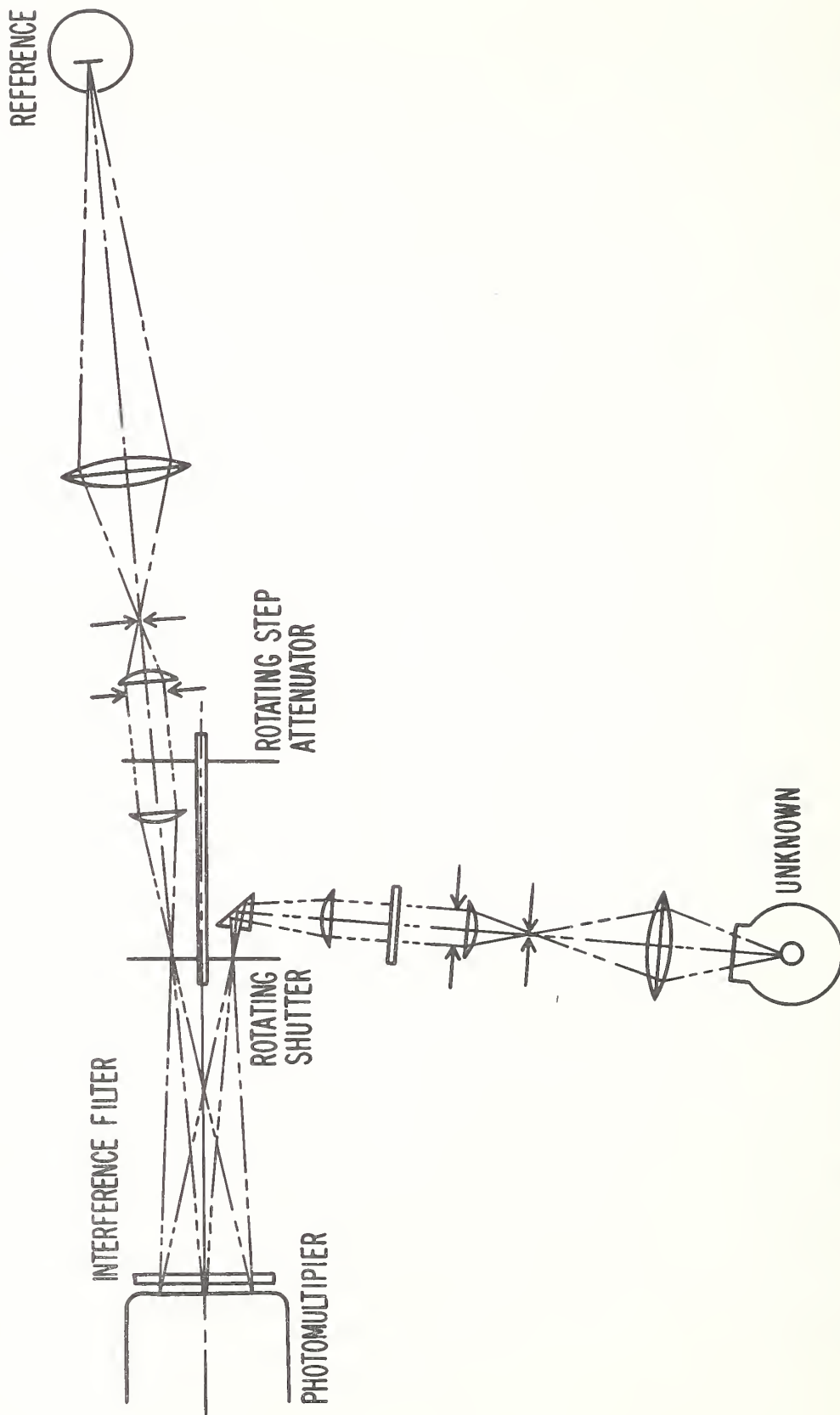


FIGURE 1. Optical system of the high-speed pyrometer (Foley⁸).

During each exposure to the reference or unknown source, the photomultiplier current is integrated and recorded, together with other data of experimental significance, by a digital data acquisition system composed of a multiplexer, an analog-to-digital converter, a magnetic core memory, and related control and interfacing equipment. At the end of an experiment, information is retrieved via a teletypewriter and is processed using a time-shared computer. The data acquisition system has a full-scale signal resolution of one part in 8000, and a time resolution of approximately 0.4 ms. The pyrometer has also been connected directly to a small dedicated computer to demonstrate temperature measurement in real time.

Since the same photomultiplier and electronic components are used to evaluate the radiance of the specimen and the reference on alternate exposures, uncertainties resulting from fatigue, drift, external magnetic fields, etc. are negligible. Inaccuracy of temperature measurements with this pyrometer is estimated to be 4 K at 2000 K. At the same temperature, sensitivity is approximately 0.5 K. This pyrometer is the most accurate photoelectric instrument in existence at the present time for transient temperature measurements above 1500 K with millisecond resolution.

4. Photographic Methods

In photographic methods, the film takes the place of both the detector and the recording system. The unknown radiance is determined from the measurement of the density of the film exposed to the unknown radiation corresponding to a bandwidth at a certain effective wavelength.

A discussion on the efficiency and other characteristics of radiation detection by photographic films is given by Bird et al.⁹.

Investigations of the possibility of using photographic techniques for temperature measurements under steady-state conditions started in the early thirties. These are summarized by Shramko¹⁰.

Applications of this technique to transient temperature measurements were initiated in the mid-forties. They were developed to study temperature variations in transient or unstable phenomena associated with combustion chambers, flames, ablation, property measurements, etc. Almost all attempts to use photographic techniques for transient temperature measurements were of a preliminary nature. Nevertheless, they have shown the potential of such techniques in experiments of short duration. A distinct advantage of photographic techniques over others is that they are capable of giving temperature distribution over the specimen surface at any given instant.

Photographic methods of transient temperature measurements are based on photographing, at high speeds, either (1) the unknown alone, or (2) the unknown and one or more reference radiance sources simultaneously. In the first method, film exposures have to be calibrated after the experiment with known radiance sources. The second method is far superior to the first since it reduces most of the calibration uncertainties. In both cases, the unknown radiance is obtained by interpolating the exposure density between the two adjacent references. Research activities along these lines since the mid-forties are summarized in the following paragraphs.

First Method (measurement and calibration at different times).

Application of the photographic method to the measurement of liquid steel temperatures using a 16-mm camera was described by Hall¹¹. Half of the film was marked off while the exposures were made on the steel streams. The mask was then reversed and the film was run through the camera four times in order to record the four images of a calibrated tungsten strip lamp at four brightness temperatures on the other half of the film. Thus, images of the unknown and references were placed side by side on each frame of the film. Temperature of the unknown was determined by the interpolation between two adjacent references. Reported inaccuracy was 10 to 20 K at 1800 K.

A photographic pyrometer utilizing a 35-mm camera was described by Londeree¹². Exposure time of each film was 1/6 s, and the measurements were made with a red filter. Film was calibrated with a tungsten filament lamp and a set of absorbing filters of known transmission. Reported inaccuracy of these temperature measurements was 5 K at 1800 K.

The photographic pyrometer described by Platunov and Fedorov¹³ operated at an effective wavelength of 630 nm with a speed of 24 frames per second.

Exton¹⁴ designed a photographic pyrometer for operation in the range 1000 to 2000 K. A 35-mm framing camera was used, which had a speed of 20 frames per second. The reported inaccuracy of temperature measurements was approximately 2 to 3 percent.

Second Method (measurement and calibration simultaneously).

A photographic pyrometer capable of photographing simultaneously an unknown source and four reference radiances is described by Male¹⁵. References were four tungsten filament lamps placed next to each other. They were viewed by the camera by means of a mirror located immediately below the optical path to the unknown and mounted 45° to the optical path to the camera lens. Temperature of the unknown was determined by an interpolation of film exposure densities between references.

The construction of a similar apparatus, also using four reference radiances was described by Simmons and DeBell¹⁶. They used their photographic pyrometer to measure the temperature of rocket exhaust flames by employing the two pathlength method. Radiance measurements were made in a narrow bandwidth at 650 nm. The reported uncertainty in temperature measurements was 10 K in the range 1300 to 2300 K. Simmons and DeBell¹⁷ later modified this technique to photograph the unknown at three wavelengths. This reduced the uncertainties due to variations in the normal spectral emittance of the unknown.

The methods summarized above had time resolutions ranging from tens of milliseconds to seconds. Faster (microsecond resolution) photographic temperature measurements in relation to shock, exploding conductor, and plasma studies were also tried. Almost all the attempts made to measure transient temperatures photographically were of an exploratory or preliminary nature. At the present time, there is no accurate and self-contained high-speed photographic pyrometer.

5. Applications

High-speed temperature measurement techniques find applications in transient experiments designed for the determination of selected thermophysical and related properties at high temperatures. Time-resolved temperature measurements are also used in studying the behavior of rapid events in complex systems, involving combustion, ablation, etc. In the following paragraphs specific applications of high-speed photoelectric and photographic temperature measurement techniques, as presented in the literature, are summarized.

Photoelectric: Applications of various photoelectric temperature measurement techniques in connection with the determination of selected thermophysical properties are presented by Rasor and McClelland¹⁸, Cezairliyan³, Affortit and Lallement⁴, and Affortit¹⁹. The accurate millisecond resolution pyrometer described by Foley⁸ was used to measure specific heat, electrical resistivity, and thermal radiation properties of molybdenum²⁰, tantalum²¹, and tungsten²² from 1900 to near their respective melting points. The same pyrometer was also used to determine the melting point of molybdenum²³ and to investigate the behavior of normal spectral emittance of tantalum during the initial melting period²⁴. The pyrometer described by Kottenstette⁶ was developed in conjunction with a study of high-energy chemical reactions. Changes in surface temperature of the cathode of an oscillating magnetron and temperature rise on the surface of thermionic cathodes were measured by Dehn^{1,25}.

Photographic: Photographic techniques have been applied particularly to cases where a knowledge of spacial temperature distribution is of importance. The pyrometer described by Male¹⁵ was developed for measurement of apparent surface temperature in a ram-jet combustion chamber. Temperature of luminous rocket exhaust flames was measured by Simmons and DeBell^{16,26}. Surface temperature variations on ablative materials were studied by Exton²⁷. Measurements of liquid steel temperature were performed by Hall¹¹. Application of photographic temperature measurements to property determinations was described by Platunov and Fedorov¹³ in connection with the measurement of thermal conductivity of tungsten above 1800 K.

6. Discussion

There are other possible optical methods of measuring transient temperatures. Spectroscopic techniques²⁸ have been useful in temperature measurements in hot gases and plasmas. However, most of the work has been concentrated in steady-state type measurements. High-speed bolometers with response times ranging from 50 μ s to 0.1 μ s have also been developed and used in connection with measurements of the radiance of nuclear fireballs²⁹ and pulsed plasmas³⁰.

In millisecond resolution experiments, the accuracy of photographic methods is, in general, lower than that of photoelectric methods. However, in faster experiments, photographic methods show great promise. A considerable amount of research and developmental work on high-speed photography and related techniques, ranging from millisecond to nanosecond resolution, is reported in the literature^{31,32,33,34}. Application of available technology on high-speed photography to temperature measure-

ments may result in the successful development of photographic pyrometers of microsecond resolution. Even after the development of accurate electronic temperature measuring equipment with microsecond resolution, photographic methods will continue to be exploited and will be useful in detecting temperature non-uniformities and measuring temperature gradients in the specimen. However, because of the relative ease and operational advantages, electronic methods are likely to be more desirable in most applications.

For the successful development of accurate high-speed temperature measuring systems utilizing electronic techniques one of the following two conditions has to be satisfied: (1) stable and reproducible radiation detectors, or (2) reliable high-speed radiation modulation.

Item (1) represents the case where the detector does not monitor alternately the radiance from the unknown and a reference. This requires the detector to be stable and reproducible between calibrations and high-speed experiments. It is also important that detector behavior is invariant under transient electromagnetic fields, which are generally present in high-speed experiments. Most of the sensitive detectors operating in the visible range, such as photomultipliers, are highly unstable photoelectrically, and in addition their output depends on environmental conditions, such as electromagnetic fields, vibration, etc. However, photomultipliers have been used because of their short response time (nanoseconds) and acceptable quantum efficiency. A detailed discussion on photomultipliers is given by Engstrom³⁵.

Recent developments in the field of solid-state detectors show considerable promise. They have submicrosecond response characteristics. However, no careful study has been made regarding their stability, reproducibility and behavior under strong electromagnetic fields. Most solid-state detectors have a maximum response in the near infrared and infrared regions, which are not very desirable for very high temperature work. Discussions on high-speed solid-state detectors may be found in articles by Amsel and Zajde³⁶, Lucovsky and Emmons³⁷, DiDomenico et al³⁸, and Anderson and McMurtry³⁹.

Given the condition of detector unstability, the alternative for accurate temperature measurements is to devise techniques for the detector to monitor alternately the radiance of the unknown and a reference. This scheme requires dependable radiation modulation methods. Relatively simple motor-driven choppers can be used for modulation at millisecond and even upper microsecond rates. However, there are no compact and reliable optical radiation modulating devices operating at lower microsecond rates. Reasonably reliable mechanical modulating schemes with microsecond resolution (such as, rotating mirrors used in high-speed cameras) are bulky, expensive, and are not easily adaptable to the rest of the system. Devices which operate on electro-optic phenomena are available, although at present their reproducibility is not adequate for accurate temperature measurements. A review on various methods of optical radiation modulation at high frequencies (up to GHz) was given by Jones⁴⁰.

In the design of high-speed pyrometers, it is important to optimize the speed with respect to temperature. If approximately 0.2 s of exposure time is required to make temperature measurements (by photoelectric methods) at the gold point (1337.58 K) corresponding to an effective wavelength of 650 nm, the following approximate exposure times are computed to be needed to perform the measurements at higher temperatures: 1000 μ s at 2000 K, 1 μ s at 5000 K, 0.1 μ s at 10,000 K, and 0.01 μ s at 50,000 K. Of course by optimizing the effective wavelength as temperature is increased, the exposure times can be further reduced.

In photographic pyrometry, characteristics of films play an important role in the proper design and operation of the overall system. Some of the items that have to be considered in connection with films are: (1) wavelength dependence of film sensitivity, (2) the shape of the film's "characteristic curve" that relates the film density to the logarithm of exposure, (3) spacial non-uniformities on the film, (4) processing the exposed film, (5) the degree of the failure of the reciprocity law for the film.

An important item that needs to be considered in the design, and operation of high-speed temperature measurement systems is the availability of reference radiance sources. At moderately high temperatures (up to 1500 K) vacuum tungsten filament lamps are generally used, in the range 1500 to 2500 K gas-filled lamps can be used. They are convenient to use, and their calibration usually stays within one degree at 2000 K after operating for ten hours. For temperatures above 2500 K, there are no reliable and well characterized radiance sources. The best

available source is the low-current graphite arc which yields a brightness temperature of approximately 3800 K. The temperature level is dependent on the composition of the graphite rods and the operating conditions, such as current, electrode separation, and atmospheric pressure.

Radiance temperature of the graphite arc and its relatively long-time (seconds to minutes) variations were investigated by Chaney et al⁴¹, Null and Lozier⁴², and Lee and Lewis⁴³. The most recent measurements⁴³ made with a photoelectric pyrometer having 1/6 s time constant gave 3 K for the standard deviation of temperature fluctuations from the mean, and up to 10 K for temperature variations over a period of 15 minutes. Recently, Cezairliyan⁴⁴ studied the short-time behavior of a graphite arc with a high-speed (millisecond resolution) photoelectric pyrometer. The standard deviation of radiance temperature fluctuations was found to be in the range 3 to 4 K; maximum deviations as much as 10 K from the mean were also observed.

Above 3800 K, lasers and high pressure arcs may become useful as reference radiance sources. However, so far very little research has been done regarding their radiance stability and reproducibility.

From the presentations in the earlier sections it may be seen that high-speed temperature measuring techniques are in their infancy as almost all approaches have been of a preliminary nature. However, continued interest in high temperature research and the possibilities of both photoelectric and photographic techniques may lead to the development of accurate and versatile high-speed pyrometers for temperature measurements in millisecond, microsecond, and even shorter times.

References

- ¹R. Dehn, Brit. J. Appl. Phys. 7, 144 (1956).
- ²N. S. Rasor and J. D. McClelland, Rev. Sci. Instr. 31, 595 (1960).
- ³A. Cezairliyan, "A High-Speed (Millisecond) Method for the Simultaneous Measurement of Enthalpy, Specific Heat, and Resistivity of Electrical Conductors at High Temperatures", in Advances in Thermophysical Properties at Extreme Temperatures and Pressures (ASME, New York, 1965), p. 253.
- ⁴G. Affortit and R. Lallement, Rev. Int. Hautes Tempér. et Réfract. 5, 19 (1968).
- ⁵G. A. Hornbeck, "High-Speed Ratio Pyrometer" in Temperature Its Measurement and Control in Science and Industry, C. M. Herzfeld, ed. (Reinhold, New York, 1962), Vol 3, Part 2, p.425.
- ⁶J. P. Kottenstette, ISA Trans. 4, 270 (1965) .
- ⁷R. B. Sims and J. A. Place, J. Sci. Instr. 31, 293 (1954).
- ⁸G. M. Foley, Rev. Sci. Instr., 41, 827 (1970).
- ⁹G. R. Bird, R. C. Jones and A. E. Ames, Appl. Opt. 8, 2389 (1969).
- ¹⁰Y. P. Shramko, High Temperature 5, 328 (1967) .
- ¹¹J.A. Hall, The Photographic Journal 86B, 117 (1946).
- ¹²J. W. Londeree, J. Am. Ceram. Soc. 37, 354 (1954).
- ¹³E. S. Platunov and V. B. Fedorov, High Temperature 2, 568 (1964).
- ¹⁴R. J. Exton, ISA Trans. 4, 365 (1965).

- ¹⁵D. W. Male, Rev. Sci. Instr. 22, 769 (1951).
- ¹⁶F. S. Simmons and A. G. DeBell, J. Opt. Soc. Am. 48, 717 (1958).
- ¹⁷F. S. Simmons and A. G. DeBell, J. Opt. Soc. Am. 49, 735 (1959).
- ¹⁸N. S. Rasor and J. D. McClelland, J. Phys. Chem. Solids 15, 17 (1960).
- ¹⁹C. Affortit, High Temp.-High Pres. 1, 27 (1969).
- ²⁰A. Cezairliyan, M. S. Morse, H. A. Berman and C. W. Beckett, J. Res. Nat. Bur. Stand. (U.S.) 74A (Phys. and Chem.), 65 (1970).
- ²¹A. Cezairliyan, J. L. McClure and C. W. Beckett, J. Res. Nat. Bur. Stand. (U.S.), 75A (Phys. and Chem.), 1 (1971).
- ²²A. Cezairliyan and J. L. McClure, J. Res. Nat. Bur. Stand. (U.S.), Section A, to be published (1971).
- ²³A. Cezairliyan, M. S. Morse and C. W. Beckett, Rev. Int. Hautes Tempér. et Réfract. 7, 382 (1970).
- ²⁴A. Cezairliyan, High Temp-High Pres. to be published.
- ²⁵R. Dehn, Brit. J. Appl. Phys. 7, 210 (1956).
- ²⁶F. S. Simmons and A. G. DeBell, Aircraft Engineering 31, 144 (1959).
- ²⁷R. J. Exton, AIAA Journal 7, 2262 (1969).
- ²⁸W. Lochte-Holtgreven, "Production and Measurement of High Temperatures", in Reports on Progress in Physics (The Physical Society, London, 1958), Vol. 21, p. 312.
- ²⁹H. E. Stubbs and R. G. Phillips, Rev. Sci. Instr. 31, 115 (1960).

- ³⁰M. Camac and R. M. Feinberg, Rev. Sci. Instr. 33, 964 (1962).
- ³¹J. S. Courtney-Pratt, "A Review on the Methods of High-Speed Photography" in Reports on Progress in Physics (The Physical Society, London, 1957), Vol. 20, p. 379.
- ³²K. R. Coleman, "Ultra-High-Speed Photography" in Reports on Progress in Physics (The Physical Society, London, 1963), Vol. 26, p. 269.
- ³³W. G. Hyzer, Engineering and Scientific High-Speed Photography (The Macmillan Co., New York, 1963).
- ³⁴Proceeding of the International Congress on High-Speed Photography. A total of eight held until 1968. The last one: High-Speed Photography, eds. N. R. Nilsson and L. Högborg (Wiley, New York, 1968).
- ³⁵R. W. Engstrom, "Photoelectric Devices", in Methods of Experimental Physics, E. Bleuler and R. O. Haxby, eds. (Academic Press, New York, 1964), Vol. 2, p. 743.
- ³⁶G. Amsel and C. Zajde, Rev. Sci. Instr. 35, 1538 (1964).
- ³⁷G. Lucovsky and R. B. Emmons, Appl. Opt., 4, 697 (1965).
- ³⁸M. DiDomenico, W. M. Sharpless and J. J. McNicol, Appl. Opt. 4, 677 (1965).
- ³⁹L. K. Anderson and B. J. McMurtry, Appl. Opt. 5, 1573 (1966).
- ⁴⁰O. C. Jones, J. Sci. Instr. 41, 653 (1964).
- ⁴¹N. K. Chaney, V. C. Hamister and S. W. Glass, Trans. Electrochem. Soc. 67, 107 (1935).

⁴²M. R. Null and W. W. Lozier, J. Opt. Soc. Am. 52, 1156 (1962)

⁴³R. D. Lee and E. Lewis, Appl. Opt. 5, 1858 (1966).

⁴⁴A. Cezairliyan, Appl. Opt., to be published (1971).

Chapter 13

SHORT-TIME (MILLISECOND) FLUCTUATIONS OF RADIANCE TEMPERATURE OF GRAPHITE ARC

Ared Cezairliyan
National Bureau of Standards
Washington, D. C. 20234

Successful development of high-speed (millisecond and sub-millisecond resolution) photoelectric and photographic pyrometers for very high temperature research requires stable high temperature reference radiance sources. Low current graphite arcs are generally considered as reference sources in the vicinity of 650 nm^{1,2,3}. However, investigations regarding their radiance temperatures have been made with relatively slow detecting and recording systems. The fastest one had an electronic time constant of $1/6 \text{ s}^3$.

The objective of this note is to investigate, with submillisecond resolution, the behavior of the radiance temperature of graphite arcs.

The positive and negative electrodes were spectroscopically pure graphite rods (National Carbon grade SPK 1/4 inch and AGKS 1/8 inch, respectively). The negative electrode was inclined -120° with respect to the positive. The radiance temperature of the crater of the positive electrode along its axis was measured with a high-speed photoelectric pyrometer⁴ which can make 1200 temperature determinations per second. The effective wavelength of radiance measurements was 650 nm with a bandwidth of 10 nm. The pyrometer target was a circular area 0.2 mm in diameter. A neutral density filter was placed between the pyrometer and the graphite arc in order to reduce the radiance of graphite arc to the level of the pyrometer reference, which was a gas-filled tungsten filament lamp. The output of the pyrometer was recorded with a high-speed digital data acquisition system⁵, which has a full-scale signal resolution of one part in 8000 and a time resolution of 0.4 ms.

A total of four experiments were performed at two locations on two positive electrodes. The arc current was kept within 0.5 A of the overload point. Each experiment, which was 150 ms in duration, consisted of 180 temperature data points. A representative temperature for each experiment was obtained by taking the average of these data. The standard deviation of the averages was approximately 4 K.

The range of low and high temperatures for the four experiments extended from 3799 K to 3808 K on the International Practical Temperature Scale of 1968⁶ (IPTS-68). The average of the four experiments was 3804 K. This compares favorably with the values 3806 ± 20 K, both on IPTS-68, reported by Lee and Lewis³, and Null and Lozier², respectively.

In order to separate the contribution of the pyrometer operation on the measured temperature fluctuations, a separate experiment was performed in which the graphite arc was replaced by a tungsten filament lamp. The neutral density filter was removed and the current flowing through the lamp was adjusted to give approximately the same pyrometer output. The average of 180 temperature data points obtained under these conditions was 2380 K with a standard deviation of 0.3 K. When this is extrapolated to 3800 K an equivalent standard deviation of 0.7 K is obtained, suggesting that the graphite arc has short-time (millisecond) fluctuations amounting to approximately 3 to 4 K in standard deviation. It is interesting to note that this is almost equal to the value 3 K, reported by Lee and Lewis³, for the standard deviation of radiance temperature fluctuation over a period of a few seconds measured with an electronic time constant of 1/6 s. Target size of the pyrometer used by Lee and Lewis was essentially the same as that used in this work.

The results of typical graphite arc and tungsten lamp experiments corresponding to approximately the same effective temperature (3800 K) are shown in figure 1. It may be seen that deviations of radiance temperature from their mean for the graphite arc are random. The lack of any cyclic pattern eliminates the possibility of the contribution of improper current rectification on the results.

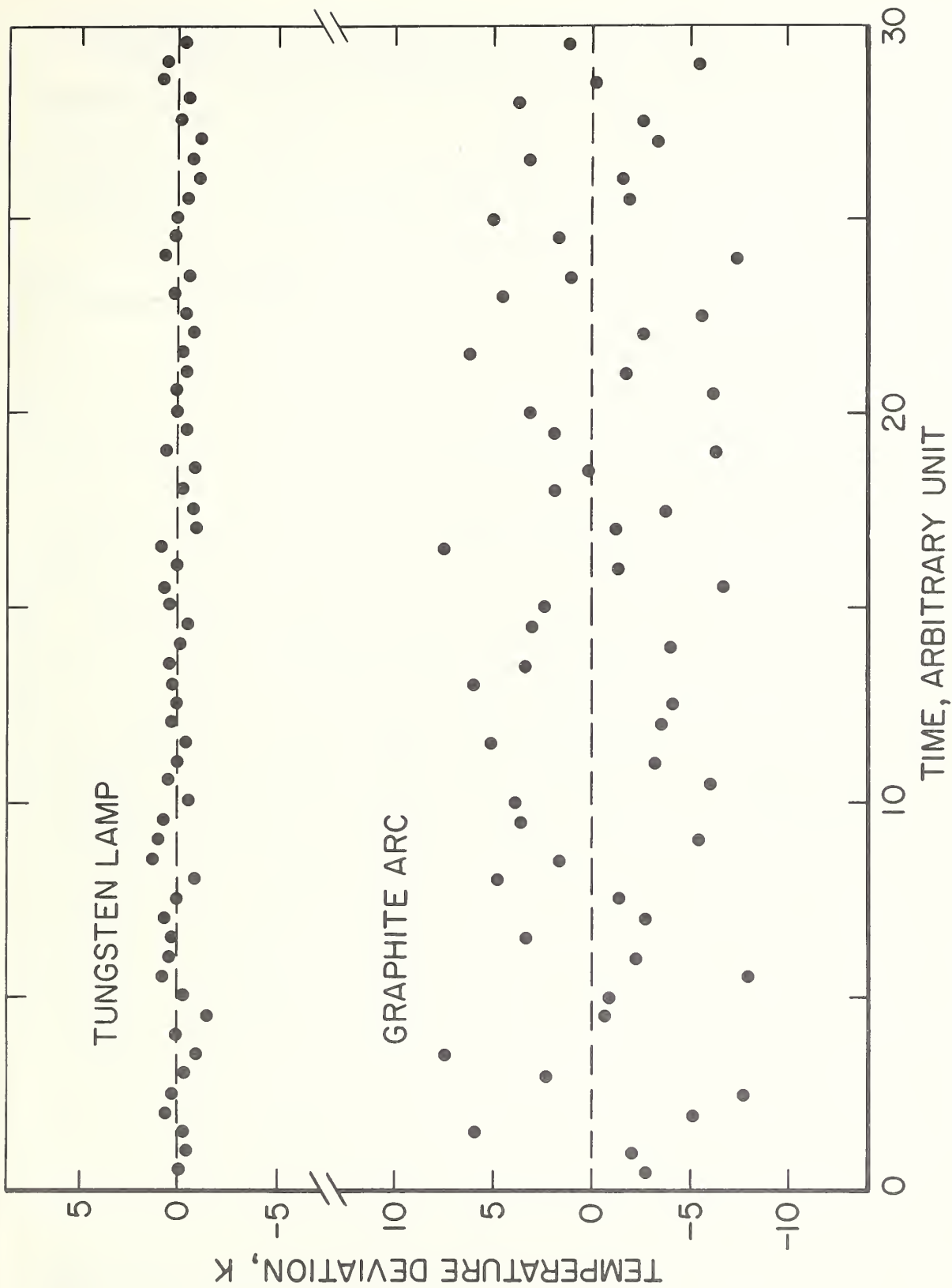


FIGURE 1. Variation of radiance temperature of graphite arc and tungsten lamp as a function of time. Both results correspond to the same effective temperature of approximately 3800 K. For simplicity every third point is plotted. 1 time unit = 2.5 ms.

The high-speed pyrometer was calibrated against a tungsten filament standard lamp, which in turn was calibrated against the NBS Temperature Standard. The estimated possible maximum error in temperature measurements at 3800 K is 10 K.

It may be concluded that short-time (millisecond) fluctuations of the graphite arc are 3 to 4 K, which is comparable to the fluctuations obtained over a period of seconds with a slower pyrometer.

References

1. N. K. Chaney, V. C. Hamister, and S. W. Glass, Trans. Electrochem. Soc. 67, 107 (1935).
2. M. R. Null, and W. W. Lozier, J. Opt. Soc. Am. 52, 1156 (1962).
3. R. D. Lee, and E. Lewis, App. Opt. 5, 1858 (1966).
4. G. M. Foley, Rev. Sci. Instr. 41, 827 (1970).
5. A. Cezairliyan, M. S. Morse, H. A. Berman, and C. W. Beckett, J. Res. Nat. Bur. Stand. (U.S.) 74A (Phys. and Chem.), 65 (1970).
6. International Practical Temperature Scale of 1968, Metrologia 5, 35 (1969).

DOCUMENT CONTROL DATA - R & D

(Security classification of title, body of abstract and indexing annotation must be entered when the overall report is classified)

1. ORIGINATING ACTIVITY (Corporate author) NATIONAL BUREAU OF STANDARDS DEPARTMENT OF COMMERCE WASHINGTON, D. C. 20234		2a. REPORT SECURITY CLASSIFICATION UNCLASSIFIED	
		2b. GROUP	
3. REPORT TITLE INTERIM REPORT ON THE THERMODYNAMICS OF CHEMICAL SPECIES IMPORTANT IN AEROSPACE TECHNOLOGY			
4. DESCRIPTIVE NOTES (Type of report and inclusive dates) Scientific Interim			
5. AUTHOR(S) (First name, middle initial, last name) THOMAS B DOUGLAS CHARLES W BECKETT			
6. REPORT DATE 1 July 1971	7a. TOTAL NO. OF PAGES 181	7b. NO. OF REFS 275	
8a. CONTRACT OR GRANT NO. ISSA-70-0002	9a. ORIGINATOR'S REPORT NUMBER(S) NBS REPORT 10 481		
b. PROJECT NO. 9750-01	9b. OTHER REPORT NO(S) (Any other numbers that may be assigned this report) AFOSR-TR-71-2584		
c. 61102F			
d. 681308			
10. DISTRIBUTION STATEMENT Approved for public release; distribution unlimited.			
11. SUPPLEMENTARY NOTES TECH, OTHER		12. SPONSORING MILITARY ACTIVITY AF Office of Scientific Research (NAE) 1400 Wilson Boulevard Arlington, Virginia 22209	
13. ABSTRACT Detailed report of recent results and critical analyses of experimental measurements completed or in progress, literature surveys, and new measurement-method developments-for high-melting metals and their Aerospace-important compounds. (Numbers in parentheses are temperature ranges or estimated general uncertainties.) Using subsecond pulse heating technique, the heat capacity (2%-3%), electrical resistivity (0.5%-1%), and hemispherical total and normal spectral emittances (3%) were measured for tungsten (2000-3600K) and niobium (1500-2700K), including 3692K(±15K) for the melting point of tungsten. Drop calorimetry gave the heat capacity (1%) of molybdenum (1170-2100K). Theoretical emissivity-resistance relation is only roughly obeyed. MoF ₅ prepared (cryoscopically, 99.85% pure), with preliminary vapor pressures and heats of vaporization measured by transpiration (after developing a technique to suppress decomposition). Preliminary heats of solution of MoF ₆ promise resolving large discrepancy with the published fluorine-combustion value. Matrix-isolation and gas-phase infrared spectroscopy gave the six active frequencies of NbF ₅ (assuming C _{4v} symmetry). Thorough review of the systems Mo-C, Ta-C, Nb-B, with criteria for sample suitability for drop calorimetry. Millisecond method for measuring high-temperature thermal expansion (5%) of electrical conductors developed and tested. Rotating attenuator for generating subsecond "sawtooth" radiance pulses (0.5%) is described. Various optical methods for measuring millisecond and microsecond high temperatures are critically reviewed (solids above 1500K, as in ramjet combustion and ablating materials). Millisecond fluctuations of 3 to 4K of the carbon-arc temperature (at about 3800K) were found comparable to those reported			

DD FORM 1 NOV 65 1473 for seconds intervals.

UNCLASSIFIED

Security Classification

14. KEY WORDS	LINK A		LINK B		LINK C	
	ROLE	WT	ROLE	WT	ROLE	WT
THERMODYNAMIC PROPERTIES						
HIGH-SPEED MEASUREMENTS						
CRITICAL LITERATURE REVIEWS						
HEAT CAPACITY						
ELECTRICAL RESISTIVITY						
THERMAL RADIATION PROPERTIES						
MELTING POINTS OF ELECTRICAL CONDUCTORS						
THERMOCHEMICAL CALORIMETRY						
VAPORIZATION BY TRANSPIRATION						
MATRIX-ISOLATION INFRARED SPECTROSCOPY						
THERMAL EXPANSION OF ELECTRICAL CONDUCTORS						
TUNGSTEN						
NIOBIUM						
MOLYBDENUM						
MOLYBDENUM FLUORIDES						
NIOBIUM PENTAFLUORIDE						
REFRACTORY-METAL CARBIDES AND BORIDES						
CARBON-ARC TEMPERATURES						

